National Library of Canada
Canadian Theses Service
Ottawa, Canada
K1A 0N4

Bibliothèque nationale du Canada
Services des thèses canadiennes

CANADIAN THESES

NOTICE

The quality of this microfiche is heavily dependent upon the quality of the original thesis submitted for microfilming. Every effort has been made to ensure the highest quality of reproduction possible.

If pages are missing, contact the university which granted the degree.

Some pages may have indistinct print especially if the original pages were typed with a poor typewriter ribbon or if the university sent us an inferior photocopy.

Previously copyrighted materials (journal articles, published tests, etc.) are not filmed.

Reproduction in full or in part of this film is governed by the Canadian Copyright Act, R.S.C. 1970, c. C-30. Please read the authorization forms which accompany this thesis.

THIS DISSERTATION
HAS BEEN MICROFILMED
EXACTLY AS RECEIVED

THÈSES CANADIENNES

AVIS

La qualité de cette microfiche dépend grandement de la qualité de la thèse soumise au microfilmage. Nous avons tout fait pour assurer une qualité supérieure de reproduction.

S'il manque des pages, veuillez communiquer avec l'université qui a conféré le grade.

La qualité d'impression de certaines pages peut laisser à désirer, surtout si les pages originales ont été dactylographiées à l'aide d'un ruban usé ou si l'université nous a fait parvenir une photocopie de qualité inférieure.

Les documents qui font déjà l'objet d'un droit d'auteur (articles de revue, examens publiés, etc.) ne sont pas microfilmés.

La reproduction, même partielle, de ce microfilm est soumise à la Loi canadienne sur le droit d'auteur, SRC 1970, c. C-30. Veuillez prendre connaissance des formules d'autorisation qui accompagnent cette thèse.

LA THÈSE A ÉTÉ
MICROFILMÉE TELLE QUE
NOUS L'AVONS REÇUE

NL 339 (r. 86/01)

Canada

199

National Library of Canada
Canadian Theses Division
Ottawa, Canada
K1A 0N4

Bibliothèque nationale du Canada
Division des thèses canadiennes

0-315-26931-6

PERMISSION TO MICROFILM — AUTORISATION DE MICROFILMER

- Please print or type — Écrire en lettres moulées ou dactylographier

Full Name of Author — Nom complet de l'auteur
M JOHN M. DUKE (MICHAEL JOHN MACLACHLAN DUKE)

Date of Birth — Date de naissance
8 NOV 1983

Country of Birth — Lieu de naissance
NORTHERN IRELAND.

Permanent Address — Résidence fixe
30, COLUMN ROAD
WEST KIRBY
WIRRAL, MERSEYSIDE

Title of Thesis — Titre de la thèse
"GEOCHEMISTRY OF THE EXSHAW SHALE OF ALBERTA - AN APPLICATAION OF NEUTRON ACTIVATION ANALYSIS AND RELATED TECHNIQUES"

University — Université
UNIVERSITY OF ALBERTA

Degree for which thesis was presented — Grade pour lequel cette thèse fut présentée
M. Sc

Year this degree conferred — Année d'obtention de ce grade
1983.

Name of Supervisor — Nom du directeur de thèse
R. D. MORTON

Permission is hereby granted to the NATIONAL LIBRARY OF CANADA to microfilm this thesis and to lend or sell copies of the film.

The author reserves other publication rights, and neither the thesis nor extensive extracts from it may be printed or otherwise reproduced without the author's written permission.

L'autorisation est, par la présente, accordée à la BIBLIOTHÈQUE NATIONALE DU CANADA de microfilmer cette thèse et de prêter ou de vendre des exemplaires du film.

L'auteur se réserve les autres droits de publication; ni la thèse ni de longs extraits de celle-ci ne doivent être imprimés ou autrement reproduits sans l'autorisation écrite de l'auteur.

Date
17/OCT/1983

Signature
John Duke

NL-91 (4/77)

THE UNIVERSITY OF ALBERTA

"Geochemistry of the Exshaw Shale of Alberta - an application of neutron activation analysis and related techniques."

by

Michael John Maclachlan Duke

A THESIS

SUBMITTED TO THE FACULTY OF GRADUATE STUDIES AND RESEARCH

IN PARTIAL FULFILMENT OF THE REQUIREMENTS FOR THE DEGREE

OF Master of Science

Department of Geology

EDMONTON, ALBERTA

Fall, 1983

THE UNIVERSITY OF ALBERTA

RELEASE FORM

NAME OF AUTHOR Michael John Maclachlan Duke

TITLE OF THESIS "Geochemistry of the Exshaw Shale of Alberta - an application of neutron activation analysis and related techniques."

DEGREE FOR WHICH THESIS WAS PRESENTED Master of Science

YEAR THIS DEGREE GRANTED Fall, 1983

Permission is hereby granted to THE UNIVERSITY OF ALBERTA LIBRARY to reproduce single copies of this thesis and to lend or sell such copies for private, scholarly or scientific research purposes only.

The author reserves other publication rights, and neither the thesis nor extensive extracts from it may be printed or otherwise reproduced without the author's written permission.

(SIGNED) ...John Duke...

PERMANENT ADDRESS:

.......30, Column Road.........

.......West Kirby, Wirral......

.......Merseyside, ENGLAND.....

DATED ......15th.. October.. 1983

THE UNIVERSITY OF ALBERTA

FACULTY OF GRADUATE STUDIES AND RESEARCH

The undersigned certify that they have read, and recommend to the Faculty of Graduate Studies and Research, for acceptance, a thesis entitled "Geochemistry of the Exshaw Shale of Alberta - an application of neutron activation analysis and related techniques." submitted by Michael John Maclachlan Duke in partial fulfilment of the requirements for the degree of Master of Science.

....

Supervisor

....

....

....

Date........18th May 1983...........

Abstract

The Mississippian Exshaw Formation of Alberta consists largely of black, and in places calcareous, radioactive shales. Forty-two core samples of the formation have been analyzed for some forty elements to quantify the naturally occurring radiosotopes U, Th and K and to study the geochemistry of these uraniferous black shales.

Uranium concentrations up to 92.2 ppm (twenty-five times the average shale value) are largely responsible for the anomalous radioactivity, though in places potassium concentrations up to three times the average black shale concentration, are also a major contributor. The median Exshaw Shale thorium concentration of 9.2 ± 1.9 ppm is in agreement with the relatively constant average shale Th values.

Uranium is found to be correlated with organic carbon, suggesting that following transportation as a soluble (most likely carbonate) complex the uranium was precipitated and adsorbed by the carbon in a reducing environment.

Thorium shows strong correlations with most of the hydrolysate elements suggesting that the element is bound mainly to clays.

Compared to average shales the median Exshaw Shale is enriched in U, V, Zn, Sb, Pb, Ni, Mo, Cu and As while Cr, Ga, Mn and the rare earth elements are depleted. The Exshaw Shale rare earth element patterns are very similar to those of the North American Shale Composite and the post-Archaean

Australian Shale except for the presence of a negative cerium anomaly. This anomaly is thought to be due to dilution of the black shales by calcareous material and a siliceous biogenetic component.

A number of instrumental methods, including instrumental and epithermal neutron activation analysis, delayed neutron counting, fission track analysis, X-ray fluorescence and gamma-ray spectrometry, utilized for uranium, thorium and potassium analysis are compared. The relative merits and drawbacks of each technique are presented in an attempt to aid the potential researcher in deciding which method is most suitable for his needs. A variation of the 'traditional' method of uranium, thorium and potassium analysis via natural gamma-ray spectrometry is presented and shown to require less sample and to be more rapid than conventional gamma-ray spectrometry, but with comparable accuracy and precision being obtained.

The accuracy, precision and multielement nature of instrumental neutron activation analysis is exemplified by the analysis of a number of the more traditional USGS rock standards together with three of the 'new' standards, SCo-1, SGR-1 and MAG-1 (two shales and a marine mud respectively). The results for these new standards are presented.

Acknowledgements

It is practically impossible to thank everyone who has helped me in some way complete this thesis. However, major thanks must go to a number of people; Dr. Roger Morton my supervisor, for his encouragement and interest throughout the thesis. To Dr. Llyod Stephens-Newsham for making available the University of Alberta SLOWPOKE reactor facilities. Many thanks to Mr. Dennis Ng and Mr. Peter Ford for their help in the counting and irradiation of samples. I am most indebted to Dr. Mike Apps my co-supervisor and would like to thank him for introducing me to neutron activation analysis, and for his help, enthusiasm, expertise and friendship which he has extended me. I thank Margaret Hunt who has always been there when I needed encouragement and who has helped me time and time again in the actual production stages of this thesis.

Finally, the finacial support for this work, which was provided by the Boreal Institute for Northern Studies is gratefully acknowledged as are the graduate teaching assistantships to the author from the Department of Geology, University of Alberta.

Table of Contents

Chapter Page

1. Introduction 1

2. Neutron Activation Analysis 4

    2.1 Introduction 4

    2.2 The theoretical background 4

    2.3 SLOWPOKE II Nuclear Reactor 8

        2.3.1 Introduction 8

        2.3.2 Fundamentals of the SLOWPOKE II Nuclear Reactor 8

        2.3.3 Irradiation facilities 11

    2.4 Instrumental Neutron Activation Analysis of Samples 13

        2.4.1 Short Irradiation (4 minute) 13

        2.4.2 Long Irradiation (2 hour) 21

    2.5 Interferences 24

        2.5.1 Spectral Interferences 24

        2.5.2 Nuclear Interferences 28

        2.5.3 (n,f) interferences 33

        2.5.4 Other Interferences 36

    2.6 Instrumental neutron activation analysis results 36

        2.6.1 Uranium, thorium and potassium 36

        2.6.2 INAA of other elements 43

    2.7 EPITHERMAL NAA 51

        2.7.1 Introduction 51

        2.7.2 Previous work 56

        2.7.3 Experimentation and results 58

3. Fission Track Analysis 68

3.1 Introduction 68

3.2 Theoretical principles 68

3.3 Sample Preparation and Analysis. 69

3.4 Results 73

4. Delayed Neutron Counting. 74

4.1 Introduction 74

4.2 Theory 74

4.3 DNC results 79

5. Gamma-ray Spectrometry. 84

5.1 Introduction 84

5.2 Sample Preparation 87

5.3 The Counting System. 88

5.4 Analysis 89

5.5 Results 101

6. X-Ray Fluorescence 108

6.1 Introduction 108

6.2 Analyses 108

7. Evaluation of the various methods for uranium analysis 111

8. The Exshaw Shale 124

8.1 Mineralogy 125

8.2 Geochemistry 126

8.2.1 Major elements 127

8.2.2 Rare Earth Element Geochemistry 136

8.2.3 Uranium and Thorium geochemisty 151

8.2.4 Geochemistry of remaining elements 155

9. Conclusions 157

9.1 Methodology 157

9.2 Geochemistry 157

References 159

Appendix 1 : Chemical Analyses. 171

Appendix 2 : Sample Locations. 186

List of Tables

Table Page

2.1 Nuclear data for short-lived radionuclide analysis..14

2.2 Specific activities and mean detection limits for short irradiation........................19

2.3 Elements determined and counting scheme employed following 2 hour irradiation...............23

2.4 Potential nuclear and spectral interferences........25

2.5 Examples of interfering transmutations..............30

2.6 Calculations of the interference effects of 1% of each of the major rock forming oxides......32

2.7 Fission interfernces due to the irradiation of natural uranium.....................36

2.8 Uranium and potassium results for selected USGS rock standards following short irradiation..................................42

2.9 Uranium, thorium and potassium results for DL-1 following a 2 hour irradiation and various decay times............................42

2.10 Uranium, thorium and potassium results for selected USGS standards following long irradiation...................................44

2.11 Short INAA results for USGS Cody Shale (SCo-1)......45

2.12 Short INAA results for USGS Green River Shale (SGR-1).......................................46

2.13 Short INAA results for USGS marine mud (MAG-1)......47

2.14 Short INAA results for USGS Dunite (DTS-1)..........48

2.15 Short INAA results for USGS Granodiorite (GSP-1)....49

2.16 Results following 2 hour irradiation of USGS Cody Shale (SCo-1)............................52

2.17 Results following 2 hour irradiation of USGS Green River Shale (SGR-1).....................53

2.18 Results following 2 hour irradiation of USGS Diabase (W1)...............................54

Table Page

2.19 Comparison of instrumental and epithermal NAA of AGV-1....62

4.1 DNC uranium results using the SLOWPOKE reactor......79

5.1 Uranium and thorium results of low energy gamma-spectrometry....102

5.2 Low energy gamma-spectrometry for the analysis of uranium, thorium and potassium in NBS Flyash 1633a....105

6.1 Detection limits for X-Ray fluorescense............110

7.1 Results of various methods of uranium analysis applied to Exshaw shale samples..........114

8.1 Comparison of average shale values with those of the Exshaw Shale determined in this study....128

8.2 Comparison of some elemental concentrations in the post-Archaean upper continental crust with the Exshaw Shale............150

8.3 Correlation coefficients for U, Th, K_2O and organic C for the Exshaw Shale................153

List of Figures

Figure Page

2.1 The University of Alberta SLOWPOKE Reactor..........10

2.2 SLOWPOKE reactor critical assembly and core.........11

2.3 The γ-ray spectrum of a shale after a 12 minute decay period..................................16

2.4 The γ-ray spectrum of a shale after a 30 minute decay period..................................17

2.5 Fission yield curve of ^{235}U induced by thermal neutrons.......................................34

2.6 Cd and B cross-section variation with neutron energy...57

2.7 The γ-ray spectrum of USGS andesite AGV-1 following ENAA......................................59

2.8 The γ-ray spectrum of USGS andesite AGV-1 following INAA......................................60

2.9 Effect of B_4C on the specific activity of selected isotopes....................................65

4.1 Comparison of SLOWPOKE and McMaster reactors DNC uranium results.........................81

5.1 ^{238}U, ^{232}Th and ^{235}U decay chains..................85

5.2 Uranium spectrum (0 to 3000 keV)...................90

5.3 Thorium spectrum (0 to 3000 keV)...................91

5.4 The low energy parts of the uranium and thorium spectra.....................................93

5.5 Uranium spectrum (0 to 1500 keV)...................98

5.6 Thorium spectrum (0 to 1500 keV)...................99

5.7 Potassium spectrum (0 to 1500 keV)................100

7.1 Linear plot of uranium content obtained by DNC versus XRF................................116

7.2 Linear plot of uranium content obtained by DNC versus low energy gamma-spectrometry NaI analysis...................117

Figure Page

7.3 Linear plot of uranium content obtained by DNC versus INAA 2 hour irradiation..............118

7.4 Linear plot of uranium content obtained by DNC versus INAA 4 minute irradiation............119

7.5 Linear plot of uranium content obtained by low energy gamma-spectrometry with and without correction for potassium..................120

7.6 Linear plot of thorium content obtained by 2 hour INAA versus XRF..........................121

7.7 Linear plot of thorium content obtained by low energy gamma-spectrometry NaI, corrected for potassium versus XRF................122

8.1 Log-log plot of Al_2O_3 versus Sc for the Exshaw Shale......................................131

8.2 Log-log plot of Al_2O_3 versus Rb for the Exshaw Shale......................................132

8.3 Diagramatic representation of ionic charge versus ionic radius of elements in the hydro-geological sedimentary environment.......133

8.4 Log-log plot of K_2O versus Rb for Exshaw Shale.....135

8.5 REE normalized patterns for Australian shales of various ages...........................139

8.6 REE normalized patterns for various sedimentary rocks................................139

8.7 REE normalized patterns of the Exshaw Shale and comparatory shales.......................141

8.8 REE pattern of the mean Exshaw Shale normalized to the post-Archaean Australian shale....................................142

8.9 Log-log plot of La versus Dy for Exshaw Shale......146

8.10 Log-log plot of Dy versus Sm for Exshaw Shale......147

8.11 Log-log plot of Dy versus Eu for Exshaw Shale......148

1. Introduction

Since the 1890's it has been recognized that marine black shales often contain anomalous concentrations of uranium (Bell, 1978). In Alberta a number of horizons are anomalously radioactive and are used by the oil and gas industry as marker horizons when logging and correlating wells. Examples of such units within Alberta include the Exshaw Formation and the Nordegg shale of the Fernie Group. Until recently however, few data existed on the uranium or potassium contents of the Exshaw Shale (Campbell, 1980; Havard,1967) and to date, no data have been published on the thorium contents of the shale.

The initial objective of this thesis was therefore to quantify, and if possible explain, the uranium, thorium and potassium contents of the anomalously radioactive pelites of the Exshaw Formation of Alberta. As this in part required the setting up, and in certain instances development, of a variety of methods for the analysis of U, Th and K (for example natural gamma-ray spectrometry, delayed neutron counting and fission track analysis) it became apparent that a description and comparison of the various techniques utilized would be both a useful and valuable contribution.

Forty-two core samples of Exshaw shale, taken from 19 wells, were analyzed largely by instrumental neutron activation analysis (INAA) and X-ray fluorescence (XRF), for some thirty-five elements in total. The locations of those wells sampled are given in Appendix 2. Samples were selected from core areas of maximum and minimum total radioactivity using an Urtec minispec with a small NaI(Tl) crystal.

Part I

Analytical Methods.

2. Neutron Activation Analysis

2.1 Introduction

The principles of neutron activation analysis (NAA) were first developed by Von Hevesy and Levi(1936). However, it was not until the development of the nuclear reactor that the technique could be used in a routine manner. Over the last four decades the increased availability of research-type nuclear reactors, together with the development of semiconductor detectors and the complementary solid-state electronics capable of collecting and reducing complex spectra have made NAA an extremely attractive method. At present the sensitivity, precision, generally non-destructive and multi-element nature of NAA makes it a competitive means of analysis when access to a nuclear reactor is available. A brief introduction on the theory of NAA will be given so that the reader might appreciate some of the later discussions. For a more complete coverage of the technique and its applications see Rakovic (1970), Kruger (1971), De Soete *et al*. (1972), Muecke *et al*.(1980), and Amiel *et al*. (1981).

2.2 The theoretical background

Unlike many techniques commonly used in the earth sciences, NAA is based upon modification of the nucleus, not the orbiting electrons of the atom. Nuclei of stable isotopes are irradiated with neutrons which, via neutron capture, produce radioisotopes. These radioisotopes then decay according to a well defined time constant (termed the half-life, T1/2). The decay of many such radionuclides is accompanied by the emission of gamma-rays characteristic of the radionuclide. Detection and counting these gamma photons affords a means of elemental analysis, the energy of the gamma peaks being used to identify the radioisotope. The photopeak intensity is related to the element mass by the activation analysis equation:-

$$A = \frac{m.N.\theta.\sigma.\phi.I.\epsilon}{M.\lambda}\,(1-e^{-\lambda ti}).e^{-\lambda td}.(1-e^{-\lambda tc})$$

where:

A = photopeak area
m = mass of element
N = Avogadros number
θ = fractional isotopic abundance of isotope
M = molecular mass of target element
λ = decay constant (0.693/T1/2)
σ = effective cross section
ϕ = neutron flux (n cm^{-2} s^{-1})
ϵ = fractional detector efficiency
I = fractional gamma yield
ti = irradiation time in seconds
td = decay time in seconds
tc = count time in seconds

Within a reactor there is a spectrum of neutron energies. They range from the highly energetic fission or fast neutrons produced by the fission process, through resonance or epithermal neutrons (also called intermediate neutrons) which are in the process of 'slowing down' due to elastic collisions with the reactor moderator; down to the lowest energy thermal neutrons. It is the thermal neutrons which are largely responsible for the (n,γ) reactions. Fast neutrons, due to their greater energy, may induce reactions which result in the emission of a charged particle (such as a proton or α-particle) or another neutron from the excited nucleus. The (n,p) and (n,α) type reactions are known as *transmutations* as the atomic number of the product nucleus differs from its stable parent. Although analytically useful in a number of instances, such reactions are often the source of interferences (see page 28).

The neutron flux ϕ, is the product of the neutron density (n.cm^{-3}) and their average velocity (cm.s^{-1}) hence giving it the units n cm^{-2} s^{-1}. Due to the different average velocities and densities of the thermal, epithermal and fast neutrons there is a particular thermal, epithermal and fast neutron flux for any particular reactor operating level and position relative to the core (the source of the fast neutrons). Flux monitors of Au, Mn and Ni for example, may be used to measure the various components of the total neutron flux (De Soete et al. p.70-72, 1972).

The probability of a particular nuclear reaction occurring is known as the *reaction cross-section*, and is given the symbol, θ . This is an energy dependent function and is measured in barns (1 barn = 10^{-24} cm^2). Practically all fast neutron reactions have very small cross-sections in the order of millibarns (mb) while the majority of thermal (n,γ) reactions range from near unity to several thousand barns. The effective or reactor cross-section for many (n, γ) reactions includes a component due to the resonance or epithermal neutron flux. This effective cross-section, for any particular (n,γ) reaction, is given by:-

$$\sigma \text{ effective} = \sigma_0 + I \text{ res.} \frac{\phi epi}{\phi th}$$

Where $Ires = I_0 + 0.45\sigma$.

The resonance integral I_0 and thermal neutron cross-section σ_0, are available in tables (e.g. Lederer *et al*. 1978, Gryntakis and Kim 1976, 1978) while the epithermal to thermal neutron ratio is dependant upon the individual reactor and irradiation position and, as noted earlier, may be measured via flux monitors.

The activity of a radioisotope following a ti second irradiation is governed in part by the isotopes half-life and is given by the growth factor $1-e^{-\lambda ti}$. The decay factor $e^{-\lambda td}$, is a measure of how much of the initial activity remains after a decay time td. If after this time the sample is counted for a period tc, the fraction of the integrated area under the decay curve is given by $1-e^{-\lambda tc}/\lambda$ (assuming all emissions are detected).

The number of gamma-photons emitted per disintegration of a particular nuclear species is known as its fractional yield or γ-branching ratio and is given the symbol I.

The area of the photopeak however, depends upon the fractional efficiency of the detector, ϵ. This is controlled by the sample geometry (i.e. the solid angle subtended by the detector) and the energy of the emitted radiation and finally upon the intrinsic efficiency of the detector itself. Efficiency curves for the various counting geometries are usually found empirically from the analysis of mixed radionuclide reference sources (e.g. ^{152}Eu, ^{88}Y, ^{60}Co and ^{125}Sb) of known activity.

2.3 SLOWPOKE II Nuclear Reactor

2.3.1 Introduction

A supply of neutrons is essential for delayed neutron counting, fission track and neutron activation analysis. Invariably, a nuclear reactor is used to generate the high neutron flux necessary for practical analyses.

As all three of the above methods of analysis were carried out using the SLOWPOKE II nuclear reactor at the University of Alberta, it is felt pertinent to include in this thesis a description of the SLOWPOKE and some of its more important features. Most of the following information is synthesised from Kay *et al.*(1973) and the Atomic Energy of Canada Limited (AECL) literature. The reader is refered to these publications for additiional information.

2.3.2 Fundamentals of the SLOWPOKE II Nuclear Reactor

The reactor was developed by AECL at the beginning of the 1970's to be used at universities and hospitals for isotope production and neutron activation analysis with a minimum of supervision. The word SLOWPOKE is an acronym for **S**afe **LOW** **PO**wer **K**ritical **E**xperiment. A maximum thermal neutron flux of 1 x 10^{12}n $cm^{-2}s^{-1}$ is attainable, which is greater than can be supplied by most neutron generators or sources (for example ^{252}Cf), but at far less cost and supervision than conventional reactors.

SLOWPOKE is a small pool-type reactor (see figure 2.1) with a critical mass of enriched (to 93%) ^{235}U of approximately 0.85 kg. The small critical mass is the result of the beryllium annulus, bottom plate and upper shims which surround the fuel cage (see figure 2.2). Due to its low atomic mass, Be reflects a certain percentage of neutrons back into the reactor core where, once thermalized, they may participate further in the fission of ^{235}U.

The insertion or removal of a central cadmium control rod is used to control the fission process. This is due to the very large thermal-neutron capture cross-section of ^{113}Cd (ca. 20,000 barn).

In addition to acting as a coolant and moderator, normal (i.e. light) water is one of the primary safety features of the reactor. Due to a loss in density as the water temperature rises its ability to moderate the fission neutrons decreases. The water is said to have a 'negative temperature coefficient of reactivity'. Consequently, fewer fission neutrons are thermalized and the chain reaction slows and may reach the point were it is no longer self-sustaining and becomes sub-critical as the fission of ^{235}U occurs dominantly with thermal neutrons. Consequently, if there was a malfunction in the water cooling system the reactor power level would fall to where the amount of heat

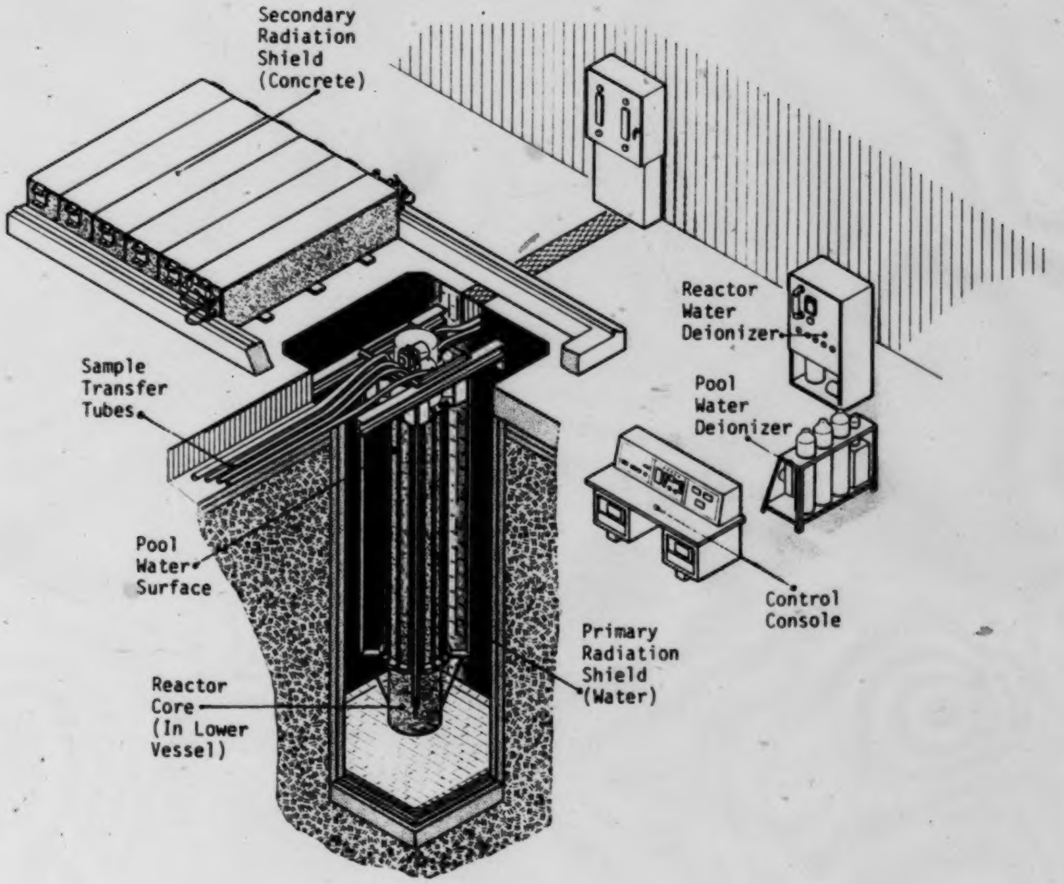
Secondary
Radiation
Shield
(Concrete)
Reactor
Water
Deionizer
Pool
Water
Deionizer
Sample
Transfer
Tubes
Pool
Water
Surface
Control
Console
Primary
Radiation
Shield
(Water)
Reactor
Core
(In Lower
Vessel)

Figure 2.1 The University of Alberta SLOWPOKE Reactor.

being generated by the fission process equalled that being lost to the pool surroundings.

2.3.3 Irradiation facilities

The University of Alberta SLOWPOKE reactor has five inner irradiation sites (within the Be annulus) and one outer irradiation site (outside the Be annulus); see figure 2.2 Samples are transfered rapidly (ca. 1.5 s one-way) to-and-from the sites pneumatically via a 'rabbit' system. The inner site vials are 7 cm^3 in volume and may accomodate two smaller 1.5 cm^3 vials while the large outer site vials

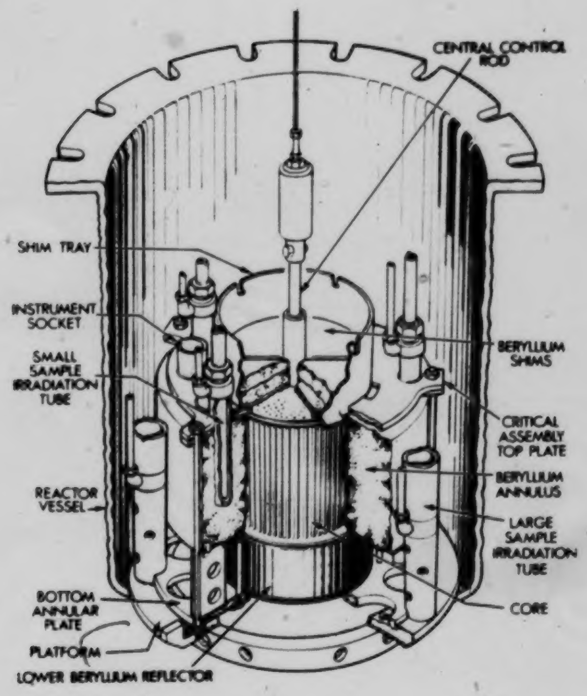
CENTRAL CONTROL ROD
SHIM TRAY
INSTRUMENT SOCKET
SMALL SAMPLE IRRADIATION TUBE
BERYLLIUM SHIMS
CRITICAL ASSEMBLY TOP PLATE
BERYLLIUM ANNULUS
REACTOR VESSEL
LARGE SAMPLE IRRADIATION TUBE
CORE
BOTTOM ANNULAR PLATE
PLATFORM
LOWER BERYLLIUM REFLECTOR

Figure 2.2 SLOWPOKE reactor critical assembly and core

have a capacity of 27 cm^3.

The U-Al alloy fuel rods are arranged so as to produce an equal, homogeneous neutron flux at each of the five inner sites. Ryan *et al*. (1978) carried out a number of flux measurements on the Dalhousie SLOWPOKE reactor. From measurements on three inner sites the neutron flux was found to differ by < ±2% (two sigma). Further measurements showed that the flux homogeneity varied <1% cm^{-1} vertically in both the inner and outer sites. Radial homogeneity was found to vary <1% cm^{-1} in the inner site but varied by 5% cm^{-1} in the outer site. From their research they concluded that the neutron flux:-

> "..is stable, homogeneous and reproducible
> from day to day over a period of months."
> Ryan *et al.* p.87,(1978).

Similiar stability was found by Bergerioux *et al*. (1979). This is extremely important as it makes the simultaneous irradiation of flux monitors and/or standards with samples unnecessary.

At the University of Alberta SLOWPOKE reactor the thermal to epithermal neutron ratio was measured via Au and Mn flux monitors (De Soete p.70, 1972) and found to be 16.9 ± 0.8 for the inner sites. The thermal to fast neutron ratio for the inner sites is 4.58 ± 0.22 (Ryan *et al*., 1978; Zikovsky and Galinier, 1981). As is shown later the epithermal and fast neutron components may be used advantageously for the analysis of certain elements.

2.4 Instrumental Neutron Activation Analysis of Samples

Two irradiation schemes were developed to maximize the number of elements determined together with a reasonable sample throughput. They included:-

a) 4 minute irradiation at 2.5×10^{11}n cm^{-2} s^{-1}

b) 2 hour irradiation at 1.0×10^{12}n cm^{-2} s^{-1}

Counting was carried out with an Ortec 80 cm^3 active volume Win[15] coaxial Ge(Li) detector, coupled to a Nuclear Data (ND) 660 multichannel analyzer with an Ortec 572 amplifer and ND 575 ADC. The detector specifications include a relative efficiency of 18.5% and a measured FWHM of 2.1 keV and peak-to-Compton ratio of 53:1 for the 1332 keV photopeak of ^{60}Co. Signals were assigned to one of 4096 channels and the spectra collected stored on floppy discs for later analysis.

2.4.1 Short Irradiation (4 minute)

A number of elements, including Al, Mn, Mg, Ti and V, only produce short-lived radioisotopes upon irradiation with thermal neutrons. For their measurement the samples must be counted soon after irradiation, before the activity from these short-lived isotopes decays away. Table 2.1 gives the relevant nuclear data for the short-lived radionuclides routinely determined in this study.

Samples and standards (both liquid and reference materials) were irradiated at 2.5×10^{11} n cm^{-2} s^{-1} for four minutes in site 1 of the SLOWPOKE reactor. Each sample was

Table 2.1 Nuclear data for short-lived radionuclide analysis

Target Isotope.	Isotopic Abundance (%)	Thermal cross-section (b)	Product nuclide	Half-life	γ-ray(s) used (keV)
^{23}Na	100.0	0.53	^{24}Na	15.00h	1368.5, 2753.9
^{48}Ca	0.185	1.1	^{49}Ca	8.72m	3084.0
^{27}Al	100.0	0.24	^{28}Al	2.24m	1778.7
^{41}K	6.8	1.2	^{42}K	12.36h	1524.6
^{26}Mg	11.3	0.027	^{27}Mg	9.46m	843.8, 1014.4
^{50}Ti	5.3	0.14	^{51}Ti	5.80m	320.1
^{51}V	99.8	4.9	^{52}V	3.76m	1434.0
^{238}U	99.28	2.72	^{239}U	23.4 m	74.7
^{86}Sr	9.86	1.3	^{87m}Sr	2.81h	388.5
^{37}Cl	24.2	0.4	^{38}Cl	37.29m	1642.7, 2167.5
^{59}Co	100.0	37.	^{60m}Co	10.47m	58.6
^{138}Ba	71.7	0.4	^{139}Ba	84.9 m	165.9
^{133}Cs	100.0	2.5	^{134m}Cs	2.91h	127.5
^{164}Dy	28.2	2700.	^{165}Dy	2.33h	94.7
^{154}Sm	22.6	5.5	^{155}Sm	22.1 m	104.3
^{151}Eu	47.8	2800.	^{152m}Eu	9.3 h	121.8
^{29}Si	4.7	---	^{29}Al	6.52m	1273.2
^{55}Mn	100.0	13.3	^{56}Mn	2.58h	846.6, 1811.2

counted twice, initially after a twelve minute decay period for 300s live time at 10 cm geometry and then for 600s live time at 1 cm geometry following a thirty minute decay period. This scheme allows for some 12-13 samples to be analyzed every four hours.

Although the majority of the elements in table 2.1 may be determined in both counting intervals the first count produces more precise results for Al, Ti and V on account of their shorter half-lives compared to the longer-lived isotopes. After the thirty minute decay period, the ^{28}Al activity and its associated Compton continuum has decayed to approximately 1/10000 of its initial value. This results in an increase in the signal-to-background ratio for the longer-lived isotopes which, together with the longer counting time, lowers the detection limit and increases the precision with which they may be determined. Figures 2.3 and 2.4 show sample spectra abtained following the two decay periods for example with a number of photopeaks identified.

Analysis was carried out via an adaptation of the comparator method of INAA (also called the 'semi-absolute' method by Bergerioux et al. 1979). Conventionally the method involves the simultaneous irradiation of a known mass of a particular element with a sample containing an unknown mass of the same element. If the counting geometries and irradiation-decay-count histories are identical for both the sample and standard, then the activities of the isotope of interest in the standard and sample are directly

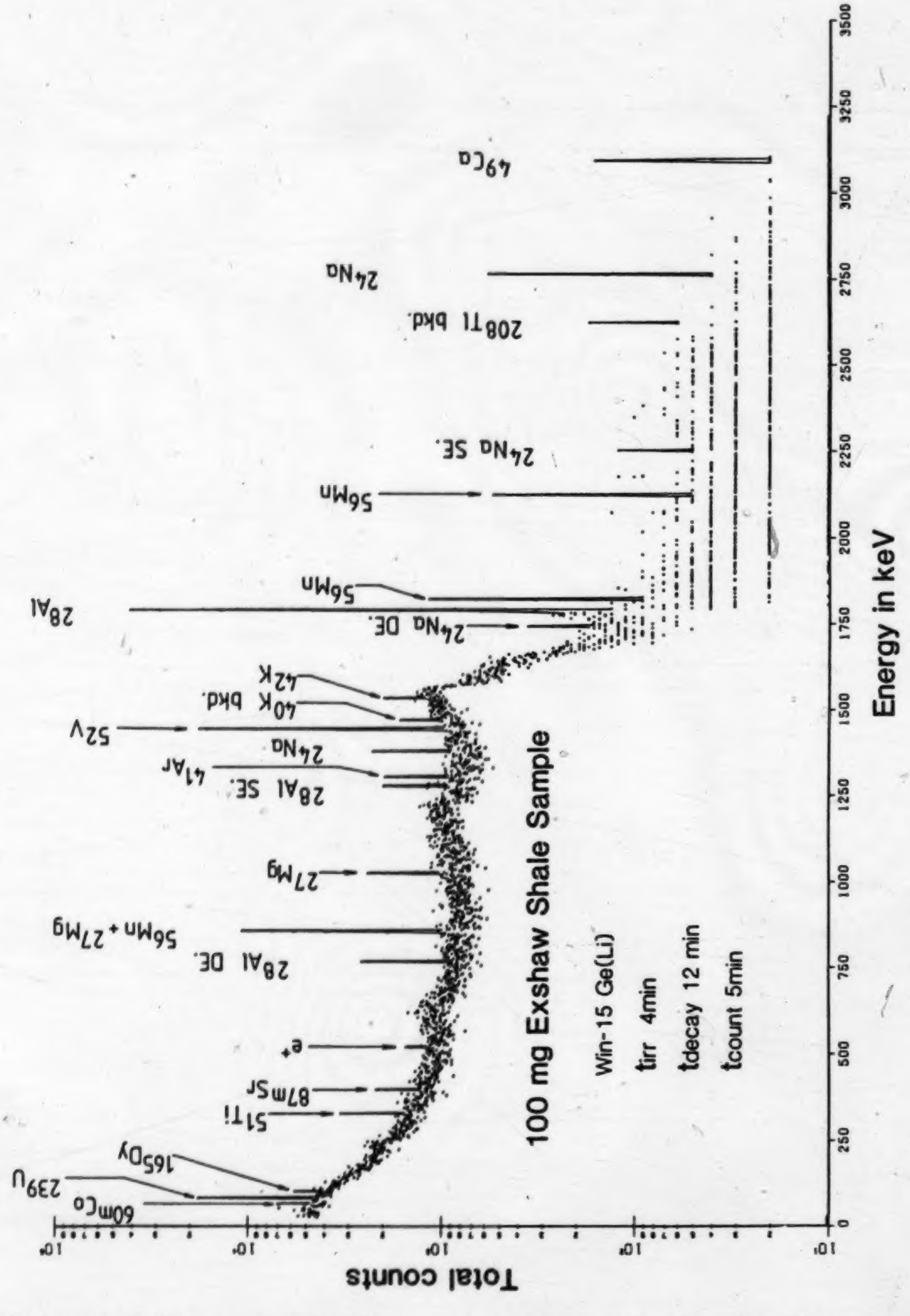

Figure 2.3 The γ-ray spectrum of a shale after a 12 minute decay period

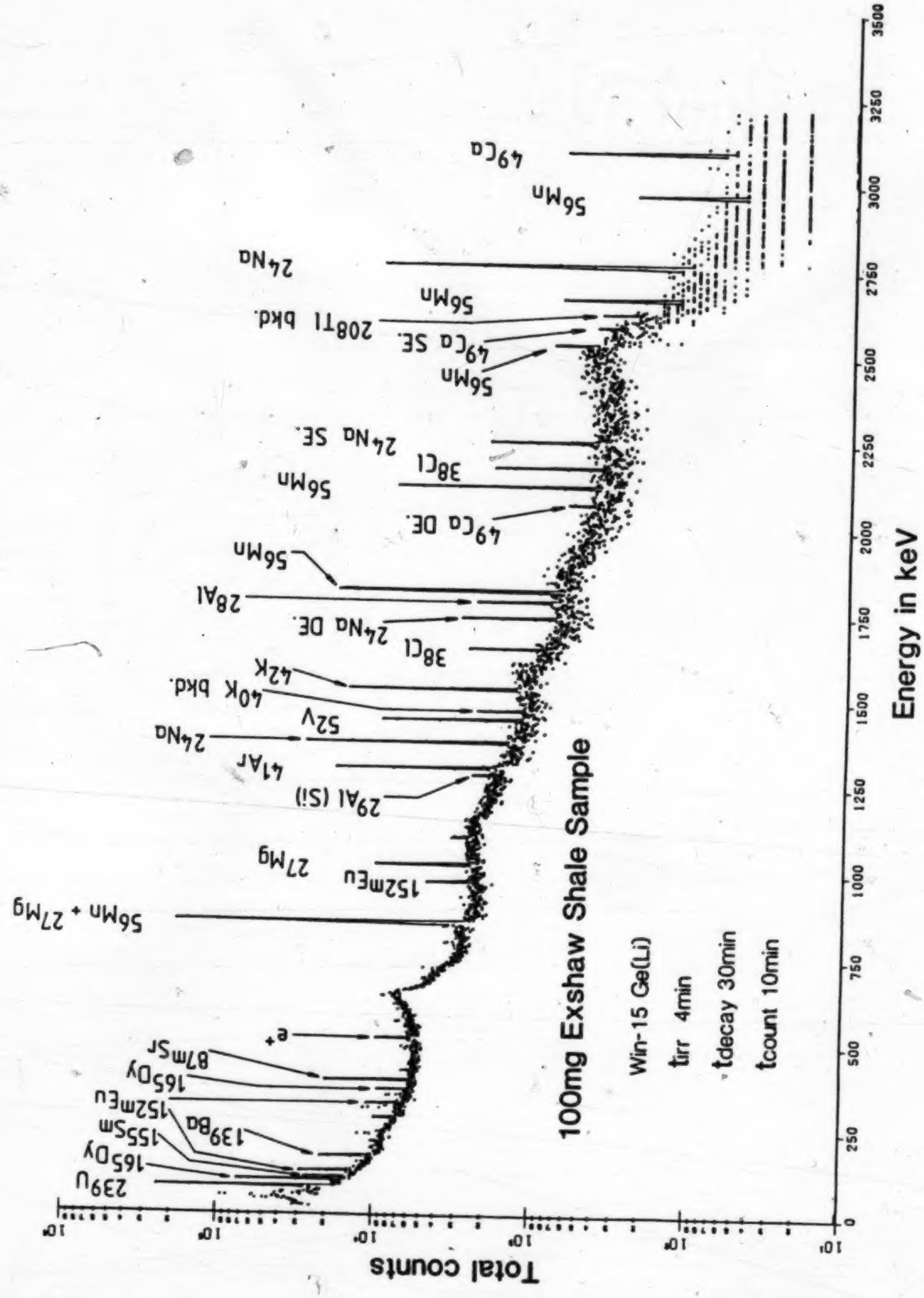

Figure 2.4 The γ-ray spectrum of a shale after a 30 minute decay period

proportional to the respective masses of the elements. An unknown mass may therefore be determined by ratioing the activities and multiplying by the known mass in the standard. As mentioned earlier, when discussing the salient features of the SLOWPOKE reactor, one of its assets is the stability and reproducibility of the neutron flux over long periods of time. This makes the simultaneous or regular irradiation of standards with, or following samples, unnecessary (Bergerioux et al. 1979).

Single element liquid standards covering a wide range of concentrations were prepared from a variety of atomic absorption standards (Aldrich, Alpha and Spex) for comparison. They were heat sealed in 1.5 ml polyethelene vials and analyzed utilizing the previously described scheme. From these runs the specific activities (counts/microgram for each nuclide) were determined for the two counting periods. To reduce the uncertainty in the specific activity determinations, the liquid standards were re-analyzed a number of times following suitable decay periods. This ultimately reduces the error when determining the elemental concentrations of the unknown samples (taking into consideration counting statistics of the individual peaks). The specific activities and mean detection limits for each element determined in the study samples are listed in table 2.2

Table 2.2 Specific activities and mean detection limits for short irradiation

Element	Net photopeak activity* (cts/ug)	Detection Limit† (in 100mg shale)
Na	65.24 ± 0.6[2]	37 ± 27
Al	2.654 ± 1.0[1]	310 ± 180
Ca	0.367 ± 1.1[2]	1900 ± 1400
K	1.56 ± 0.5[2]	1550 ± 1100
Mg	0.761 ± 2.1[1]	1300 ± 800**
Ti	1.88 ± 2.5[1]	900 ± 540
Mn	5782 ± 0.2[2]	0.44 ± 0.30
V	158.4 ± 1.0[1]	10.5 ± 7.0
U	17276 ± 0.2[2]	0.4 ± 0.3
Sr	42.5 ± 0.4[1]	90 ± 57
Cl	2.26 ± 3.0[2]	50 ± 30
Co	1516 ± 0.4[2]	4 ± 1
Ba	103.1 ± 0.2[2]	45 ± 27
Cs	616.4 ± 0.5[2]	7 ± 4
Dy	30172 ± 0.2[2]	0.2 ± 0.1
Sm	5980 ± 0.2[2]	1.0 ± 0.6
Eu	2394 ± 2.9[2]	0.2 ± 0.1
In	48954 ± 0.1[2]	$4.6\times10^{-3} \pm 3.0\times10^{-3}$
Si	0.0084 ± 3.0[2]	$2.4\times10^{5} \pm 1.2\times10^{5}$

---

* coefficient of variation in %

† mean detection limit in ppm calculated from 40 shale samples (± 1 std. deviation)

[1] from the 4:12: 5 min scheme at 10 cm geometry

[2] from the 4:30:10 min scheme at 1 cm geometry

** Assumming no ^{27}Al(n,p)^{27}Mg interference

Dead time and Pulse Pile-up Effects

Highly active samples (due largely to ^{28}Al, ^{56}Mn and ^{24}Na for example) can introduce significant error when determining element concentrations due to dead time and pulse pile-up (also called 'random summing') effects. As unknown samples and standards rarely, if ever, have the same activities, corrections must be applied. Consequently, a dead time correction (after Takeuchi _et_ _al_. 1980) for short-lived radioisotopes in the presence of a high, longer lived background (e.g. ^{24}Na and ^{56}Mn) was applied to each peak and a correction factor for random summing effects was calculated and applied following the procedure of Wyttenbach (1971).

Data reduction

All analyses were carried out off-line, in batch mode using the peak search programme PREP10 (Apps, 1978). The programme calculates amongest other data the energy, net area, background, counts s^{-1}, FWHM and % uncertainty in the net area determination of each peak. The user may select a variety of parameters including the minimum size a 'peak' must be before being processed, the Gaussian sensitivity (i.e. how much a peak may deviate from an ideal Gaussian shape before analysis for multiplet or overlapping peaks is initiated) and finally the number of iterations or 'peak fit attempts' that are applied to multiplets (see also ND660 Operator's Instruction manual). Recently, the programme was made available on the University of Alberta computer (an

AMDAHL 470V/6). In the future this will greatly reduce analysis time.

A programme was written by the author in FORTRAN IV which given the sample mass, live and clock times, together with the identity, area and uncertainty associated with each peak (taken from the PREP10 output) corrects for dead-time and pulse pile-up losses and calculates the corrected counts, mass, concentration and 1 sigma standard deviation for each element measured. Where necessary the programme also converts major element concentrations to oxides. Where a particular radionuclide decays with the emission of two or more quantifiable gamma-rays (for example ^{24}Na, ^{56}Mn and ^{38}Cl) the additional photopeaks have on occasion been used when calculating the element concentration. As each peak has its own associated uncertainty the best estimate of the mean value of the element and its associated uncertainty, was found by taking the weighted mean of the individual peak determinations. The reported mean values, determined from replicate analyses of USGS standard rocks, were calculated in the same manner.

2.4.2 Long Irradiation (2 hour)

Certain elements including As, Cr, Au, La, Fe and Tb only produce long-lived ($T1/2 > 1$day) radioisotopes when irradiated with thermal neutrons. Other elements, such as Ce, Sc, Sb and Th, produce both long- and short-lived nuclides when irradiated. Invariably however, these elements are determined via their long-lived products for convenience and increased sensitivity or precision.

To determine a number of the longer-lived isotopes standards and the 100 mg samples used in the short irradiation were re-irradiated for 2 hours in one of the five inner SLOWPOKE sites at a flux of 1 x 10^{12}n cm^{-2} s^{-1}. They were counted five times over the 21 days following irradiation in order to maximize the number of elements determined with optimium precision. The decay times, counting conditions and elements determined in each counting interval are given in table 2.3. The table shows that the concentrations of a number of elements are repeatedly determined via the same isotope. To reduce analysis time it would be possible to replace the first three counting intervals with a single one hour count after two days or just abandon the second day count altogether. Increased precision is however obtained by taking the weighted mean of these independant analyses.

Sample throughput is limited by the 10 hour sample count approximately 3 weeks after irradiation. Therefore, so as not to monopolize the ND 660 spectrometry system this 10 hour count was usually carried out overnight and only four samples were irradiated per week. Using approximately 0.75 ml vials (cut-in-half 1.5 ml vials) 4 samples, each 100 mg mass, may easily be packed into one medium sized (7 ml) irradiation vial.

Table 2.3 Elements determined and counting scheme employed following 2 hour irradiation.

Decay interval	Counting goemetry*	Counting time	Elements Determined
1 d.	10 cm.	20 min	Na,K,La,Eu,Sm,As,Ga,Sb,U(Np)
2 d.	1-3 cm.	1 hr	Na,K,La,Eu,Sm,As,Ga,Sb,U(Np)
3 d.	1-3 cm.	1 hr	Na,K,La,Sm,U(Np),As,Sb,Sc
6 d.	1 cm.	1 hr	Sc,Fe,Co,La,Ce,Sm,Lu,Hf, U(Np),Th(Pa)
c 21d.	1 cm.	10 hr	Sc,Rb,Sr,Sb,Ba,Cs,Ce,Cr,Hf, Ni(Co),Fe,Co,Se,Tb,Yb,Lu, Ta,Th(Pa),Fe(Mn), ± Nd

* initial 1 day count outside Pb cave, all other counts in 10 cm Pb cave to reduce background.

Data reduction

As with the short-lived INAA, spectra were stored on floppy discs for off-line analysis. All spectra were reduced using the batch programme NAARUN (Apps and Apps, 1981). The programme is an extension of PREP10 (Apps, 1978) and is fully interactive. In addition to the peak search output of PREP10, NAARUN identifies the isotopes possibly responsible for the emissions. Given the sample mass, counting time, plus the dates and times the samples were removed from the reactor and counting began, it calculates the mass (in ug) and concentration (in ppm) of each element identified. At present the data reduction is done off-line on the mini-computer based ND 660 system.

It cannot be over-emphasised how important the development of this programme has been in making long-lived INAA at the SLOWPOKE reactor facility routine in nature. Using the programme analysis of a single spectrum takes approximately 10 minutes. Where a similar analysis attempted manually using the PREP10 output and pocket calculator it would require a minimum of 5 or 6 hours. Once on the University computer, analysis time will be cut to a fraction of the present ten minutes.

2.5 Interferences

Like most other methods of elemental analysis neutron activation analysis may suffer interferences which, if not considered, can result in significant error. Such interferences fall into one of two catergories, namely:

1) spectral and
2) nuclear.

Table 2.4 lists examples of both interference types which may occur when analyzing geological materials via short-lived radionuclides.

2.5.1 Spectral Interferences

As the name suggests, spectral interferences result when two or more photopeaks (produced by different nuclides) lie within the resolving power of a spectrometry system. Generally, with Gaussian curve fitting applied to spectra, the Win[15] Ge(Li) detector and its associated electronics can

Table 2.4 Potential nuclear and spectral interferences

	Potential Nuclear Interference	Potential spectral Interference
^{28}Al	^{28}Si(n,p)^{28}Al ^{31}P (n,α)^{28}Al	-----------
^{24}Na	^{24}Mg(n,p)^{24}Na ^{27}Al(n,α)^{24}Na	-----------
^{56}Mn	^{56}Fe(n,p)^{56}Mn ^{59}Co(n,α)^{56}Mn	843.8 keV ^{27}Mg 9.46m
^{134}Cs	----------	127.2 keV ^{101}Tc 14.3m
^{165}Dy	----------	90 keV ^{152}m$_2$ Eu 96m
^{152}Eu	----------	846.6 keV ^{56}Mn 154.6m 843.8 keV ^{27}Mg 9.6m
^{27}Mg	^{27}Al(n,p)^{27}Mg ^{30}Si(n,α)^{27}Mg	846.6 keV ^{56}Mn 154.6m 841.7 keV ^{152}m$_1$ Eu 9.3h
^{52}V	^{52}Cr(n,p)^{52}V ^{55}Mn(n,α)^{52}V	----------
^{139}Ba	^{235}U (n,f)	-----------
^{155}Sm	^{158}Gd(n,α)^{155}Sm	103.2 keV ^{153}Sm 46.7h 106.1 keV ^{239}Np 2.35d
^{51}Ti	^{51}V (n,p)^{51}Ti ^{54}Cr(n,α)^{51}Ti	320.2 keV ^{151}Nd 12.4m
^{239}U	----------	74.97 keV Pb Kα X-rays
^{60}mCo	----------	57.5 keV ^{182}Ta 15.84m 58.0 keV ^{159}Gd 18.56h

satisfactorily resolve two gamma peaks whose centroids are ≥2.5 keV apart.[1] Such is the case with the ^{27}Mg and ^{56}Mn photopeaks at 843.8 and 846.6 keV respectively following the 12 minute decay period of the short irradiation scheme. Following the 30 minute decay period however, broadening of the 846.6 keV Mn photopeak (due to the increased photopeak area resulting from the longer counting period and increased counting efficiency) makes the determination of Mg from the 843.8 keV peak difficult. In such instances, or where more than two peaks are involved, or two peaks are too close to be satisfactorily resolved, the analyst may use another gamma-emission for analysis (if available, of sufficient intensity and free from interferences). In the above Mn and Mg example the analyst may use the 1014.4 keV (28.5% intensity) and 1811.2 keV (27% intensity) gamma peaks of ^{27}Mg and ^{56}Mn respectively for analysis.

Where the nuclide being interfered with decays with only a single gamma-ray (e.g. ^{51}Cr and ^{52}V) or with only one emission of sufficient intensity for quantification (e.g. ^{139}Ba or ^{42}K), two options are open to the analyst. Firstly, if the interfering nuclide decays with the emission of two or more gamma-rays the ratio of the area of the interfering photopeak with the area of an interference-free 'monitor' peak may be determined by irradiating and counting a standard of the interfering element and a correction factor calculated. Regardless of the irradiation, decay and count history of this standard, the ratio of the photopeak areas will be constant. Consequently, the counts to be stripped from the *'photopeak'* of the unresolved peaks may be calculated by multiplying the area of the interference-free monitor peak by the empirically determined correction factor. Alternatively, if the interfering isotope has a half-life which is significantly shorter than that of the nuclide of interest the analyst may, by extending the 'cooling' period, reduce the interference to insignificance while still retaining a satisfactory level of precision when determining the longer-lived nuclide. Analysis of the rare earth elements (REE) may be used to exemplify this latter point. Due to the extremely similar geochemistries of the REE in practically all cases the presence of one REE implies the presence of the other members of the group. Thus, the determination of Lu soon after irradiation via the 113.0 keV photopeak of ^{177}m Lu (T1/2=155d) is interfered with by the 113.5 keV photopeak of ^{175}Yb (T1/2=4.21d). Following a decay period of 30 days however, the activity of ^{175}Yb will have decayed to <1% of its initial activity while ^{177}m Lu will be at 87.5% of its initial activity. Similarly, if the interfering nuclide has a half-life much greater than that of an element of interest, the interference may be calculated and corrected for by counting the sample twice. From an initial measurement the unresolved peak area may be measured while from a second analysis (some time later when the isotope of interest has decayed away to insignificance) the interference from the long-lived isotope may be measured and when corrected for decay, the interference may be stripped from the *photopeak* measured earlier giving the net peak area due to the short-lived isotope.

---

[1] This is in part a function of the photopeak energy as, with increasing energy the FWHM also increases and resolution deteriorates.

Less obvious spectral interferences may also result. For example, where a gamma emission is greater than 1022 keV, single- and double-escape peaks may be the source of interferences. Once again however, the main photopeak may be used to monitor the effect if corrections are necessary.

The coincident counting of two photons (gammas and/or X-rays) at high countrates, or that decay in cascade, will result in a pile-up or coincidence peak that may be an interference. In the case of the single photopeak at 320.0 keV of ^{51}Cr, summing of the two ^{177}m Lu photopeaks at 208.4 and 113.0 keV would produce an unresolved peak at 321.4 keV. Such peaks are difficult to identify and correct for as the severity of the interference is largely related to the sample activity, matrix composition and various radioisotope decay schemes. The effect is therefore best avoided by keeping the spectrometer busy time <10% by varying the irradiation:decay histories and/or counting geometry.

2.5.2 Nuclear Interferences

Such interferences result when the radionuclide under investigation is produced via a reaction other than that under consideration. INAA using thermal neutrons largely utilizes (n,γ) reactions. Consequently (n,p) and (n,α) reactions are potential interferences.

As a reactor flux is rarely completely thermalized, neutron activation by fast neutrons followed by the emission of a proton or alpha particle is in certain instances a favoured form of decay. As noted earlier when discussing the SLOWPOKE reactor a fast flux of approximately 2.2×10^{11}n cm^{-2} s^{-1}, may be obtained at full power. This is utilized favourably in some instances[2] however, in other cases corrections need to be made.

Zikovsky and Galinier (1981) calculated interference factors (IF) for some 50 (n,p) and 100 (n,α) reactions for the flux conditions occurring in a SLOWPOKE II reactor. The interference factor (IF) may be defined as the mass (in ug for example) of an element which, via an (n,p) or (n,α) reaction, produces a specific activity equal to that produced by an (n,γ) reaction of 1 ug of the element of interest. A selection of transmutational reactions and their IF values of particular interest to the geologist are given in table 2.5. From these values it may be calculated that 1000 ug of Al would produce, via the reaction $^{27}Al(n,p)^{27}Mg$, the equivalent ^{27}Mg activity produced by the irradiation of 185 ug of Mg via the reaction $^{26}Mg(n,\gamma)^{27}Mg$.[3] From the irradiation of Al standards of various concentrations when determining the specific activity for Al it was found that

---

[2] in the determination of Ni via the reaction $^{58}Ni(n,p)^{58}Co$ and Fe via $^{54}Fe(n,p)^{54}Mn$ for example.

[3] 1000ug Al/5.4 = 185ug Mg (equivalent)

Table 2.5 Examples of interfering transmutations.

Reaction	IF (ppm)
^{28}Si (n,p) ^{28}Al	690
^{24}Mg (n,p) ^{24}Na	980
^{56}Fe (n,p) ^{56}Mn	1×10^{5}
^{27}Al (n,p) ^{27}Mg	5.4
^{52}Cr (n,p) ^{52}V	4.2×10^{4}
^{51}V (n,p) ^{51}Ti	71
^{31}P (n,α) ^{28}Al	1600
^{27}Al (n,α) ^{24}Na	1200
^{59}Co (n,α) ^{56}Mn	3.2×10^{5}
^{30}Si (n,α) ^{27}Mg	6000
^{55}Mn (n,α) ^{52}V	1.8×10^{5}
^{54}Cr (n,α) ^{51}Ti	2.7×10^{4}
^{158}Gd (n,α) ^{155}Sm	4.9×10^{6}

(taken from Zikovsky and Galinier, 1981).

for the 12 minute decay period at 10 cms geometry:

$$\frac{^{27}\text{Mg cts at 843.8 keV photopeak}}{\text{ug Al}} = 0.16 \pm 7.2\% \ (N=7) \qquad (1)$$

and for the 30 minute decay period at 1 cm geometry.

$$\frac{^{27}\text{Mg cts at 843.8 keV photopeak}}{\text{ug Al}} = 0.71 \pm 0.8\% \ (N=5) \qquad (2)$$

while the specific activities for the Mg (n,γ) reaction following the short irradiation scheme are:

$$0.761 \text{ cts / ug Mg} \pm 2.1\% \ (N=5) \text{ at 10 cms geometry} \qquad (3)$$

$$4.04 \text{ cts / ug Mg} \pm 0.8\% \ (N=5) \text{ at 1 cm geometry} \qquad (4)$$

Thus from equations (1) and (3) 1000ug Al would give the equivalent ^{27}Mg activity of 210±28ug (7.5%) Mg, while equations (2) and (4) give the equivalent of 176±4ug (2.3%) Mg. The weighted mean of these two results gives 181±4ug Mg. The agreement between the theoretical and empirical results is not quite as excellent as it first appears. Zikovsky and

Galinier (1981) used a øth/øfast ratio of 5 in their calculations. In reality a value of 4.6 is more accurate. This would change the IF for the $^{27}Al(n,p)^{27}Mg$ reaction from 5.4 to 5.0 thus 1000ug Al would give a theoretical value of 200 ug Mg. However, considering the theoretical nature of Zikovsky and Galinier's method, the agreement between the two results is still very good and may be used as a first approximation of the potential interferences.

So that the geologist might more fully appreciate the **possible** extent of such interferences this author calculated the interfering effects of 1% of each of the ten major oxides routinely determined in geological materials from the IF values of Zikovsky and Galinier. From the results shown in table 2.6 one may conclude that the majority of the transmutations may be ignored unless rock-types of extreme composition are being analyzed. The 65-70% SiO_2 content of an average granitoid would produce the equivalent of c.525 ppm Al (0.1% Al_2O_3) which constitutes <1% of the typical content of such rock-types. Conversely, the 40.5% SiO_2[4] content of the USGS rock standard DTS-1 (dunite) would produce the equivalent of c.320 ppm Al(0.06% Al_2O_3) which represents 25% of the recommended Al_2O_3 content of the rock (0.24% Al_2O_3). The Mg content of such ultramafic rock-types may also result in significant errors when determining Na. Still using DTS-1 as the example the recommended MgO content of 49.8% would produce the equivalent of c.300 ppm Na (0.04%

---

[4] all recommended values taken from Flanagan(1976).

Table 2.6 Calculations of the interference effects of 1% of each of the major rock forming oxides.

Oxide	(n,p)	(n,α)
SiO_2	7.8 ppm Al	0.9 ppm Mg
Al_2O_3	980 ppm Mg	4.4 ppm Na
TiO_2	0.07 ppm Sc	-----
Fe_2O_3	0.04 ppm Mn	<0.2 ppm Cr
MgO	6.15 ppm Na	1.8 ppm Ne
CaO	3.3 ppm K	-----
Na_2O	-----	57 ppm F
K_2O	0.24 ppm Ar	1.2 ppm Cl
MnO	64.5 ppm Cr	0.04 ppm V
P_2O_5	4700 ppm Si	0.35 ppm Al

Na_2O) which is almost 600% greater than the recommended value of 0.007% Na_2O. The MnO content of most rock-types is <1%, therefore the V interference is generally negligible, this is not always the case with regards to the (n,p) reaction. In the USGS standard W1 (diabase) the recommended MnO content of 0.17% would produce the approximate equivalent of 11 ppm Cr which represents almost 10% of the recommended 114 ppm. The importance of the Si production via $^{31}P(n,p)^{31}Si$ is, in reality, irrelevant as the Si content of samples when measured is determined via the reaction $^{29}Si(n,p)^{29}Al$ at SLOWPOKE.

Where necessary corrections for these transmutations may be made by monitoring the (n,γ) photopeaks of the parent nuclides responsible.[5] It is extremely important to note however, that if the analyst runs a standard of a particular element to determine the extent of its transmutation interferences the corrections obtained may only be used for the particular decay and count histories that the corrections were determined for.[6] This is because the half-lives of the parent and the nuclide of interest are rarely if ever identical and the ratio of the monitor and peak of interest would be continually changing with time (as would be the correction factor).

---

[5] see for example Kerr and Spyrou(1977) where the 1368.4 keV photopeak of ^{24}Na is used to monitor and correct for the $^{23}Na(n,\alpha)^{20}F$ interference to ^{20}F produced via the reaction $^{19}F(n,\gamma)^{20}F$.

2.5.3 (n,f) interferences

The fission products of ^{235}U (upon which uranium analysis by delayed neutron counting and fission track analysis are based) are also a potential primary interference source. The fission of ^{235}U may be written as:

$$^{235}_{92}U + ^{1}_{0}n \longrightarrow ^{236}_{92}U \longrightarrow X + Y + f\,^{1}_{0}n + Q$$

where:

Q = the energy released per reaction (c. 200 MeV)
f = the number of neutrons produced (c. 2.5/reaction)
X = fission product nuclei
Y = fission product nuclei.

The two most probable masses of the fission nuclei are 95 and 139, about the maxima of the bimodally distributed fission yield curve (figure 2.5). Following the method outlined in De Soete et al. p.481 (1972) correction factors for the fission of ^{235}U in natural uranium were calculated. Those that were significant when analyzing geological materials are listed in table 2.7. The fission yields, thermal and resonance cross-sections, and remaining nuclear

---

[6] unless the activities of both sample and standard are calculated to some reference time.

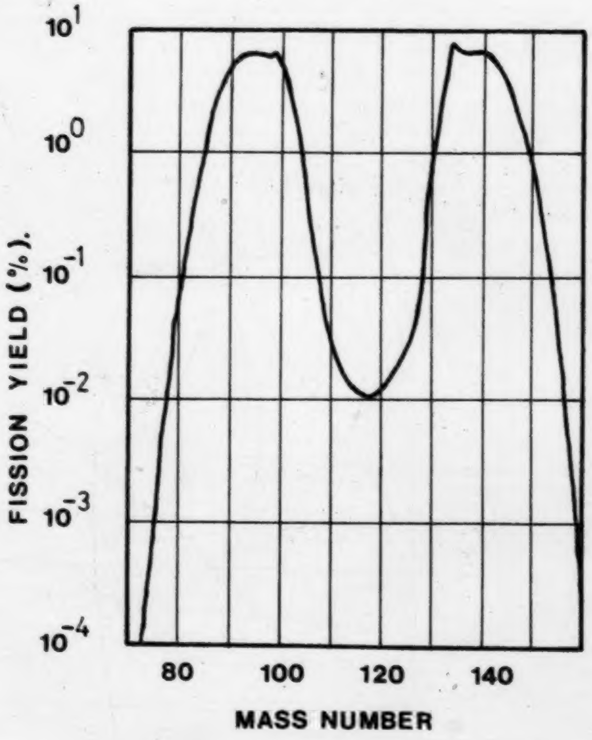

(Source: Katcoff, 1960)

Figure 2.5 Fission yield curve of ^{235}U induced by thermal neutrons

data were taken fron Katcoff(1960), Gryntakis and Kim(1976, 1978) and Lederer _et_ _al._(1974).

Most severely affected are the determinations of Zr, Mo and Ba via the radioisotopes ^{95}Zr, ^{99}Mo and ^{139}Ba. In addition, the light REE are also affected. This interference may be very important as it is the **relative** abundances of the REE that is of particular interest to the geologist. Consequently, care must be exercised when analyzing for the REE by NAA in the presence of uranium.[7] If a uranium standard is prepared and analyzed to measure the fission interferences empirically it is obviously very important to insure that the standard is of natural (or at least known) isotopic abundance. Empirical and theoretical (n,f) interferences were determined in this work. Their effectivness was tested whan analyzing the Canadian Radioactive Reference Ore DL-1 (U = 41 ± 2 ppm) and the corrected results obtained for this standard were found to be in good agreement with those found by Jagam and Muecke (to be published, pers. comm. G. Muecke, 1982). Consequently, were necessary, these corrections have been applied to the samples of this study. While this thesis was in the latter stages of being produced a paper addressing the problem of ^{235}U (n,f) interferences to REE analyses was published by Kennedy and Fowler (1983). Their findings are very similar to those measured and reported by this author in table 2.7.

---

[7] 100 ppm U in a sample would give the equivalent concentration of approximately 26 ppm Nd and 24 ppm Ce.

Table 2.7 Fission interferences due to the irradiation of natural uranium

Isotope	Fission Yield(%)	1ug U equivalent(ug)
^{139}Ba	6.55	0.62 Ba
^{95}Zr	6.2	6.15 Zr
^{99}Mo	6.06	0.78 Mo
^{140}La	---*	0.02 La
^{141}Ce	6.0	0.24 Ce
^{147}Nd	2.7	0.26 Nd

* produced during the decay of the fission product ^{140}Ba via the reaction $^{140}\mathrm{Ba} \longrightarrow \beta \longrightarrow {}^{140}\mathrm{La}$ (T1/2=12.8d), interference for decay time = 4 days.

2.5.4 Other Interferences

Secondary reactions induced by prompt gammas or charged particles emitted from the compound nucleus were considered but were concluded to have negligible effect when analyzing 'typical' geological samples at the SLOWPOKE reactor.

Similarly, second order reactions[1] need not be considered here as they usually only present a problem when analyzing for a particular trace element in a near monoelemental sample that lies next to the trace element in the periodic table (see Kubota, 1977).

2.6 Instrumental neutron activation analysis results

2.6.1 Uranium, thorium and potassium

Uranium analysis

Invariably uranium has been determined via one or more of the gamma-emissions of ^{239}Np as it decays to ^{239}Pu (see

---

[1] when the product of an (n,γ) or transmutation reaction is itself further activated eg. $^{30}\mathrm{Si}(n,\gamma)^{31}\mathrm{Si} \longrightarrow \beta \longrightarrow {}^{31}\mathrm{P}(n,\gamma)$ ^{32}P resulting in a gain in P or $^{181}\mathrm{Ta}\ (n,\gamma)^{182}\mathrm{Ta}\ (n,\gamma)^{183}\mathrm{Ta}$ for a loss of an isotope.

Morgan and Lovering, 1963; Schock, 1977; Baedecker *et al.*, 1977; and Hart *et al.* 1980). However, when ^{239}U decays to ^{239}Np it emits a 74.5 keV gamma photon of sufficient intensity to be used in quantifing the uranium content of many geological samples (see for example Vukotic, 1981).

In this work uranium was determined from both the short- and long-lived (n,γ) radioproducts of ^{238}U.

The detection limit (Currie, 1968) for uranium varied with the sample background when using the 74.5 keV emission of ^{239}U. However, based on some forty shale samples, the mean detection limit for a 100 mg sample was 0.4 ± 0.3 ppm U (at the 90% confidence level).

Following the two hour irradiation at a flux of 1×10^{12} n cm^{-2} s^{-1} the detection limit for uranium, determined solely from the 106.1 keV emission of ^{239}Np was found to fall from 2.3 ± 0.7 ppm U following a decay period of approximately 24 hours to 1.0 ± 0.3 ppm U after 2 days, down to 0.3 ± 0.2 ppm U after a decay period of 6 days. This reduction is largely due to the simultaneous, but more rapid decay of ^{24}Na and its associated Compton continiuum. One major problem associated with the use of the 106.1 keV gamma emission is that it may suffer interference from the 103.2 keV photopeak of ^{153}Sm (T1/2 = 1.94d) even when a Ge(Li) detector and counting system of superior resolution is used (see Kuleff and Koslodinov, 1981) and Gaussian spectral fitting is applied.[1]

---

[1] Use of a low energy photon spectrometer (LEPS) detector, with superior resolution to that of a Ge(Li) detector avoids

Similarly, the same interference to the 103.7 keV peak (K X-rays of ^{239}Pu) makes this peak of little use for analysis unless corrections are made. The 209.7 and 117.7 keV photopeaks of ^{239}Np are interfered with by ^{177}Lu (T1/2 = 155 d) and ^{169}Yb (T1/2 = 30.6d) respectively. Of the 277.5 and 228.2 keV photopeaks of ^{239}Np the 277.5 keV emission is to be prefered as the 228.2 keV line suffers an interference from the 229.3 keV photopeak of ^{182}Ta (T1/2 = 115d) which becomes increasingly significant the longer the decay period. In addition, the ^{235}U fission product ^{132}Te (fission yield 4.7%) with a half-life of 78.0 hours also emits a gamma photon at 228.2 keV (G. Muecke, pers comm. 1982). Spectral interferences to the 277.5 keV photopeak were found to be negligible and the results obtained from it more accurate than those obtained from the other emissions. Unfortunately however, due to the combination of decreasing detector efficiency with increasing energy, and the lower intensity of this emission, the uncertainty associated with this line is greater than that of the 106.1 or 228.2 keV emissions. Under the present irradiation:decay:count scheme, and using only the 277.5 keV emission, a concentration of 4 ppm U in a 100 mg sample may be determined with a precision of ±10 % or better (single analysis) following a decay period of 6 days. Conversely, the 74.7 keV photopeak of ^{239}U may be regarded as interference-free unless samples

---

[1](cont'd)this interference but these detectors are generally not as efficient as the coaxial Ge(Li) detector and hence longer counting times are required for a precise analysis.

containing an appreciable amount of lead are to be analyzed. Upon excitation by more energetic gamma- and/or X-rays, lead may emit secondary fluorescent Kα X-rays with an energy of 74.97 keV which cannot be resolved from the 74.7 keV gamma photons of ^{239}U. Such samples were not found in this study.

Thorium analysis

Unfortunately, unlike ^{239}U, the sensitivity for Th analysis via the short-lived ^{233}Th was found to be quite poor (c. 360 cts/ug Th vs. 17600 cts/ug U). For the shales analyzed, this resulted in a mean detection limit of 16 ppm Th and a quantification limit of 50 ppm Th (Currie, 1968). Consequently, although the 86.2 keV photopeak (2.7 % intensity) of ^{233}Th was positively identified in a number of instances it could rarely be used for precise or routine Th analysis in this study.

Following the two hour irradiation, and using only the 311.9 keV gamma emission of ^{233}Pa, the mean detection limit for thorium was calculated to be 0.3 ± 0.1 ppm following a decay period of approximately 21 days. Based solely on counting statistics, 10 ppm Th in a 100 mg sample may be determined with an uncertainty of ± 1% or better (1 sigma standard deviation). As is shown later accurate and sufficiently precise results may be obtained following a decay period of 6 days.

Potassium Analysis

Potassium was determined via its most intense gamma emission at 1524 keV (18% intensity). The emission is interference-free and because of the half-life of ^{42}K (12.2h) the same isotope is used following both the short and long irradiations. Following the short irradiation and a decay period of thirty minutes the mean detection limit for potassium (based on 42 shale samples) was calculated to be 0.155% ± 0.110% (0.186% ± 0.132% K_2O) in a 100mg sample (90 % confidence level). After the two hour irradiation the most precise and accurate results were obtained following a decay period of 3 days.

Accuracy of the U, Th and K analyses

To assess the accuracy of the U, Th and K analyses by both the short and long irradiation schemes, four 100 mg aliquots of the Canadian Radioactive Reference Ore DL-1 (U =41 ±2ppm, Th = 83±5ppm and K = 2.50%) were prepared and analyzed in accordance with the previously described procedures. The weighted means, one sigma standard deviations, number of determinations and scatter of results obtained following the four minute irradiation are as follows:

U = 40.8±0.1 ppm (N=4) scatter=6.54%
Th = 79.2±1.9 ppm (N=4) scatter=8.05%
K = 2.48±0.07 % (N=4) scatter=2.50%

Clearly the agreement between the recommended values and the results of this work are excellent. The scatter of the uranium and thorium results suggests however, that there may be some sample inhomogeneity and/or that variations in the counting geometry have produced the scatter and may therefore introduce a significant source of random error.

To further assess the four minute irradiation scheme for both accuracy and precision the USGS rock standards GSP-1, AGV-1, BCR-1 and W-1 were analyzed, the results are given in table 2.8 As thorium was only quantified in GSP-1 values are not reported. As with DL-1, the agreement between the recommended and measured concentrations are excellent.

Following the two hour irradiation of DL-1, and utilizing only the 277.9, 311.9 and 1524 keV photopeaks of ^{239}Np, ^{233}Pa and ^{42}K respectively, the individual results and weighted means of two separate analyses of DL-1 are reported in table 2.9 As can be seen the most accurate and precise results for potassium were obtained following a decay period of three days. Both the six day and ca. twenty-one day determinations of thorium are in excellent agreement with the recommended concentration. The uranium results obtained from the two 100 mg aliquots gave significantly different results with a mean of 38.0±0.2 ppm (N=6) scatter=6.58%. As with the short irradiation results the scatter of the results from the long irradiation may be due to sample inhomogeneity and/or slight variations in counting geometry. Fission track analysis of an aliquot of DL-1 would show whether inhomogeneity was a serious problem.

Finally, the standards GSP-1, AGV-1, BCR-1 and W-1 were also analyzed in keeping with the long irradiation scheme to

Table 2.8 Uranium and potassium results for selected USGS rock standards following short irradiation

	URANIUM (ppm)		POTASSIUM OXIDE (%)	
	This work	Recommended	This work	Recommended
GSP-1	2.61 ± .07 (n=3)	1.96 (a) 2.56 ± .13 (b)	5.50 ± .07 (n=3)	5.53 (a)
AGV-1	1.98 ± .14 (n=2)	1.88 (a) 2.05 ± .08 (b)	2.91 ± .10 (n=2)	2.89 (a)
BCR-1	1.69 ± .24 (n=1)	1.74 (a) 1.81 ± .09 (b)	1.68 ± .16 (n=1)	1.70 (a)
W-1	0.55 ± .14 (n=2)	0.58 (a)	0.54 ± .08 (n=3)	0.64 (a)

(a) Flanagan (1976)
(b) Millard (1976)

Table 2.9 Uranium, thorium and potassium results for DL-1 following a 2 hour irradiation and various decay times

	Decay Period				
	1 Day	3 Day	6 Day	c. 21 Day	Weighted mean
U	43.0 ± 1.5	39.4 ± 0.3	36.6 ± 0.2	-----	38.0 ± 0.2 ppm.
Th	-----	-----	84.2 ± 0.5	85.4 ± 0.5	84.7 ± 0.6 ppm.
K_2O	2.43 ± 0.04	2.47 ± 0.02	2.69 ± 0.10	-----	2.46 ± 0.11 %

evaluate the accuracy and precision of the U, Th and K determinations. The results, and a selection of recommended values, are given in table 2.10. Once again the agreement between the two is in general excellent. The uranium determinations are quite accurate though rather imprecise as a consequence of the low levels being analyzed.

2.6.2 INAA of other elements

Results of 4 minute irradiation of standard rocks

Utilizing the short irradiation scheme and data reduction method described the, USGS rock standards GSP-1(granodiorite), AGV-1(andesite), W-1(diabase), BCR-1(basalt), PCC-1(peridotite), DTS-1(dunite), SCo-1(Cody shale), SGR-1(Green River shale) and MAG-1(marine mud) were analyzed. The results obtained for GSP-1, DTS-1, SCo-1, SGR-1 and MAG-1 are given in tables 2.11 to 2.15 together with recommended and other literature values. As can be seen, the method is accurate and for most elements, precise. From the variety of geological materials analyzed the method is applicable over a wide compostional range. Its application to the analysis of ultramafic rocks is however limited due to the extremely low levels of many elements in such rocks.

Analyses of the new USGS rock standards SCo-1, SGR-1 and MAG-1 show that acceptable results may be obtained for argillaceous materials and, in addition, adds to the limited data base on these materials (compared to the 'traditional'

Table 2.10 Uranium, thorium and potassium results for selected USGS standards following long irradiation

	URANIUM (ppm)		THORIUM (ppm)		POTASSIUM OXIDE (%)	
	This work	Recommended	This work	Recommended	This work	Recommended
GSP-1	1.87 ± .51	1.96 (a) 2.56 ± .13 (b)	110 ± 3	104 (a) 106.9 ± 2.1 (b) 114.6 (c)	5.11 ± .24	5.53 (a)
AGV-1	2.17 ± .46	1.88 (a) 2.05 ± .08 (b)	5.93 ± .24	6.41 (a) 5.37 ± 1.07 (b) 6.44 (c)	2.52 ± .34	2.89 (a)
BCR-1	1.81 ± .45	1.74 (a) 1.81 ± .09 (b)	7.05 ± 1.17	6.0 (a) 5.26 ± .89 (b) 6.12 (c)	1.56 ± .26	1.70 (a)
W-1	0.78 ± .15	0.58 (a)	2.39 ± .13	2.42 (a)	0.61 ± .06	0.64 (a)

(a) Flanagan (1976)
(b) Millard (1976)
(c) Potts et al. (1981)

Table 2.11 Short INAA results for USGS Cody Shale (SCo-1)

Element /Oxide	This work (± 1 std.dev.)	Literature values†
Al_2O_3	13.71 ± 0.12	13.80±0.13[1],13.6[8]
MgO	2.59 ± 0.16	2.32±0.05[1],2.60±0.02[2],2.6[8]
CaO	2.63 ± 0.10	2.56±0.01[1],2.63[7]
Na_2O	0.92 ± 0.04	0.78±0.05[1],0.918±0.008[2],0.9[8],0.857[7]
K_2O	2.78 ± 0.12	2.65±0.04[1],2.675±0.017[2],2.7[8],1.795[7]
TiO_2	0.54 ± 0.04	0.61±0.01[1],0.64[8],0.544[2]
Ba	588 ± 9	622±19[1],474±82[3],560[8],544[7];598[4]
Cl	46 ± 9	68±9[1]
Co	8.8 ± 0.7	9.66±0.36[3]
Cs	8.3 ± 1.5	6.82±0.68[3],8.85[4]
Dy	3.47 ± 0.04	4.21±0.13[6],3.79[4],3.50[7],4.7[5]
Eu	1.13 ± 0.04	1.24±0.06[3],1.02±0.02[6],1.16[5],1.03[4]
In	0.05 ± 0.01	--------------
Mn	380 ± 16	398±5[2],381[7]
Sm	5.11 ± 0.18	5.13±0.14[6],5.40[5],5.07[4]
Sr	191 ± 19	153±5[2],193±2[1],<200[7],175[8]
U	3.36 ± 0.07	3.15±0.09[9],2.49[4]
V	132 ± 3	138±2[2],128[7],115[8]

(Major oxides in weight percent, trace elements in ppm.)

† References.

[1] Fabbi and Espos (1976)   [2] Thomas *et al*. (1976)
[3] Katz and Grossman (1976)   [4] McLennan and Taylor (1980)
[5] Potts *et al*. (1981)   [6] Kosiewicz *et al*. (1974)
[7] Chattopadhyay and Katz (1978)

(references continued on table 2.11)

Table 2.12 Short INAA results for USGS Green River Shale (SGR-1)

Element /Oxide	This work (± 1 std.dev.)	Literature values
Al_2O_3	6.60 ± 0.06	7.24±0.26[1],6.5[8]
MgO	4.05 ± 0.14	4.50±0.35[1],4.32±0.02[2],4.5[8]
CaO	8.62 ± 0.16	8.37±0.10[1]
Na_2O	3.19 ± 0.08	2.66±0.06[1],3.03±0.01[2],3.0[8]
K_2O	1.66 ± 0.05	1.71±0.05[1],1.60±0.01[2],1.6[8]
TiO_2	0.40 ± 0.03	0.36±0.01[1],0.26[8]
Ba	308 ± 12	328±8[1],225±120[3],278[4]
Cl	39 ± 27	44±4[1]
Co	9.4 ± 1.0	10.3±0.5[3],12.0[5]
Cs	4.7 ± 1.6	4.61±0.36[3],5.16[4]
Dy	1.84 ± 0.05	1.77[4],2.0[5]
Eu	0.52 ± 0.04	0.52±0.07[3],0.50[4],0.50[5]
In	n.d.	-------------
Mn	250 ± 8	251±1[2],232[8]
Sm	2.73 ± 0.20	2.66±[4],3.0[5]
Sr	397 ± 24	445±6[1],332±10[1]
U	5.66 ± 0.09	5.60±0.17[9],4.85[4]
V	130 ± 3	134±3[1]

(Major oxides in weight percent, trace elements in ppm.)

contd. from table 2.10
[8] Abbey (1980)
[9] Millard (1976)
[10] Brunfelt and Steinnes (1978)
[11] Flanagan (1976)
[12] Baedecker *et al*. (1977)
[13] Brenner and Harel (1976)

Table 2.13 Short INAA results for USGS marine mud (MAG-1)

Element /Oxide	This work (± 1 std.dev.)	Literature values
Al_2O_3	16.35 ± 0.12	16.77±0.24[1],16.4[6]
MgO	3.10 ± 0.17	3.00±0.03[2],2.83±0.01[1],3.0[6]
CaO	1.24 ± 0.28	1.42±0.03[1],1.35[6]
Na_2O	3.88 ± 0.11	3.43±0.04[1],3.792±0.026[2],3.8[6]
K_2O	3.36 ± 0.12	3.57±0.02[1],3.528±0.011[2],3.6[6]
TiO_2	0.75 ± 0.05	0.75±0.01[1],0.73[6]
Ba	551 ± 38	513±8[1],311±78[3],453[4]
Cl	3.13 ± 0.04	3.127±0.057[1]
Co	21.3 ± 3.0	18.8±0.14[3],20.6[5]
Cs	9 ± 6	9.49[4]
Dy	5.24 ± 0.10	5.02[4],5.5[5]
Eu	1.32 ± 0.10	1.64±0.06[3],1.47[4],1.43[5]
In	n.d.	------------
Mn	746 ± 23	713±7[2],775[6]
Sm	7.31 ± 0.49	7.96[4],7.22[5]
Sr	109 ± 50	167±3[1],173±1[2]
U	2.22 ± 0.17	2.82±0.11[9],2.38[4]
V	142 ± 4	142±2[1]

(Major oxides and Cl in weight percent,
trace elements in ppm.)

Table 2.14 Short INAA results for USGS Dunite (DTS-1)

Element /Oxide	This work (± 1 std.dev.)	Literature values
Al_2O_3	0.29 ± 0.02†	0.25[8]
MgO	48.5 ± 0.9	49.8[8]
CaO	n.d.	0.14[8]
Na_2O	n.d.	0.01[8]
K_2O	n.d.	0.00[8]
TiO_2	n.d.	----
Ba	n.d.	5[8]
Cl	n.d.	11[8],9.4[10]
Co	150 ± 3	122[3],140[10]
Cs	n.d.	0.006[8]
Dy	n.d.	----
Eu	n.d.	----
In	n.d.	0.0025[8]
Mn	923 ± 27	929[8]
Sm	n.d.	----
Sr	n.d.	----
U	n.d.	----
V	9.9 ± 1.2	11[8]

(Major oxides in weight percent, trace elements in ppm.)
† corrected for ^{28}Si(n,p)^{28}Al interference.

Table 2.15 Short INAA results for USGS Granodiorite (GSP-1)

Element /Oxide	This work (± 1 std.dev.)	Literature values
Al_2O_3	15.26 ± 0.18	15.25[11],15.28[8]
MgO	0.91 ± 0.08	0.96[11],0.97[8]
CaO	2.10 ± 0.10	2.02[11],2.03[8]
Na_2O	2.85 ± 0.07	2.80[11],2.81[8]
K_2O	5.50 ± 0.06	5.53[11],5.51[8]
TiO_2	0.66 ± 0.04	0.66[11],0.66[8]
Ba	1300 ± 20	1300[8],1190[10]
Cl	331 ± 14	300[11],311[10]
Co	3.0 ± 1.0	6.4[11],7.8[8],6.4[10]
Cs	n.d.	1.0[11],0.96[10]
Dy	5.60 ± 0.08	5.40[11]
Eu	2.57 ± 0.06	2.80±0.07[3],2.4[11]
In	n.d.	-----------
Mn	317 ± 11	331[11]
Sm	26.1 ± 0.2	25.2[10],27.1[11]
Sr	225 ± 24	240[8],193[10],233[11]
U	2.61 ± 0.07	2.56±0.09[9],2.1[8],1.96[11]
V	51.7 ± 2.9	52.9[11]

(Major oxides in weight percent, trace elements in ppm.)

standards).

The four minute irradiation results obtained for the Exshaw Shale samples are tabulated in Appendix 1 together with the results of the long irradiation scheme.

Results of 2 hour irradiation of standards rocks

Following the 2 hour irradiation at full power, element concentrations were determined via a variant of the 'absolute method' of activation analysis. This method normally requires the determination of the neutron flux and its distribution via a flux monitor(s), irradiated simultaneously with samples. This, as is apparent from the earlier discussions on the SLOWPOKE II reactor, is unnecessary as it has been shown by various workers that the neutron flux of the SLOWPOKE reactor is both stable and reproducible over extended periods of time. With the knowledge of the neutron flux, the mass (and hence concentration) of an unknown element may be determined from the activation analysis equation (page 5). Although in most cases precise, the method is often inaccurate due to uncertainties in the nuclear and isotopic data (e.g. half-life, cross section etc.). Analysis of the USGS rock standards GSP-1, AGV-1, BCR-1, PCC-1 and DTS-1 showed this to be the case for a number of elements. Consequently, in a manner similiar to that employed by Potts _et_ _al_. (1981) correction factors, based on the average discrepancy between the 'found' and recommended values for the standards, were calculated. To test the method with corrections, samples of the old USGS rock standard W-1, and two of the new standards SCo-1 and SGR-1, were analyzed.[18] The results obtained are reported in tables 2.16 to 2.18 and as with the other standards, recommended and published values are given for comparison. In practically every case there is very good agreement between the results of this work and those of other workers.

Using these correction factors therefore, the Exshaw Shale results following the long irradiation, were corrected. These results are tabulated in Appendix 1 together with the short irradiation results.

2.7 EPITHERMAL NAA

2.7.1 Introduction

As mentioned in an earlier section, the effective or reactor cross-section for any particular (n,γ) reaction is made up of two components. These being the thermal neutron cross-section σ, and the resonance integral I_0 (see page 7). With increasing neutron energy the majority of (n,γ) reactions follow the so-called '1/V law', that is, the thermal cross-section is inversely proportional to the velocity (and therefore energy) of the incident neutrons. Examples of such reactions include $^{27}Al(n,\gamma)^{28}Al$, $^{23}Na(n,\gamma)^{24}Na$ and $^{55}Mn(n,\gamma)^{56}Mn$. Certain isotopes however, with large I_0/σ ratios, are preferentially activated by the

---

[18] These samples were not included when calculating the 'correction' factors.

Table 2.16 Results following 2 hour irradiation of USGS Cody Shale (SCo-1)

Element /Oxide	This work (± 1 std.dev.)	Literature† values
Fe_2O_3	5.32 ± 0.24	$5.23\pm0.04^{1},5.1^{8},5.34^{12}$
Na_2O	0.923 ± 0.016	$0.78\pm0.05^{1},0.918\pm0.008^{2},0.9^{8},0.857^{7}$
K_2O	2.53 ± 0.07	$2.65\pm0.04^{1},2.675\pm0.017^{2},2.7^{8},1.795^{7}$
As	13.7 ± 0.6	10.8 ± 2.6^{1}
Ba	572 ± 46	$622\pm19^{1},474\pm82^{3},593^{12}$
Co	10.7 ± 0.2	$9.66\pm0.19^{3},11.7^{12}$
Cr	75.5 ± 4.5	$75.3\pm4.4^{3},65.2\pm8.1^{13}$
Cs	6.62 ± 0.21	$6.82\pm0.66^{3},7.56^{12}$
Ga	15.8 ± 3.4	13.9 ± 2.5^{13}
Hf	3.9 ± 0.4	$4.38\pm0.29^{3},4.27^{12}$
Rb	111 ± 15	$122\pm1^{1},68.9\pm15.9^{3},113^{12}$
Sb	2.59 ± 0.26	$2.40\pm0.22^{3},2.51^{12}$
Sc	12.3 ± 1.5	$19.3\pm2.1^{1},11.4\pm0.4^{3},11.1^{12}$
Ta	0.98 ± 0.07	$0.56\pm0.03^{3},0.98^{12}$
Th	9.75 ± 0.13	$10.5\pm0.4^{3},9.52\pm0.95^{9},9.64^{12}$
U	2.72 ± 0.17	$3.15\pm0.09^{9},2.49^{4}$
La	29.7 ± 0.5	$29.7^{4},30.3^{5},29.2^{6}$
Ce	65.5 ± 0.6	$62.1\pm4.7^{3},63.4^{4},60.1^{5},64.8^{12}$
Eu	1.16 ± 0.06	$1.24\pm0.06^{3},1.03^{4},1.16^{5},1.24^{12}$
Tb	0.69 ± 0.06	$0.78\pm0.02^{3},0.64^{4},0.75^{5},0.73^{12}$
Yb	2.45 ± 0.20	$2.25^{4},2.43^{5},2.33^{6},2.86^{12}$
Lu	0.32 ± 0.03	$0.34^{4},0.35^{5},0.37^{6}$

(Major oxides in weight percent, trace elements in ppm.)
† references as in tables 2.10 to 2.14.

Table 2.17 Results following 2 hour irradiation of USGS Green River Shale (SGR-1)

Element /Oxide	This work (± 1 std.dev.)	Literature values
Fe_2O_3	3.32 ± 0.15	3.20±0.06[1],3.2[8],3.20[12]
Na_2O	3.08 ± 0.05	2.66±0.06[1],3.0[8]
K_2O	1.75 ± 0.09	1.71±0.05[1],1.6[8]
As	70.7 ± 1.1	74.5±0.9[1]
Ba	363 ± 33	328±8[1],225±120[3],278[4],323[12]
Co	11.4 ± 0.2	10.3±0.5[3],12.8[12],12.0[5]
Cr	34.6 ± 2.3	32.5±3.2[3]
Cs	4.01 ± 0.12	4.61±0.36[3],5.32[12],5.16[4]
Ga	n.d.	----------
Hf	1.13 ± 0.13	1.31±0.26[3],1.36[12],1.43[4]
Rb	78 ± 11	92±1[1],66.5±9.1[3],82[12]
Sb	3.68 ± 0.37	3.05±0.36[3],3.00[12]
Sc	5.54 ± 0.66	4.78±0.19[3],5.02[12]
Ta	0.48 ± 0.05	0.22±0.05[3],0.52[12],0.4[6]
Th	5.36 ± 0.10	4.86±0.23[3],7.66±1.68[9],4.91[12]
U	4.66 ± 0.29	5.60[9],4.55[4],5.60[12]
La	18.4 ± 0.6	20.5[4],20.5[5]
Ce	37.1 ± 0.4	31.2±2.2[1],38.1[4],35.6[5],41.6[12]
Eu	0.56 ± 0.03	0.52±0.07[3],0.50[4],0.50[5],0.52[12]
Tb	n.d.	0.33[4],0.33[5],0.34±0.14[3],0.35[12]
Yb	n.d.	0.97[4],0.98[5]
Lu	0.17 ± 0.03	0.15[4],0.14[5]

(Major oxides in weight percent, trace elements in ppm.)
references as in tables 2.10 to 2.14

Table 2.18 Results following 2 hour irradiation of USGS Diabase (W1)

Element /Oxide	This work (± 1 std.dev.)	Literature values
Fe_2O_3	11.6 ± 0.32	11.11[8],10.66[8]
Na_2O	2.157 ± 0.037	2.15[8]
K_2O	0.61 ± 0.06	0.64[8]
As	n.d.	1.9[8],2.22[19]
Ba	134 ± 47	160[8],187[10],146[11]
Co	43.6 ± 0.2	41.0±0.3[3],46.0[11],44.5[10]
Cr	131 ± 8	102±3[3],110[11],115[10]
Cs	1.09 ± 0.18	0.63±0.46[3],0.91[10],0.97[10]
Ga	23.7 ± 5.5	18.4[10],16[8]
Hf	1.93 ± 0.23	2.24±0.31[3],2.50[11],2.5[10]
Rb	31 ± 6	20.5[11],21.8[10],21[8]
Sb	1.00 ± 0.13	1.10±0.33[3],1.05[11],0.91[10],1.0[8]
Sc	38.3 ± 4.6	35.4±0.06[3],33.9[11],33.3[10],35[8]
Ta	0.51 ± 0.09	0.68[11],0.42[10],0.5[8]
Th	2.39 ± 0.13	2.67±0.27[3],2.50[11],2.1[10],2.4[8]
U	0.78 ± 0.15	0.59[11]
La	10.0 ± 0.2	10[10],9.8[8]
Ce	22.0 ± 0.5	23[10],22.0[11],23[8]
Eu	1.14 ± 0.06	1.18±0.08[3],1.08[11],1.2[10],1.1[8]
Tb	n.d.	0.92±0.13[3],0.65[8],0.68[11],0.64[10]
Yb	n.d.	2.1[8],2.3[10]
Lu	0.43 ± 0.03	0.35[10]

(Major oxides in weight percent, trace elements in ppm.)
references as in tables 2.10 to 2.14

higher energy neutrons in the epithermal or resonance neutron range. By 'filtering out' the thermal neutrons, so that only the epithermal and fast neutrons may activate the sample, one may preferentially enhance the signal-to-background ratio of those isotopes that have large resonance integrals over those which follow the 1/V law. This method or technique is known epithermal neutron activation analysis (ENAA) and may be used advantageously in certain instances as it:-

1). lowers the detection limits for those elements which have isotopes with major resonance peaks (e.g. U and Th, see Gladney et al. (1978) and certain REE, Baedecker et al. (1977)) by reducing the background due to the major Compton producing isotopes e.g. ^{28}Al, ^{24}Na, ^{56}Mn and ^{46}Sc (common constituents of many geological materials). .

2). reduces the sample activity which:

    a) makes post-irradiation handling safer.

    b) results in shorter decay times being necessary following irradiation.

    c) allows for more sample to be irradiated if necessary (which allows a more representative sample to be taken and thus lowers the detection limit for many elements).

    d) reduces corrections resulting from highly active samples (e.g. pulse pile-up and dead-time corrections).

3). reduces the ^{235}U (n,f) interference to certain isotopes e.g. ^{99}Mo, ^{139}Ba and some of the REE.

2.7.2 Previous work

Due to their very large thermal neutron absorption cross-sections, cadmium and boron have been utilized by a number of workers in ENAA (see Steinnes (1970), Bem and Ryan (1981), Ehmann et al. (1980) and Stuart and Ryan (1981)). The cross cross-sections for ^{113}Cd and ^{10}B plotted against neutron energy are shown in figure 2.6. At approximately 0.2 eV ^{113}Cd has an absorption cross-section of about 8,000 b. Above this it falls off rapidly to <10 b between 1 and 10 eV. This abrupt change is known as the 'cadmium cut-off'. Boron-10 on the other hand rigidly follows the 1/V law. At first sight cadmium appears an ideal thermal neutron filter for ENAA. Unfortunately however, the metal is toxic, thus fabrication of shields must be carried out with care. In addition, upon irradiation Cd produces a number of radioisotopes. One of the radioproducts, ^{115}Cd (T1/2=53.5 hrs), has a high specific activity which makes handling of a shield soon after a long irradiation undesirable. Conversely, ^{10}B activates via the reaction $^{10}B(n,\alpha)^{7}Li$ producing stable nuclei (see under DNC) resulting in a minimum of shield produced radioactivity. In addition, by varying the B_4C wall thickness one can control the neutron energy cut-off as ^{10}B follows the 1/V law. As a result there has been recently been a number of publications regarding ENAA utilizing boron as a thermal neutron filter (e.g. Bem

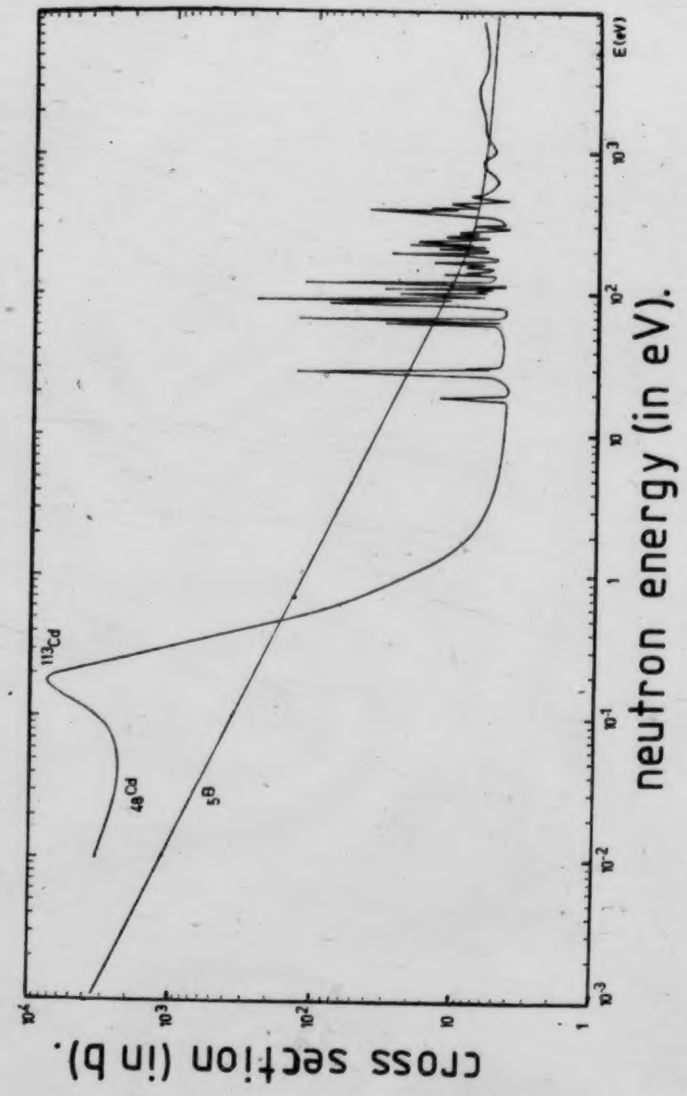

(source De Soete et al., 1972)

Figure 2.6 Cd and B cross-section variation with neutron energy

and Ryan (1980), and Stuart and Ryan (1981)). None of these workers apply ENAA to the analysis of geological samples however. In both these works, shields were fabricated by mixing B$_4$C with paraffin wax for both the outer and inner sites of a SLOWPOKE reactor respectively.

2.7.3 Experimentation and results

Following the work of Bem and Ryan(1981) B$_4$C shields were made for the outer site of the University of Alberta SLOWPOKE reactor. The 4 mm thick walls of the B$_4$C saturated paraffin wax shields have a cut-off energy of about 10 eV (Rossitto _et_ _al_. 1972, Stuart and Ryan 1981). To access the effectivness of the shields a 277.4 mg aliquot of the USGS standard AGV-1 was irradiated behind a shield for 10 minutes at maximum flux (5.0 x 10^{11}n cm^{-2} s^{-1}) in the outer site. Following a decay period of 20 minutes the sample was counted for 600 seconds livetime at 1 cm geometry on the Win ^{15} Ge(Li) detector. Figure 2.7 shows a segment of the obtained spectrum with the major peaks identified. For comparison, a plot of a spectrum obtained from the unshielded irradiation of an 88.0 mg aliquot of AGV-1 is shown in figure 2.8. This sample was irradiated for 4 minutes at 2.5 x 10^{11}n cm^{-2} s^{-1} in site 1 of the reactor. Following irradiation, except for a slightly longer decay time for the INAA work (30 minutes vs. 20 minutes) the geometry, detector, and counting periods utilized were identical to those employed in the ENAA of the larger

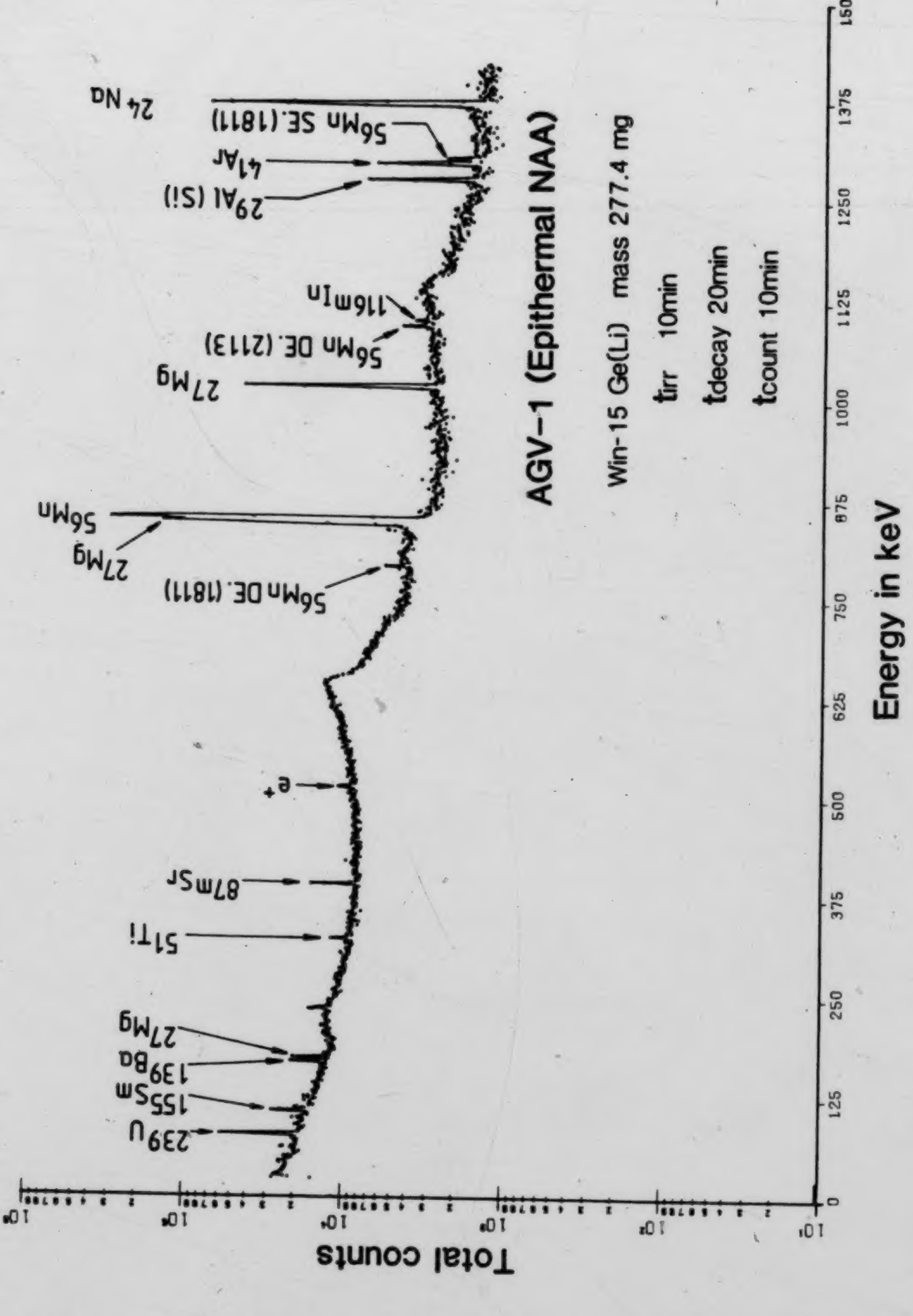

Figure 2.7 The γ-ray spectrum of USGS andesite AGV-1 following ENAA

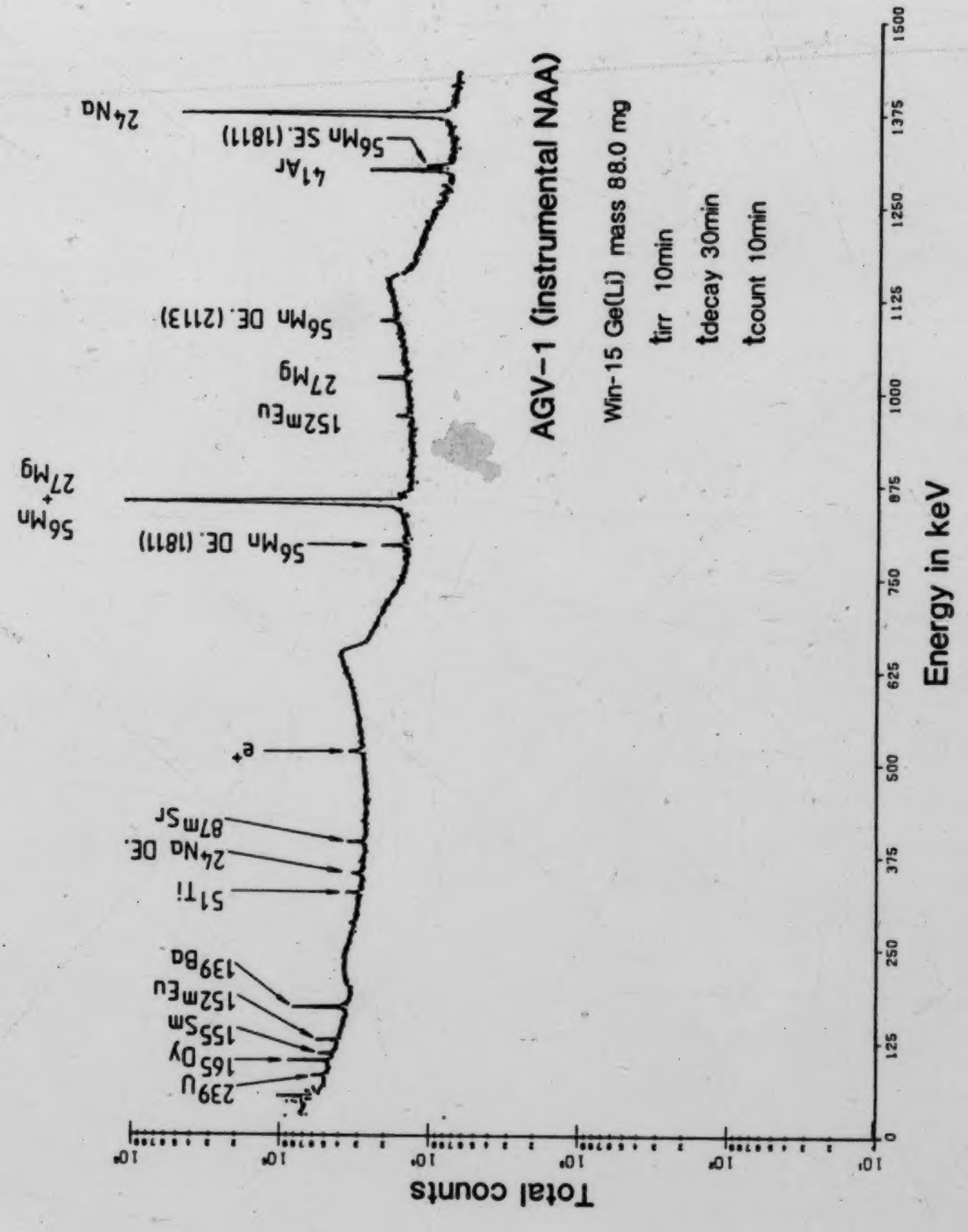

Figure 2.8 The γ-ray spectrum of USGS andesite AGV-1 following INAA

sample. Table 2.19 lists the area, background and % error of a number of identified peaks, taken from the peak search output of each analysis. From the tabulation it can be seen that the ENAA shows a clear advantage over INAA in the analysis of U, Sr and Si (via ^{28}Al). There is also a decrease in the uncertainty of the photopeak area determination of Co and Sm, due to the reduction of the background component. Note that the photopeaks of ^{24}Na are reduced by a factor of approximately 6, while ^{56}Mn and ^{41}Ar are lowered by a factor of approximately 4. In addition to the benefits of increased sensitivity for some elements due to background reduction, corrections for pulse pile-up and dead-time effects, with their associated uncertainties, are reduced.

For example, following ENAA the sample gave a spectrometer busy time of 6.15 % as opposed to the 21.76 % busy of the INAA irradiation of the 88.0 mg sample.

It should be noted that there is an increase in the areas of the 843 and 1014 keV photopeaks of ^{27}Mg even though the ^{26}Mg (n,γ) ^{27}Mg reaction follows the '1/V law'. This is the result of the larger sample mass, which, due to the increased amount of Al, leads to an increase in the production of ^{27}Mg via the transmutation reaction ^{27}Al(n,p)^{27}Mg.[11]

---

[11] Using the 'IF factors' discussed earlier the production of ^{27}Mg via the reaction ^{30}Si(n,α)^{27}Mg may be considered negligible.

Table 2.19 Comparison of instrumental and epithermal NAA of AGV-1

		INAA. of AGV-1			ENAA. of AGV-1		
Isotope	keV	Area	Background	%Error	Area	Background	%Error
^{60m}Co	58	1414	25271	16.1	1043	13134	15.8
^{239}U	75	2503	28574	9.8	9007	18365	2.4
^{165}Dy	95	8454	40586	3.5	632	10061	22.8
^{155}Sm	104	2832	29885	8.8	2664	15433	6.9
^{152m}Eu	122	3594	28035	6.8	685	9931	20.9
^{139}Ba	166	9719	32184	2.8	1692	3635	5.6
^{87m}Sr	388	1971	21604	10.8	1953	7088	6.5
^{27}Mg	1014	2368	14790	7.5	12343	3471	1.1
^{29}Al	1273	163	5506	64.9	1860	1881	4.0
^{41}Ar	1294	6316	3779	1.9	1723	845	3.4
^{24}Na	1368	164382	12990	0.3	22971	2239	0.7
^{42}K	1524	2989	7992	4.6	524	1860	12.4
^{56}Mn	1811	41947	10646	0.6	10452	1792	1.1
^{24}Na	1732	15654	7774	1.1	2258	1496	3.2
^{56}Mn	2114	19331	7320	1.0	4753	1555	1.9
^{24}Na	2243	14791	10280	1.3	1984	1639	3.7
^{24}Na	2754	81092	3653	0.4	11111	385	1.0
^{49}Ca	3084	945	1331	6.1	213	194	11.5

The readers attention is drawn to the increased size of the ^{28}Al photopeak (produced via the reaction ^{28}Si(n,p)^{28}Al) following ENAA. The analysis of Si in geological samples via this method has, suprisingly enough (considering the importance of this element to the geologist) recieved little attention. This may be due to the short-lived nature of ^{28}Al, or because SiO_2 is routinely determined by XRF. This author knows of only one example in the literature where Si has been determined in a 'geological-like' matrix (pot shards) using the isotope ^{28}Al (Hancock 1982).

There are however disadvantages associated with the use of the outer site for ENAA. Being further from the core than the inner sites the epithermal component of the flux is reduced, the øth/øepi being 58.1±1.5. A shield the size described contains some 8g of B_4C which, due to the large reactivity of ^{10}B, probably 'draws' the neutron flux, thus rendering the inner sites of little use for conventional NAA while carrying out ENAA in the outer site (unless flux monitors are simultaneously irradiated).[12] At maximum, only two or three geological samples, each 100 mg or so in mass, may be simultaneously irradiated within the shielded central cavity (unless pelletized) thus making analysis of long-lived isotopes relatively expensive.

Stuart and Ryan (1981) used an inner SLOWPOKE site and shield thus utilizing the greater epithermal flux component

---

[12] To date measurement of inner site flux variations during the irradiation of a boron shield have not been made to verify this hypothesis.

(øth/øepi = 16.9±0.8). Their shields would also have rather a high reactivity as they contain some 5g B_4C. Their main drawback is however, that samples must be placed in a central cavity some 6 mm diameter and 45 mm long which requires some delicate sample preparation, permits only one or two samples to be irradiated simultaneously and when counting, presents geometry problems.

In an attempt to determine both uranium and thorium by delayed neutron counting Rosenberg (1981) irradiated samples mixed with and without B_4C powder. From this paper came the idea of mixing B_4C with samples for ENAA.

It was important to determine the effectiveness of the B_4C in reducing the thermal neutron component and to find empirically the optimum B_4C to sample ratio. To this end 25 mg increments of B_4C from 0 to 150 mg were throughly mixed with 150 mg aliquots of a well homogenized coal. The samples were were then analyzed in accordance with the short INAA iradiation scheme. Figure 2.9 shows the effect on the activity of a number of isotopes with the increasing B_4C content. The data are plotted as a percentage of the activity of the respective isotopes in the untreated coal against the mass of B_4C added. The error bars shown take into account the uncertainties in the determination of the photopeak areas in both the untreated and treated coals. Clearly it can be seen that with increasing boron content the activity of the major Compton producing radionuclides, which follow the 1/V law are supressed far more than ^{239}U.

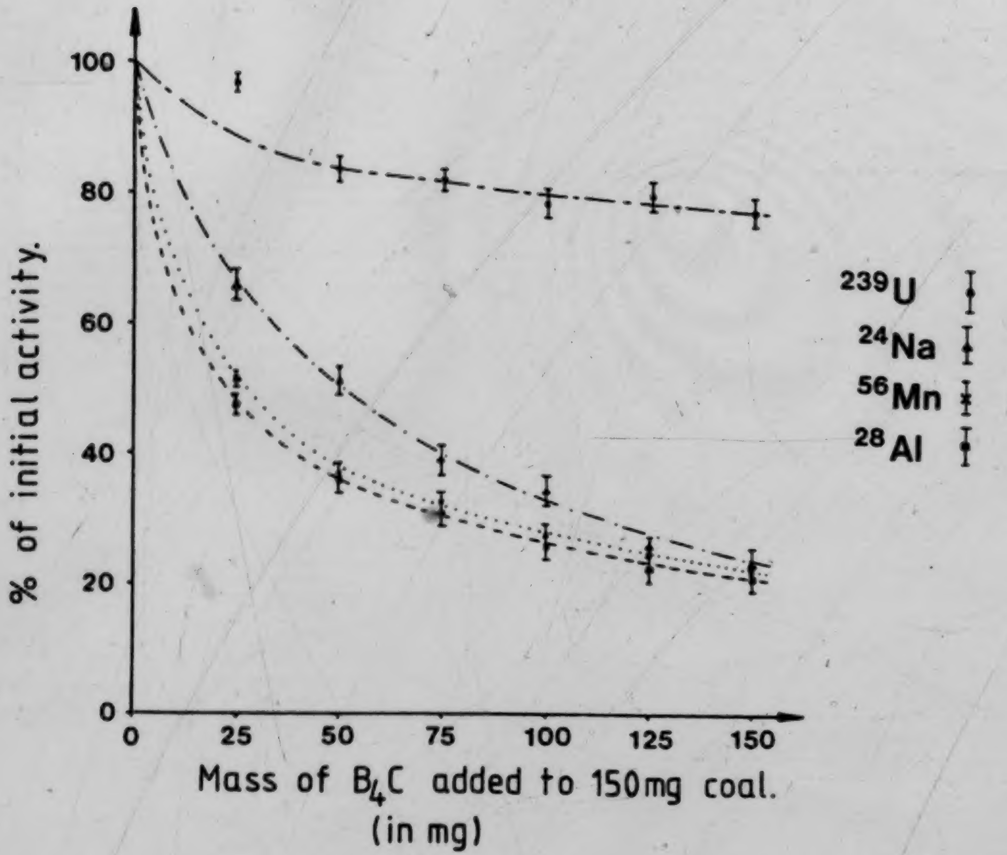

Figure 2.9 Effect of B_4C on the specific activity of selected isotopes

There seems little to be gained by increasing the B_4C to sample ratio above 1:3 (by weight). Further experimentation envolved running 100 mg of shale, 100 mg shale + 30 mg B_4C and 150 mg shale + 30 mg B_4C. When analyzed it was found that the reduction in ^{24}Na and ^{56}Mn activity was greater than in the coal samples at a similar boron to sample ratio. Although this may be attributed to incomplete mixing in the coals, statistical error or that the effectivness of the B_4C is related to its density or packing within the sample rather than weight, it may in part be due to the large percentage of organic carbon making up the coals which might, to a certain extent, thermalize the epithermal neutrons. A similar effect due to the moderating effect of hydrogen in water was found by Reynolds and Mullins (1963). With increasing B_4C (and hence C) content this might also be a problem.

A die was made to pelletize mixed sample and B_4C, producing discs 10 mm in diameter and approximately 1 mm in thickness for irradiation. In this way up to 20-24 samples (100-200 mg each) may be simultaneously irradiated in one of the inner SLOWPOKE sites with only about 600-700 mg B_4C (which is much less than used by Stuart and Ryan *ibid*). In addition, flux monitors of dried Au and Mn solutions, on sealed filter papers, may be placed between samples thus allowing the flux magnitude and distribution to be well monitored. Unfortunately, time did not permit further evaluation of the method.

The extremely well defined geometry of the pellets would reduce errors resulting from non-reproducible counting conditions. This effect is particularly important when using the LEPS detector where small variations in counting geometry are the difference between accurate and reproducible results and unreliable data. For a fuller appreciation of the importance of this effect the reader is refered to the paper by Hoede and Das (1981).

Unfortunately, due to the paucity of time, the preliminary work could not be followed up and consequently a number of questions still remain unanswered, these include:-

1) is it mixing by weight or by volume that controls the effectivness of the B_4C ?

2) once pelletized, will the increased packing of the B_4C result in a more effective thermal neutron absorber?

3) what are the advantage factors for the longer lived radioisotopes (particularly the rare earth elements)?

3. Fission Track Analysis

3.1 Introduction

Quantitative uranium measurements by fission track analysis (FTA) have been reported and the method discussed previously by a number of workers including Price and Walker (1963), Fleischer and Price (1964) and Fisher (1970). The method has a number of attractive features including its sensitivity, low cost and the variety of samples that may be analyzed. Full appreciation of this latter point can be found in Fisher (1975).

3.2 Theoretical principles

When a sample is irradiated in a nuclear reactor, the mixed neutron flux may induce (n,f) reactions (fission) in any heavy ($Z \geq 90$) nuclei present. There are however only three major naturally occurring fissionable isotopes, ^{238}U, ^{235}U and ^{232}Th. Of the three, only ^{235}U undergoes fission in a dominantly thermal flux. This is due to the large thermal fission cross-section of ^{235}U (577b) compared to the thermal fission cross sections of ^{238}U and ^{232}Th (less than 0.5 and 0.2 mb respectively, Lederer *et al.* (1978)).

When ^{235}U fissions, two highly energetic nuclei are produced with masses bimodally distributed about A=95 and 139 (see figure 2.5). In addition to these two large fragments, on average, two to three 'prompt' neutrons are also emitted. The fission fragments produced recoil in essentially opposite directions to conserve both energy and momentum. The fragments may be recorded by placing a suitable detector in intimate contact (due to the short range of the fission products) with the sample prior to irradiation. The fission fragments create damage trails or tracks of atomic proportions in the detector. After removal from the reactor and upon etching with a suitable reagent, the tracks or dislocations are enhanced to the point where they may be examined with an ordinary optical microscope.

3.3 Sample Preparation and Analysis.

Fission track studies of polished thin sections (Kleeman and Lovering, 1967; Hamilton, 1966 and Duke et al. 1980) have shown that uranium is invariably heterogeneously distributed throughout many rock forming phases. While this is useful for mapping the spatial distribution of uranium, samples must first be homogenized for whole rock quantitative analysis. Following the work of Fisher (1970) and Nishimura (1970) the samples of this study were first crushed to pass through a -120 mesh sieve and then throughly mixed.

Sample aliquots 10-20 mg each, with rims and backing of cellulose powder, were pressed at approximately 1000 kg cm^{-2} (c.14000 lbs in^{-2}) into discs 25 mm in diameter and about 1 mm thick. Each sample had an exposed surface area of approximately 50 mm^2. With care, to avoid contamination, it is possible to pelletize three or four samples on the face of a disc.

Lexan plastic discs were placed in contact with the samples and held firmly in place with scotch tape. NBL-, NBS- and USGS- standard materials were similarly prepared to the unknowns and the discs stacked in polyethelene capsules 54 mm long with an inside diameter of 29 mm.

All irradiations were carried out at the University of Alberta using the SLOWPOKE II reactor. The large outer site of the reactor, with a maximum thermal neutron flux of 5 x 10^{11} n cm^{-2} s^{-1} was used for the majority of irradiations.

After irradiation the samples were allowed to 'cool' for three or four days to allow the ^{24}Na activity to decay to acceptable handling levels. Upon separation the Lexan discs were washed in water and then etched in a 6.25 N NaOH solution at 50°C for 20 minutes (Fisher,1970). The solution was held at a constant temperature by a thermostatically controlled dry bath. This was found to be important as over etching results in damage to the polycarbonate plastic which makes track recognition difficult. Once etched the detectors were washed in distilled water and let dry.

The track densities of the samples were calculated using an ordinary optical microscope in transmitted light at 500x magnification (40x objective, 12.5x ocular) together with a graticule and point counter.

The weight fraction of uranium C, in a sample is given by:

$$C = f.M.d \,/\, \theta.\phi.t.\sigma.N.R.\rho.\epsilon$$

Where:

f = geometry factor (c.1 for fission tracks)
M = molecular weight of uranium (238.98)
d = track density observed
θ = isotopic abundance of ^{235}U (0.72%)
ϕ = thermal flux
t = irradiation time
σ = fission cross section of ^{235}U (577b)
N = Avogadros Number
R = range of fission fragments
ρ = density of material
ϵ = efficiency of detector in registering tracks
C = weight fraction of uranium

(Price and Walker, 1963; Fleischer and Price, 1964).

Determining all of the components in the above equation would make absolute uranium analysis by FTA extremely tedious. This is circumvented by applying a comparator technique similar in many ways to that used in INAA. This is achieved by ratioing the track densities of unknowns with those of standards irradiated and etched at the same time as the samples (Fisher, 1970). This allows the cancelling of many of the components allowing uranium to be determined by:-

$$C(u) = \frac{d(u)}{d(std)} \cdot \frac{I(u)}{I(std)} \times C(std) \quad \text{ppm U}$$

Where:

$C(u)$ = concentration of uranium in unknown
$C(std)$= concentration of uranium in standard
$d\ (u)$ = track density of unknown
$d(std)$= track density of standard
$I\ (u)$ = Isotopic abundance of ^{235}U in unknown
$I(std)$= isotopic abundance of ^{235}U in standard

If we assume a constant isotopic ratio for ^{238}U/^{235}U, the uranium content of the unknown is given by:

$$C(u) = \frac{d(u)}{d(std)} \times C(std)$$

The track densities were calculated by counting ten randomly selected, equal areas and taking their mean value. The standard error of the means of the known and unknown samples were calculated and the total error or uncertainty in the uranium being the square of the sum of squares of these two errors.

The total uncertainty is largely controlled by the known and unknown standard deviations which in turn reflect the spread of the data points about their respective means. Consequently, assuming a statistically significant number of tracks produced (which is proportional to the integrated neutron flux) and counted, the precision of the method is largely controlled by how well homogenized the samples are. Where results with a precision consistently ≤±5 % are required, standard glasses are available for comparison (supplied by the U.S. National Bureau Of Standards in four concentrations : 461 ppm, 37.4 ppm, 0.82 ppm and 0.072 ppm U).[13]

---

[13] There is however some doubt regarding the homogeneity of the uranium distribution in the 0.072 ppm U standard (Fisher,1975 p.295)

3.4 Results

Twenty Exshaw Shale samples were prepared and analyzed by FTA. As can be seen from a comparison of the results of the various methods of uranium analysis given in table 7.1 FTA is sufficiently accurate for the routine analysis of uranium in geological materials. The method does not suffer any major matrix effects, and is very sensitive. The results are however, rather imprecise. This is largely a consequence of heterogeneities found in the NBL-81A (20 ppm U) comparator standard used, as exemplified by fission track 'stars' in the detectors. Similar stars were observed in some of the Exshaw Shales, particularly those with higher than average uranium concentrations. Use of the NBS-glasses would avoid this problem.

Theoretically, if the material used to register the fission tracks has an extremely low U concentration then DNC is one of the most sensitive metods available for uranium analysis. The method requires very little sample and may be applied over 5 to 6 orders of magnitude of uranium concentration.

4. Delayed Neutron Counting.

4.1 Introduction

Approximately 110 samples (including replicates) were analyzed for uranium by delayed neutron counting (DNC) at McMaster Nuclear Reactor (MNR) and later at the SLOWPOKE reactor. Only a short review of the principles will be given here and the reader is referred to Amiel (1962), Gale (1967) and Boulanger *et al*. (1975) for a more complete discussion of the theory and practice of DNC.

4.2 Theory

As noted when discussing the principles behind fission track analysis, it was pointed out that fission of ^{235}U is selectively induced by thermal neutrons when a sample is irradiated in a nuclear reactor. The fission fragments produced are unstable and decay with relatively short half-lives (maximum of approximately 55 s) with the emission of β^--particles. In some of these decays (1.58% Keepin *et al.* (1957)) this is followed by the immediate emission of a 'delayed' neutron. These delayed neutrons, unlike the prompt neutrons emitted during the fission event, continue to be emitted after irradiation. The number of delayed neutrons produced is proportional to the amount of ^{235}U present and when counted can provide a rapid, low cost, precise, accurate and extremely sensitive means of uranium analysis. There are however some light radionuclides, produced by fast neutron reactions, which also decay with the emission of delayed neutrons. Of these ^{9}Li (T1/2=0.17 s) and ^{17}N (T1/2=4.17 s) produced in the reactions ^{9}Be(n,p)^{9}Li and ^{17}O(n,p)^{17}N are the most important. The possible interference due to these two isotopes is discussed later.

As it is actually ^{235}U that is determined via DNC, for quantatitive total uranium analyses, it must be assumed that the ^{238}U/^{235}U isotopic ratio is constant. Fortunately, when analyzing geological samples, this is nearly always the case.[14]

Amiel ibid. calculated that there is little to be gained by irradiating a sample for more than one minute. The reasons for this are twofold. Firstly, due to the short half-lives of the neutron emitting fission products, the signal-to-background ratio is not increased significantly by a longer irradiation. Secondly, the induced (n,γ) activity (largely due to ^{28}Al, T1/2 = 2.24 min) may interfere when counting and also presents a potential radiation hazard.

A counting period similar in length to the irradiation time is recommended as it allows the majority of the delayed neutron emissions to occur and be detected. Counting for shorter periods of time (as compared to the irradiation time) increases the sample throughput but reduces the sensitivity of the method. Too long a counting time on the other hand reduces the precision by increasing the background contribution without increasing the net signal significantly.

---

[14] There is only one well documented variation from this situation, at Oklo in Gabon where ^{235}U is depleted due to its natural fission (see Bouzigues et al., 1975).

The delay or 'decay' time chosen must necessarily be at least that taken for the transfer of the sample from the reactor to the counting facility (generally ≤ 3 second). Theoretically it should be kept as short as possible to maximize the sensitivity. In practice however, for a number of reasons, delays of between 10 and 20 seconds are commonly employed. A 20 second delay allows the complete decay of ^{9}Li and a reduction of the ^{17}N interference mentioned previously to 3.6 % of its initial value (a 10 second delay reduces this to 19.0 % of the original value). Furthermore, small variations in the delay time become more significant the shorter the delay time.

At MNR an irradiation:delay:count scheme of 10s:10s:10s at a thermal flux of 3 x 10^{12} n cm^{-2} s^{-1} was employed (written comm E. Hoffman). This does not maximize the sensitivity of the method, but does allow for an hourly throughput of some 100 samples (the prime concern of a commercial outfit). The 10 second irradiation does however, reduce the ^{28}Al activity by more than a factor of five from the activity that would be produced by a one minute irradiation at the same flux.

Because neutrons have no charge, their detection is more difficult than that of charged particles such as electrons or alpha particles. They must therefore generally be detected indirectly. The most popular detectors for registering slow neutrons are enriched BF_3 proportional gas counters. The neutrons interact with the enriched ^{10}B to produce alpha particles and ^{7}Li nuclei via the reaction $^{10}B(n,\alpha)^{7}Li$ (thermal cross-section of 3840 barns). Being positively charged, alpha particles are readily detected when a high voltage is applied across the detector. Due to the extremely large thermal cross-section of the above reaction (and small fast neutron cross-section) maximum detector efficiency only occurs when the higher energy delayed neutrons have been slowed down to thermal energies. This is accomplished by placing the irradiated sample in the centre of an array of BF_3 tubes (8 at MNR) set in paraffin wax or polyethylene. The latter materials, being rich in hydrogen, slow down the delayed neutrons by elastic scattering, thus increasing their chance of detection.

On account of the large reaction cross-section and availibility of enriched boron, the BF_3 detectors are comparatively speaking, highly efficient and well-suited for this application. The voltage pulses generated during the detection of the neutrons are passed through a pre-amplifier and amplifier to a single-channel analyzer (SCA) where they are accumulated. The gross counts at the end of the count interval may be read directly or output to a line printer. Once the system is calibrated against a number of uranium standards of varying concenratations (of known isotopic abundance) samples may be run on a routine basis.

Towards the end of this study a DNC system was built at the University of Alberta SLOWPOKE facility for uranium analysis.

The SLOWPOKE counting system consists of 6 BF_3 tubes (5 cm in diameter 30 cms active length) arranged in a circular array 25 cms in diameter and embedded in paraffin wax. A lead cylinder (8 cms diameter, 25 cms long) was placed coaxially in the middle of the BF_3 tube array to attenuate the gamma photons due predominantly to the short-lived radioisotope ^{28}Al (T1/2=2.24 min). The whole counting system was surrounded by a further 3 cms of borated paraffin wax in an attempt to reduce the external background component.

The BF_3 tubes were connected in parallel and operated at a common high voltage of 2200 V supplied by a Tennelec TC951 HV power supply. Signals were passed through a TC175 preamplifer to a Tennelec TC216 linear amplifer and SCA and on to a TC534 counter and timer. Raw data were printed out on a decwriter via a Tennelec TC588 buffer printout control/interface.

The discriminator bias on the counter/timer was adjusted with the aid of a Canberra Series 30 MCA so that all of the electronic noise and low amplitude pulses produced by the interaction of gamma-rays and the detector tubes were eliminated with only a small reduction in the neutron detector efficiency.

4.3 DNC results

Preliminary measurements, using an irradiation : decay : count scheme of 20:10:20 s, at a flux of 1×10^{12}n cm^{-2} s^{-1} gave a sensitivity of 50.1±1.1 cts μg^{-1} natural uranium. Decision and detection limits (Currie,1968) for uranium are 50 and 120 ppb respectively in a 5g sample.

Analysis of a liquid atomic absorption thorium standard under identical conditions gave a sensitivity for thorium of 0.63±0.03 cts μg^{-1}, that is, 1.25% ± 0.06% that of uranium. As expected, this ratio is in good agreement with the sensitivity ratio of 1.17%±0.05% determined by AECL Commercial Products (see Boulanger *et al*. 1975) who also used a SLOWPOKE reactor (but different irradiation, decay and count times).

Using the Canadian Radioactive Reference Standard BL-1 (U=220±10 ppm; Th=15±1 ppm) as the calibration standard, the accuracy of the method was assessed by analyzing a number of reference standards, the results of which are given in table 4.1.

Table 4.1 DNC uranium results using the SLOWPOKE reactor

Sample ID	Th/U Ratio	U(ppm) (±1 sigma)†	Corrected U (ppm)*	Recommended value
USGS-W1	3.0	0.61±0.05	0.59±0.05	0.58
DL-1	2.0	41.0±1.2	39.9±1.2	41±2
DL-1	2.0	41.0±1.2	39.9±1.1	41±2
NBS 1632a	2.4	10.9±0.4	10.6±0.4	10.2±0.
NBS 1633a	3.5	1.54±0.12	1.48±0.12	1.28±0.12

† results of a single analysis of each standard.
* correcting for the known Th content of the sample.

As can be seen, even without correction for the thorium content of each sample, the uranium results are quite accurate. Following correction, all results, except NBS 1632a, lie within one standard deviation of the recommended uranium values.

The thorium interference need only be considered significant when analyzing samples in which the Th/U ratio is greater than about 5. For such samples, determination of the thorium content, and hence the interference to uranium, should be made. One possible method is to re-irradiate each sample in a predominantly fast neutron flux (see Amiel *ibid.* and Gale *ibid*.). This effect may be seen in figure 4.1 where the uranium results obtained by delayed neutron counting at McMaster Nuclear Reactor are plotted against those obtained at the SLOWPOKE reactor. In general, the values obtained at SLOWPOKE are consistently higher than those from MNR due to the greater øth/øfast at SLOWPOKE (approximately 4.6) compared to the ratio at MNR (14.6 pers. comm. E. Hoffman).

Millard and Keaton (1982) throughly investigated the factors affecting the error in the DNC technique for U and Th analyses and concluded that counting statistics are the major source of uncertainty. Consequently, under the present scheme a concentration of 0.4 ppm uranium in a 5g sample may be determined with a precision of better than ±10% (one sigma).

Replicate analyses of five aliquots of the same sample analyzed using the SLOWPOKE DNC system gave a mean value of

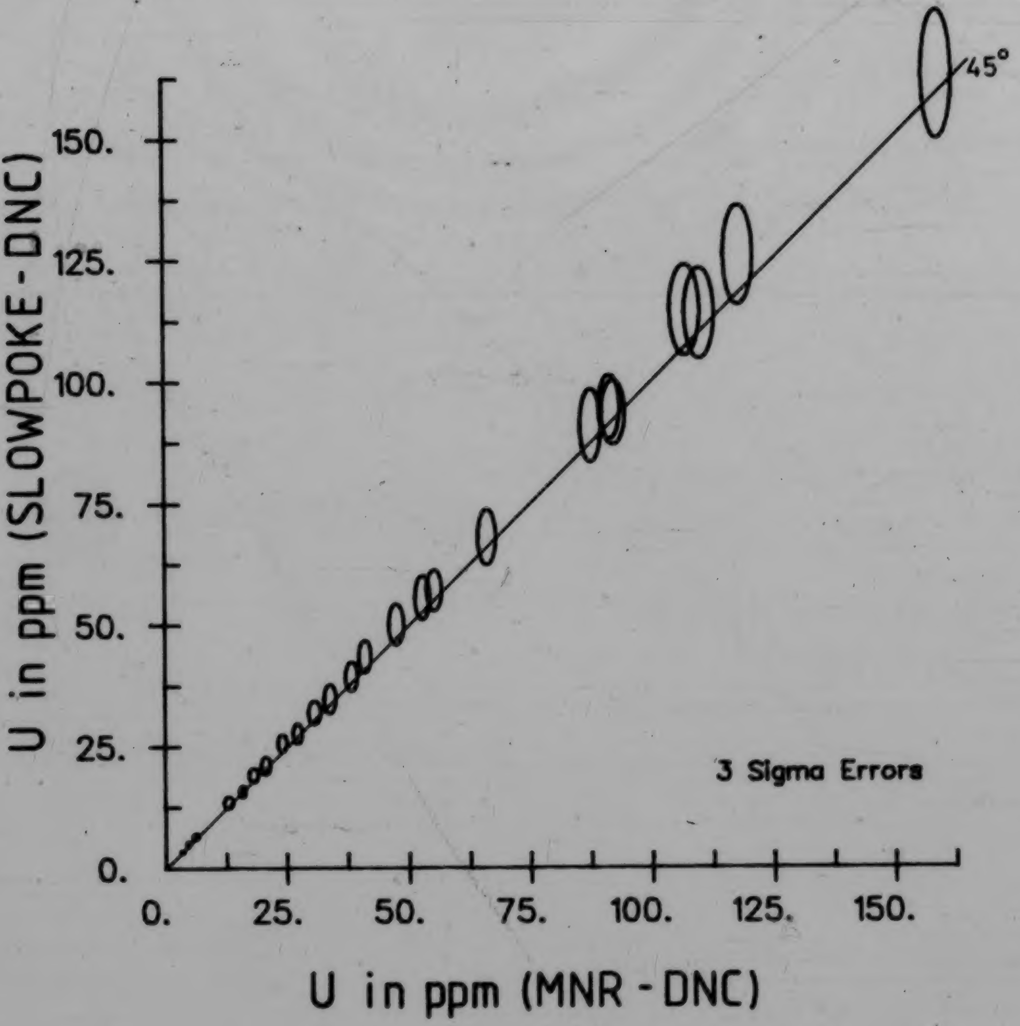

Figure 4.1 Comparison of SLOWPOKE and McMaster reactors DNC uranium results

28.03±0.32 ppm U, 1.15% (N=5, scatter = 1.56 %). The same five samples analyzed at MNR gave a mean value of 27.01±0.15 ppm U, 0.55% (N=5, scatter = 1.10%). Clearly then, as a method of uranium analysis, DNC is extremely reproducible in nature.

With the present irradiation:decay:count scheme it is possible to analyze some 60 samples per hour which, with the operating constraint of 4 hours at maximum flux at the University of Alberta SLOWPOKE reactor allows for some 240 samples to be analyzed per day.

A FORTRAN IV programme was written by the author which given the sample identity, mass and raw counts for each sample and calculates the mass and concentration of uranium together with the total error of the analysis (based on background removal, counting statistics and division by the standard sensitivity).

For an excellent coverage of the potential interferences to the analysis of uranium by DNC the reader is referred to Kunzendorf and Løvborg (1981). They conclude that the method is fast and reliable, and well-suited for the analysis of all kinds of geological samples. In their work they found errors due to variations in timing together with sample preparation negligible and enhancement of fission due to ^{239}Pu or ^{233}U in normal geological samples unlikely. The typical concentrations of B and Cd in geological samples was found to have a negligible effect on the neutron flux. Absorption of thermal neutrons was only found to be a problem when the rare earth elements Sm and Gd were present at concentrations levels of the order of 1000 ppm and then corrections were necessary.

5. Gamma-ray Spectrometry.

5.1 Introduction

Traditionally when analyzing rocks, sediments and soils for uranium and thorium by gamma-spectrometry, only the higher energy gamma emissions of the daughter products are usually utilized as they are more interference-free. Typically uranium has been quantified indirectly using the 1.76 MeV gamma-ray of ^{214}Bi, and thorium indirectly via the 2.62 MeV gamma emission of ^{208}Tl (see figure 5.1 for the ^{238}U, ^{232}Th and ^{235}U decay chains). The reasons for this are essentially three-fold. First of all, ^{238}U and ^{232}Th themselves decay by α-emission with insignificant gamma production.[15] Secondly, few of their immediate daughters which do decay by gamma emission emit sufficiently intense gamma radiation for quantification. Finally, during exploration for hidden mineralization only the higher energy gamma emissions may be used as the lower energy photons are totally absorbed by a thin soil cover. Even if this absorption did not occur, the low energy spectrum would ride on a significant low energy background which would decrease the sensitivity of the method appreciably.

Consequently, when determining U and Th via their daughter products the assumption is usually made that the

---

[15] ^{235}U does decay directly emitting a low energy gamma photon at 0.18 MeV which has been used to quantify U in the laboratory (Bunker and Bush, 1966). The method is limited to samples with a Th/U ratio ≤ 10. Above this the interference due to ^{228}Ac (a ^{232}Th daughter product) is too great for accurate U determination.

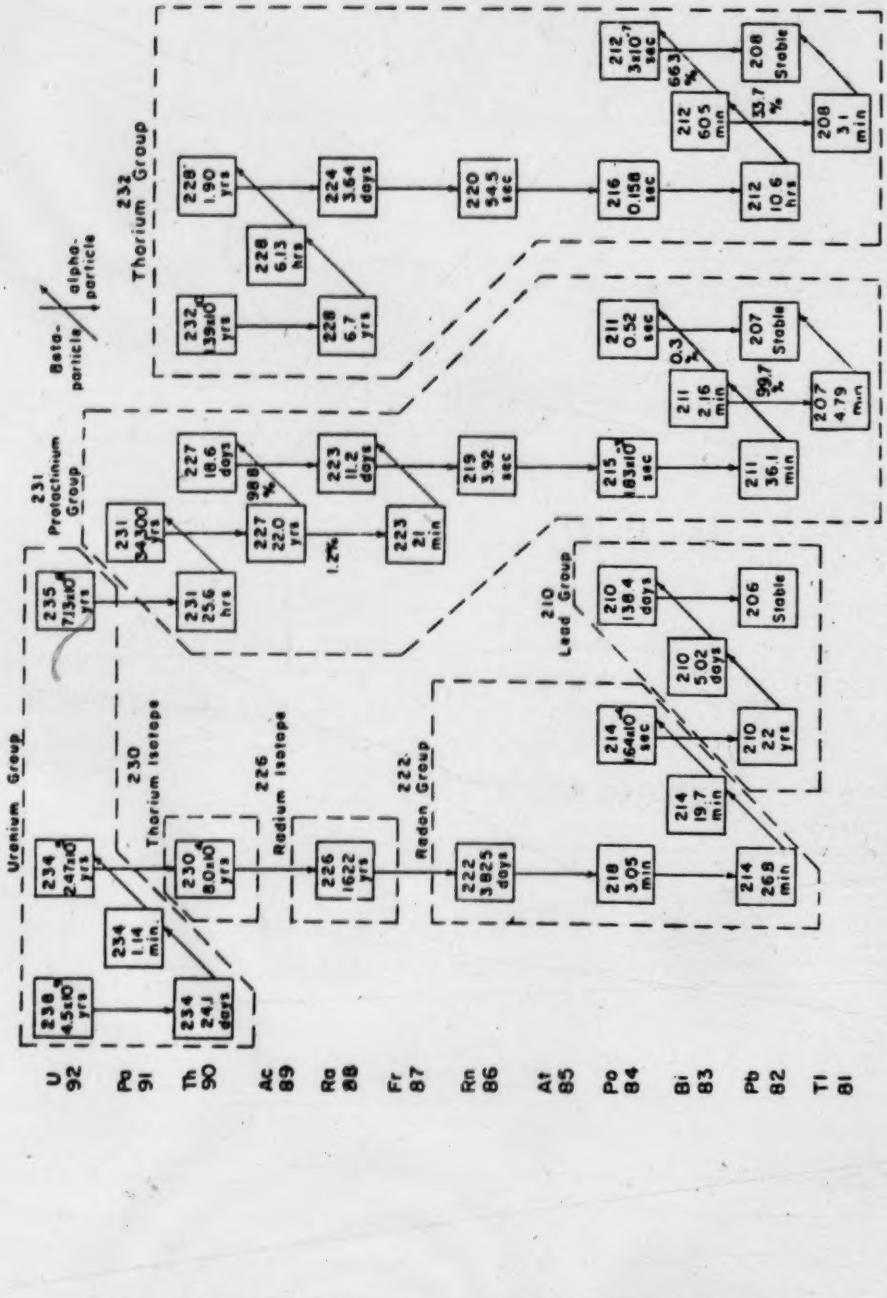
U 92
Pa 91
Th 90
Ac 89
Ra 88
Fr 87
Rn 86
At 85
Po 84
Bi 83
Pb 82
Tl 81
Uranium Group
230 Thorium Isotope
226 Radium Isotope
222 Radon Group
210 Lead Group
231 Protactinium Group
232 Thorium Group
Beta-particle
alpha-particle
238 4.5x10⁹ yrs
234 24.1 days
234 1.14 min.
234 2.47x10⁵ yrs
230 8.0x10⁴ yrs
226 1622 yrs
222 3.825 days
218 3.05 min
214 26.8 min
214 19.7 min
214 1.64x10⁻⁴ sec
210 22 yrs
210 5.02 days
210 138.4 days
206 Stable
235 7.13x10⁸ yrs
231 25.6 hrs
231 34,300 yrs
227 22.0 yrs
98.8 %
1.2%
227 18.6 days
223 21 min
223 11.2 days
219 3.92 sec
215 1.83x10⁻³ sec
211 36.1 min
211 2.16 min
0.3 %
99.7 %
211 0.52 sec
207 4.79 min
207 Stable
232 1.39x10¹⁰ yrs
228 6.7 yrs
228 6.13 hrs
228 1.90 yrs
224 3.64 days
220 54.5 sec
216 0.158 sec
212 10.6 hrs
212 60.5 min
66.3 %
33.7 %
212 3x10⁻⁷ sec
208 3.1 min
208 Stable

(after Rosholt, 1958).

Figure 5.1 ^{238}U, ^{232}Th and ^{235}U decay chains parent radionuclides are in secular equilibrium with their daughters. In secular equlibrium the number of atoms of each daughter being produced is equal to the number of atoms of the same daughter decaying. This requires that the system remain closed to gains and/or losses of radioisotopes of the decay chain under consideration. When such conditions are not met disequilibrium results. Some eight or nine half-lives of the 'offending' radioisotope are then necessary for equilibrium to be regained.

Due to the relatively short half-lives of the decay products in the ^{232}Th decay chain, disequilibrium in this chain is rarely a problem.[16] However, many of the daughter products in the ^{238}U decay chain are sufficiently long-lived and chemically distinct that selective mobilization, by leaching for example, can result in loss of equilibrium that is not rapidly regained (see Levinson and Coetyee, 1978., Szoghy and Kish, 1978, and Rosholt, 1959).

Only disequilibrium due to the diffusion of ^{222}Rn (part of the ^{238}U decay chain) is of immediate concern in the laboratory (see under "Sample Preparation"). A comparison of the uranium results obtained by gamma-spectrometry with those from INAA or DNC (where uranium is determined directly) will identify samples in which disequilibrium is a problem.

---

[16] ^{228}Ra has the longest half-life of the daughter products in the ^{232}Th decay scheme (T1/2 = 6.7 yr). Hence, >99% equilibrium is attained after 46 years (approximately seven half-lives).

Potassium may be determined via its monoenergetic gamma emission at 1.46 MeV due to the decay of ^{40}K following electron capture. As potassium is determined directly by gamma-spectrometry disequilibrium is not a problem.

5.2 Sample Preparation

Samples to be analyzed were washed briefly with tap water to remove any traces of drilling mud. Then, after drying, they were crushed in a tungsten-carbide swing mill to approximately -120 mesh. They were then vacuum dried for 24 hours and weighed into tared plastic vials (5.4 cm long with an inside diameter of 1.4 cm) to a height of 4 cm. This was found to be important for two reasons. Firstly, a non-reproducible counting geometry will result in non-reproducible results. Secondly, and having the same effect, the efficiency of the NaI(Tl) well detector utilized was found to decrease rapidly towards the top of the well as the near 4π geometry was lost. To avoid later settling the vials were tapped to the above height during packing. The mass of crushed rock was measured to the nearest milligram and recorded.

The plastic vials were then hermetically sealed and left for some thirty days before being counted. This is necessary as it allows the ^{238}U decay chain to regain secular equilibrium as, when crushed, the gaseous ^{222}Rn daughter is lost. Consequently, ^{214}Bi which occurs even later in the decay chain (see figure 5.1) may only be used to quantify the uranium once equilibrium has been regained. In this work a minimum of seven half-lives of ^{222}Rn (T1/2 = 3.825 days) were allowed for the gas and its daughter products to build up and regain >99% equilibrium. However, Ritchie and McHenry (1973) found from their work on uranium analysis by gamma spectrometry that:

> "measured gamma-ray equilibrium was achieved in 10-15 days." (Ritchie and McHenry p.577, 1973).

Radon-220 (T1/2 = 55.3 secs) occurs in the ^{232}Th decay chain, however, due to its short half-life, equilibrium is regained approximately eight minutes after sealing.

5.3 The Counting System.

Samples were counted using a 3" x 3" well-type Bicron NaI(Tl) crystal detector with a measured resolution of 7.65% at the ^{137}Cs 0.662 MeV photopeak. The crystal was mounted on a photomultiplier tube which was in turn connected to an Ortec 276 photomultiplier base and preamplifier. A lead castle some 10 cm in thickness housed the detector system. The 1 kV detector bias was supplied by an Ortec 456 high voltage power supply. The preamp signals were fed to a Canberra Series 80 multichannel analyzer (MCA) where they were amplified and assigned to one of 1024 channels. Spectra thus obtained were stored on floppy-discs using a Canberra Model 8660 Series 80 Floppy-Disc System for later numerical analysis.

Any drift in the system was monitored using an Ortec 419 precision pulse generator.

5.4 Analysis

As noted earlier U and Th have generally been determined via the high energy gamma emissions of ^{214}Bi and ^{208}Tl (Adams et al. 1956). Although convenient for field analysis this method has two main drawbacks for routine laboratory work. These are:

a) large samples and

b) long counting times

are necessary when measuring low levels of U and Th (0-50 ppm). Figures 5.2 and 5.3 show typical spectra of uranium and thorium standards over the range of 0 to 3 MeV. From them it can be seen that the low energy regions of the spectra (0 to 0.5 MeV) contain the greatest amount of potential information. This is due in part to the greater intensity of the low energy peaks, together with the increased efficiency of the detector at about 0.1 MeV. Both factors result in an increased countrate and better counting statistics.

After a series of preliminary studies at the concentrations of uranium expected in the samples of this study (0-100 ppm) it was decided that 'conventional' gamma spectrometry would not be sufficiently sensitive or rapid for the routine analysis of a large number of samples. It was therefore decided to investigate the lower part of the

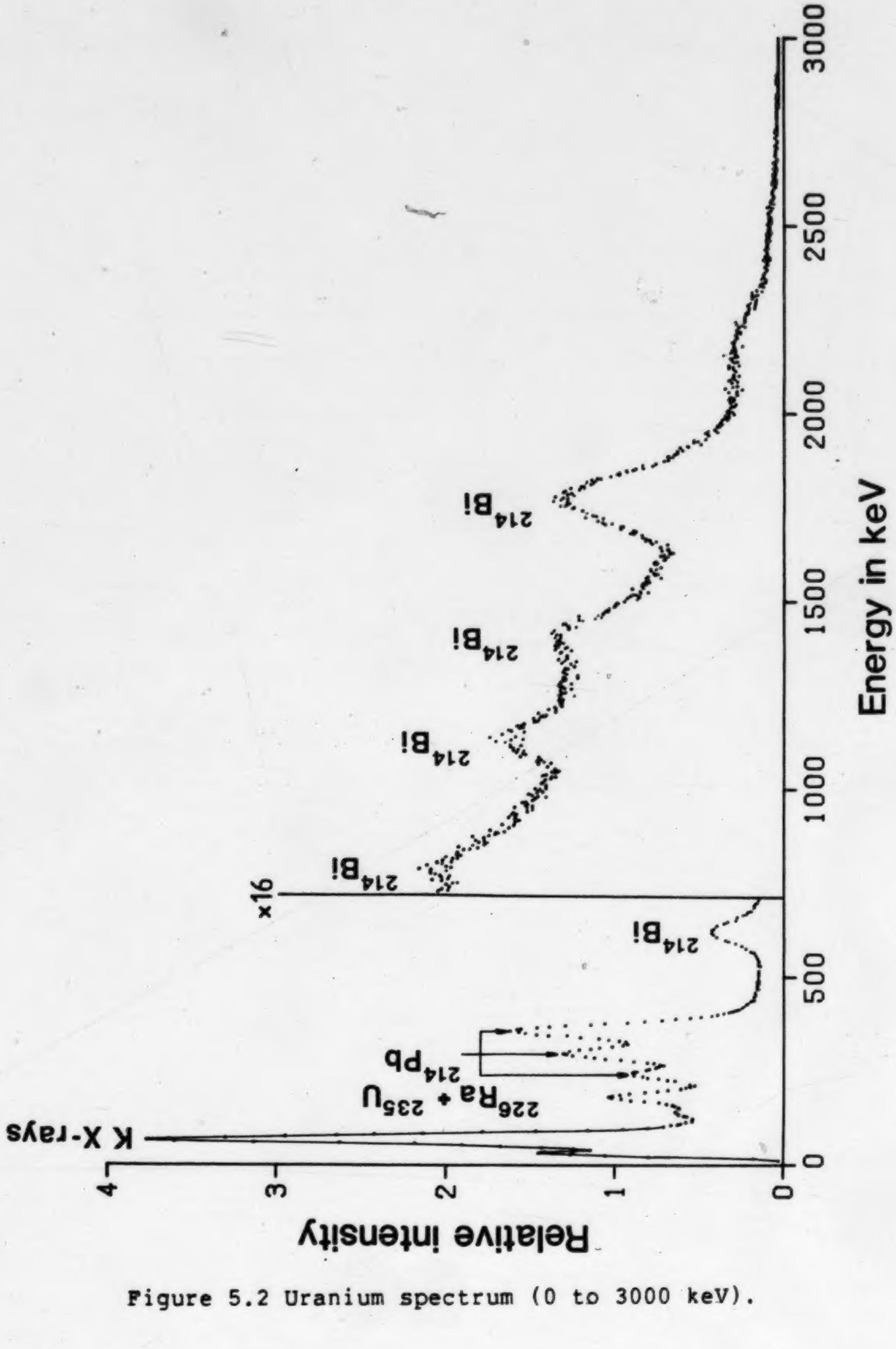

Figure 5.2 Uranium spectrum (0 to 3000 keV).

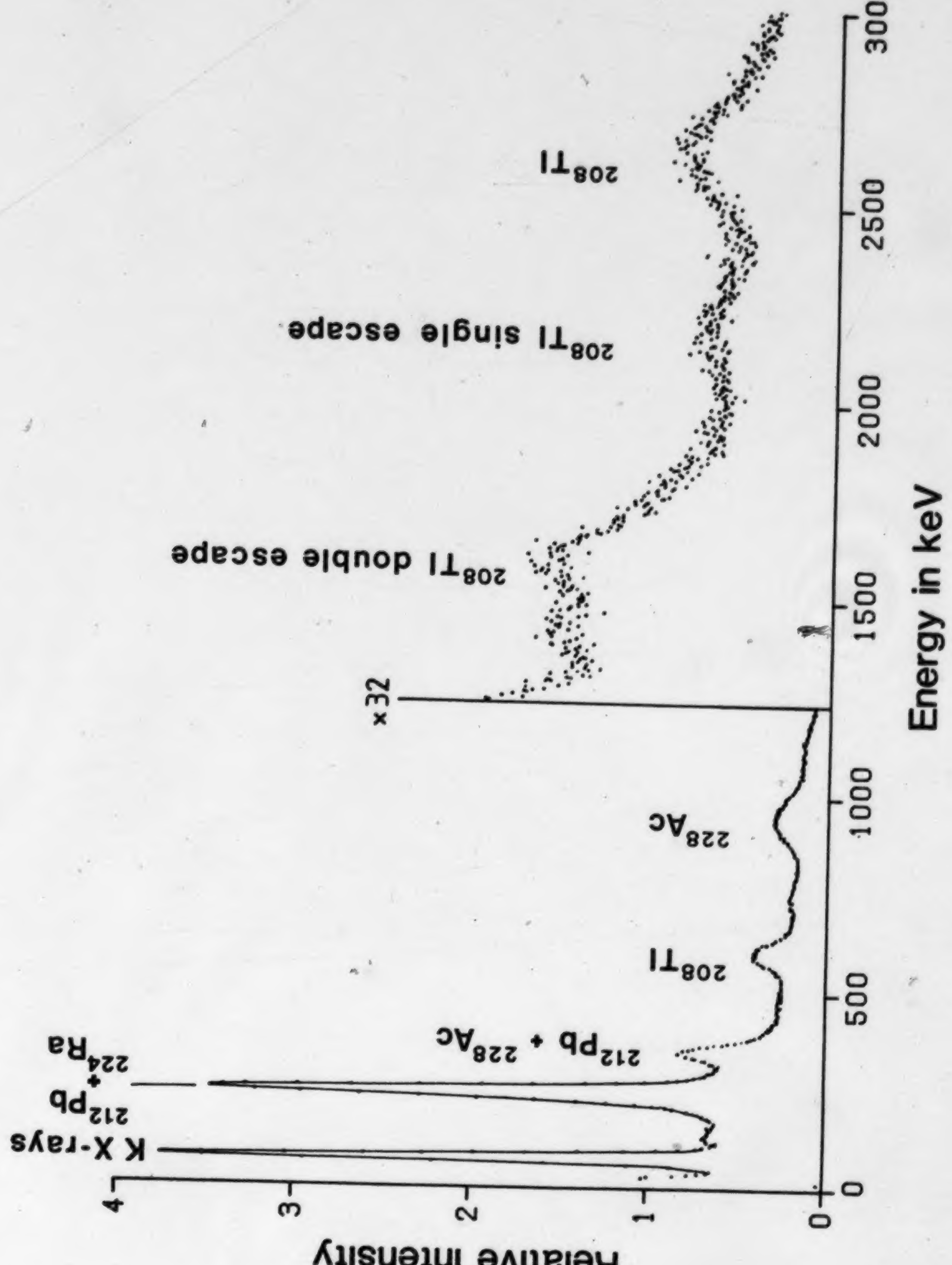

Figure 5.3 Thorium spectrum (0 to 3000 keV).

spectrum.

In an attempt to utilize the mass of information contained in the lower energy part of the spectrum (see Hurley, 1954, 1956; Bunker and Bush, 1966; Culbert and Leighton, 1981) the method of Culbert and Leighton was adopted for U and Th measurement. Following their work the amplifier gain was adjusted so that only the lower energy part of the gamma spectrum (0-400 keV)[17] was assigned to the 1024 channels of the MCA. Two windows, or regions of interest (53-112 keV and 208-269 keV) were set up to encompass the 80 keV photopeak of ^{214}Pb and 235 keV photopeak of ^{212}Pb (daughters of ^{238}U and ^{232}Th respectively). Figure 5.4 shows spectra of the uranium and thorium standards superimposed, with the photopeaks and windows identified. As can be seen, neither window is interference-free and consequently stripping coefficients or ratios must be determined. Knowing the mass and U and Th concentrations of two standards, the stripping coefficients for U and Th were calculated after repeatedly counting the background and standards. For the equipment and operating conditions employed, the coefficients were calculated to be:-

$S1U = 4.447 \times 10^{-3}$ cts $s^{-1}g^{-1}ppm^{-1}$U
$S2U = 1.396 \times 10^{-3}$ cts $s^{-1}g^{-1}ppm^{-1}$U
$S1T = 1.604 \times 10^{-3}$ cts $s^{-1}g^{-1}ppm^{-1}$Th
$S2T = 1.631 \times 10^{-3}$ cts $s^{-1}g^{-1}ppm^{-1}$Th

---

[17] While discussing low energy gamma spectrometry γ-ray energies will be given in kilo electron volts (keV) for ease.

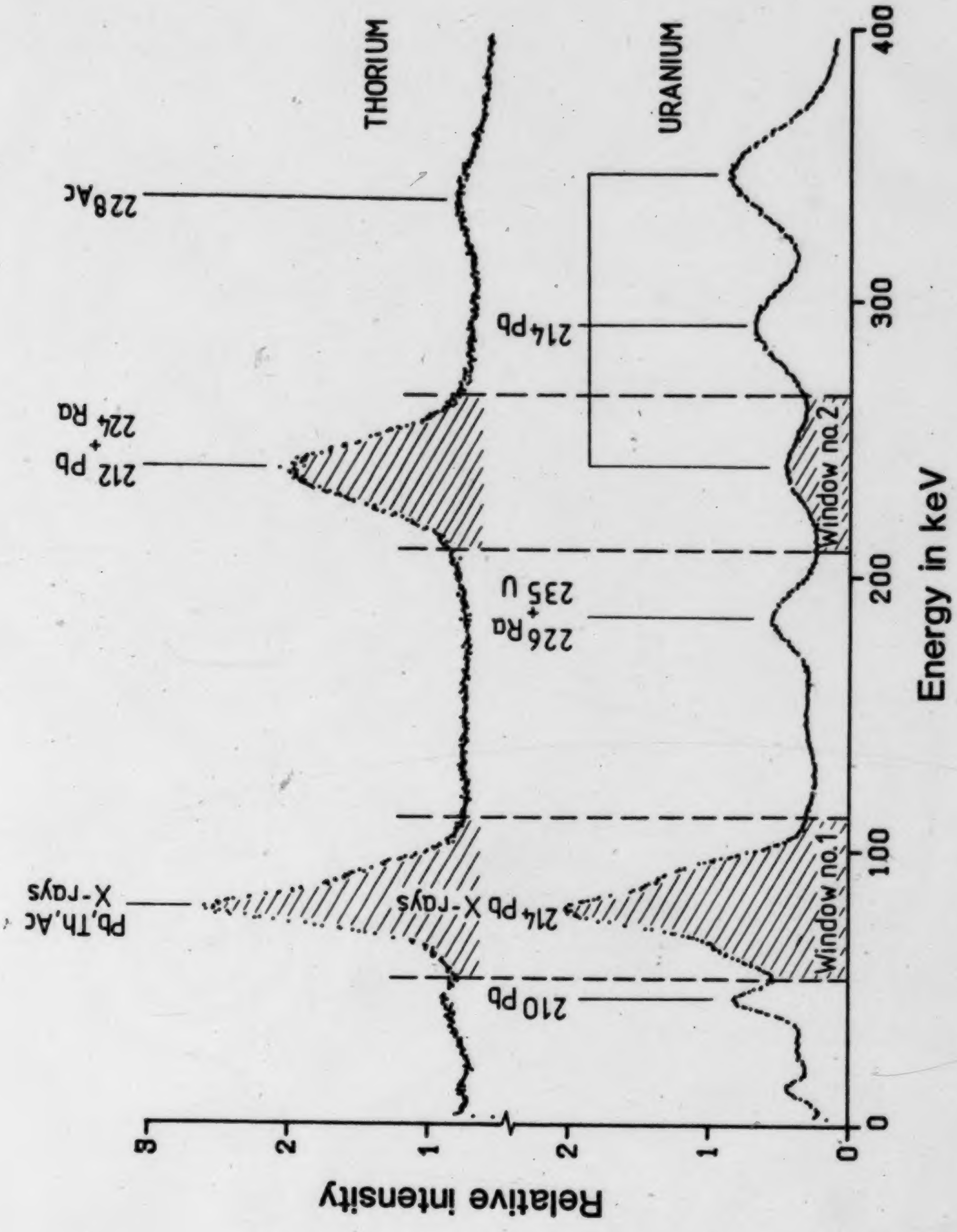

Figure 5.4 The low energy parts of the uranium and thorium spectra

Once the background counts have been subtracted, the uranium and thorium concentrations of the sample may be calculated from the following equations:-

$$U\ (\text{ppm}) = \frac{(N_1.S1T - N_2.S1T)}{m\ (S1U.S2T - S2U.S1T)}$$

$$Th\ (\text{ppm}) = \frac{(N_1.S2U - N_2.S1U)}{m\ (S2U.S1T - S1U.S2T)}$$

where:-

N_1 = net counts per second in window 1
N_2 = net counts per second in window 2
m = mass of sample in grams
SnX = stripping coefficient for element X in window n

Following this method, the detection limits (Currie, 1968) in a thorium- and uranium-free matrix are 0.63 ppm U and 1.57 ppm Th respectively, for an 8-9 gram sample counted for 10,000 seconds.

Such short counting times, together with the above sensitivity, are a great improvement on conventional gamma-spectrometry. In order to increase the sensitivity further, either the sample size must be increased and/or the background decreased. Much of the background in window 1 is due to 75 keV fluorescent Pb Kα X-rays produced by the interaction of cosmic radiation and high energy background gamma-rays with the lead shield. In an attempt to reduce this component, a copper shield (1.25 mm thick) was made to surround the detector to absorb the Pb Kα X-rays. A background reduction of approximately 33% was found in window 1 when the shield was used. With a thicker copper shield this reduction could be further increased.

One major problem associated with this method is the contribution to windows 1 and 2 by *bremsstralung* X-rays. These X-rays result from the kinetic energy loss during interaction of energetic β^--particles (produced during the decay of ^{40}K) with the sample matrix. To examine the extent of this interference, a 6g sample of reagent grade KCl was prepared and run in accordance with the above method. From this it was calculated that 1% K (1.205% K_2O) in an 8g sample results in an apparent uranium and thorium concentration of 0.75 ppm and 0.34 ppm respectively. Typically shales contain between 0 and 4% K_2O, therefore uncorrected U and Th determinations could be high by as much as 3 ppm U and 1.5 ppm Th. This does not represent a significant error when measuring U and Th levels >50 ppm. However, it should not be ignored when measuring lower levels, particularly in the 1-10 ppm range.

As the samples of the study could lie in this range, it was clear that a method to correct for the potassium content needed to be developed. Culbert and Leighton (ibid.) suggest that the induced fluorescent photopeak of iodine (29.8 keV) in the NaI crystal could be used to monitor the potassium interference. However, this procedure was found inadequate by the present author. For the purpose of this study, it was decided that the low energy gamma-spectrometry method be modified to include the analysis of K and hence correct for the interference. Alternatively, the potassium content of the sample may be determined by an independent method such as X-ray fluorescence spectrometry and a correction made in conjunction with the above empirical measurements.

In order to measure the potassium content, the gain of the amplifer was altered so that the range 0 to 1600 keV was assigned to the 1024 channels of the MCA. A third window (see figures 5.5, 5.6 and 5.7) was set up to encompass the 1460 keV photopeak of ^{40}K in addition to the U and Th windows discussed above. Extended counts (100,000 seconds) with an empty vial placed in the detector well were repeatedly taken so as to reduce the error in the determination of the background component of the windows. As in the case of the low energy gamma-spectrometry, stripping coefficients and equations for calculating the U, Th and K contents of samples had to be determined. Repeated measurements on a series of U, Th and K standards were preformed. Analysis of these measurements yielded the following stripping coefficients:-

S1U = 4.170 x 10^{-3}cts $s^{-1}g^{-1}ppm^{-1}$U
S2U = 1.397 x 10^{-3}cts $s^{-1}g^{-1}ppm^{-1}$U
S3U = 3.641 x 10^{-3}cts $s^{-1}g^{-1}ppm^{-1}$U
S1T = 1.454 x 10^{-3}cts $s^{-1}g^{-1}ppm^{-1}$Th
S2T = 1.655 x 10^{-3}cts $s^{-1}g^{-1}ppm^{-1}$Th
S3T = 8.447 x 10^{-5}cts $s^{-1}g^{-1}ppm^{-1}$Th
S1K = 2.927 x 10^{-4}cts $s^{-1}g^{-1}$% K^{-1}
S2K = 1.220 x 10^{-4}cts $s^{-1}g^{-1}$% K^{-1}
S3K = 3.328 x 10^{-4}cts $s^{-1}g^{-1}$% K^{-1}

The U, Th and K content of samples may be determined from the equations on page 97.

Where three 'pure' standards are not available the stripping coefficients may be calculated from three mixed

$$\frac{(N_1.S2T.S3K) + (S1T.S2K.N_3) + (S1K.N_2.S3T) - (N_1.S3T.S2K) - (S1T.N_2.S3K) - (S1K.S2T.N_3)}{D}$$

$$\frac{(S1U.N_2.S3K) + (N_1.S2K.S3U) + (S1K.S2U.N_3) - (S1U.N_3.S2K) - (N_1.S2U.S3K) - (S1K.N_2.S3U)}{D}$$

$$\frac{(S1U.S2T.N_3) + (S1T.N_2.S3U) + (N_1.S2U.S3T) - (S1U.S3T.N_2) - (S1T.S2U.N_3) - (N_1.S2T.S3U)}{D}$$

where:-

D = m (S1U.S2T.S3K)+(S1T.S2K.S3U)+(SIK.S2U.S3T)−(S1K.S2T.S3U)−(S1K.S2U.S3T)−(S1U.S2K.S3T)

Nn = net counts per second in window n

m = weight of sample in grams

SnX = stripping coefficient for element X in window n

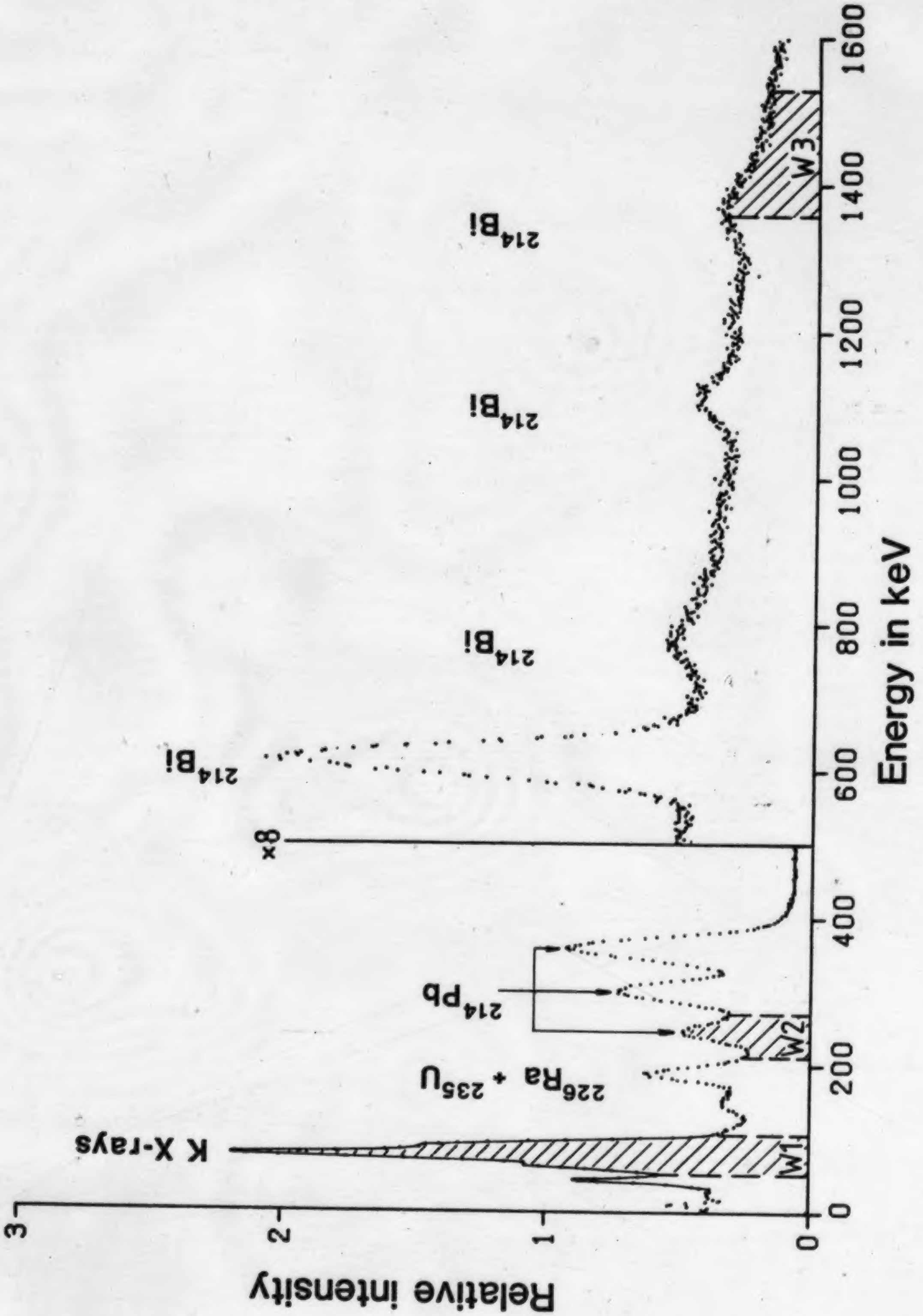

Figure 5.5 Uranium spectrum (0 to 1500 keV)

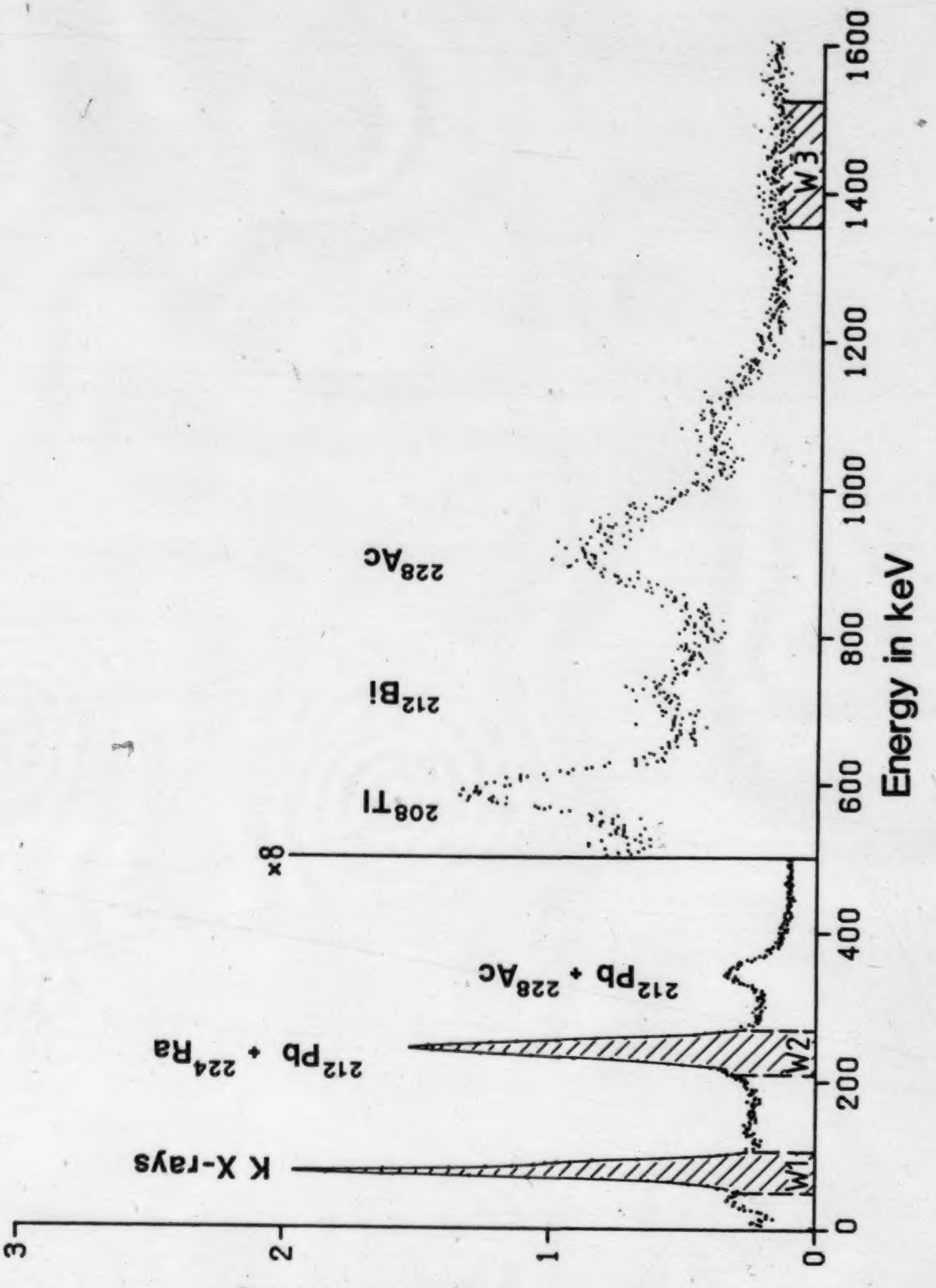

Figure 5.6 Thorium spectrum (0 to 1500 keV)

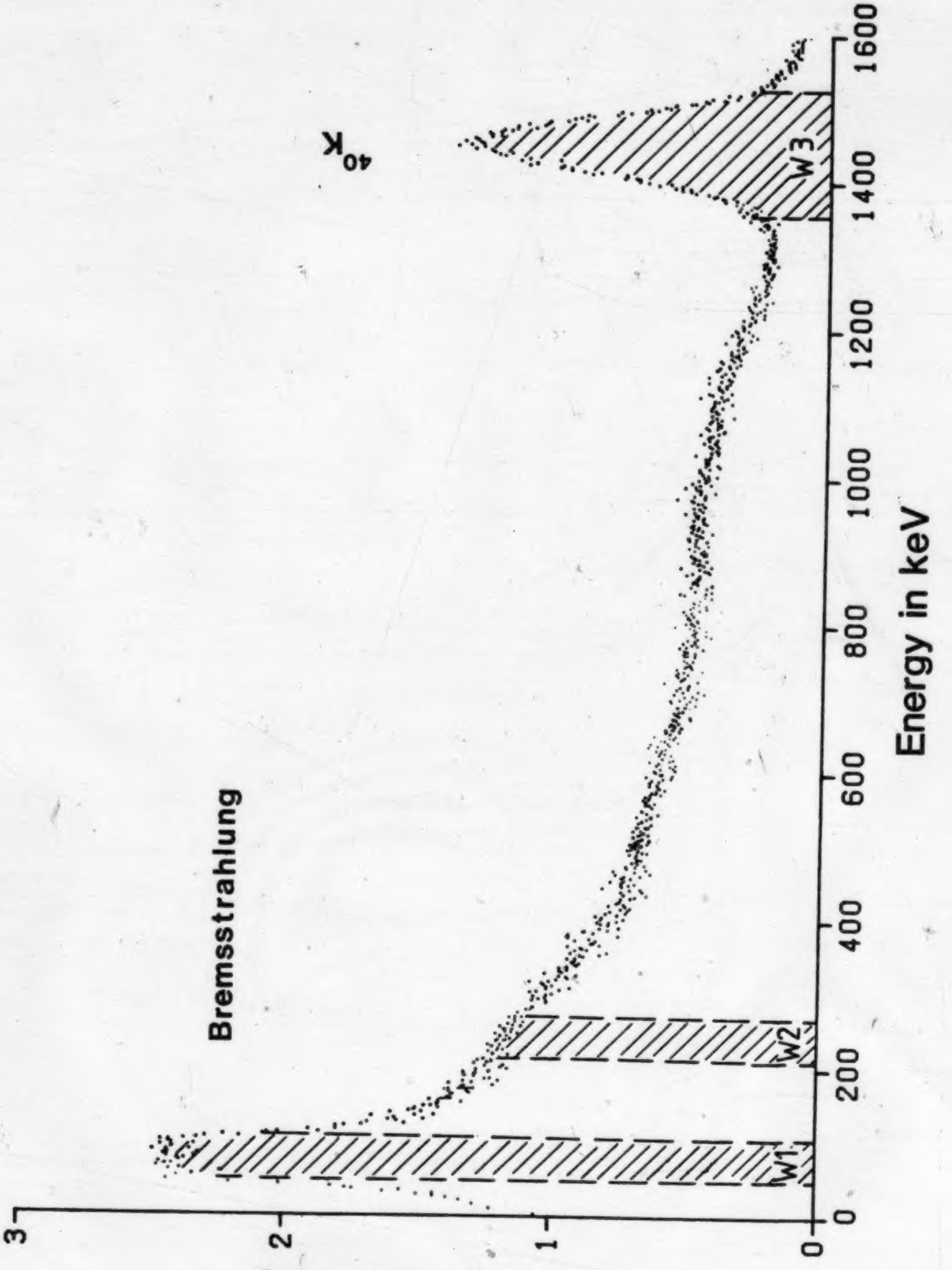

Figure 5.7 Potassium spectrum (0 to 1500 keV)

samples/standards of well known U, Th and K content.

To simplify the numerical analysis of the results, an interactive FORTRAN IV programme was written by the the author. Given the counting time, integrated counts in windows 1, 2 and 3, plus the sample mass, the programme calculates the U, Th and K concentrations, errors, ratios, etc. for each sample.

5.5 Results

To examine the accuracy and precision of the low energy gamma-spectroscopy method for uranium and thorium analyses the reference standards BL-1, DL-1 and NBS 1633a (coal fly-ash) were prepared and analyzed a number of times over a three month period. The recommended and measured uranium and thorium values are given in table 5.1.

Uranium determinations for the radioactive reference standard BL-1 are in each case well within the recommended limits. For the same sample however, the accuracy of the thorium determinations varies and in all cases the one sigma uncertainty ≥50% (usually much greater). The large uncertainty is due to the unfavourable Th/U ratio (0.07) of the standard. The method is most precise for **both** thorium and uranium determinations when the Th/U ratio lies between 0.5 and 2.5 (this being well exemplified by the analyses of DL-1).

When counted for 10,000 seconds, uranium and thorium concentrations down to 1 and 3 ppm respectively may be

Table 5.1 Uranium and thorium results of low energy gamma-spectrometry

Canadian Radioactive Reference Ore BL-1

	Uranium (ppm)	Thorium (ppm)	T count (s)
a)	233 ± 6	6.4 ± 3.6	10,000
b)	226 ± 7	7.2 ± 8.0	1000
c)	224 ± 8	12.3 ± 10.1	600
rec.	220 ± 10	15 ± 1	

Canadian Radioactive Reference Ore DL-1

	Uranium (ppm)	Thorium (ppm)	T count (s)
a)	38.9 ± 1.8	82.8 ± 2.0	10,000
b)	40.6 ± 1.9	80.6 ± 2.2	7200
rec.	41 ± 2	83 ± 5	

NBS Flyash 1633a.

	Uranium (ppm)	Thorium (ppm)	T count (s)
a)	13.9 ± 0.6	24.0 ± 0.7	36,000
b)	12,4 ± 0.7	24.0 ± 1.0	10,000
rec.	10.2 ± 0.1	24.7 ± 0.3	

(all values plus or minus one standard deviation) determined with a precision better than ±10% in a thorium- and uranium-free matrix respectively.

The variable counting times necessary for analyses show that accurate and precise results may be obtained with short (e.g. 10 minute) counting intervals when the uranium and/or thorium concentrations are sufficiently high (>100ppm). Consequently, as noted by Culbert and Leighton ibid. the procedure may be used to rapidly 'screen' samples in an exploration programme.

The thorium results obtained for NBS 1633a are in good agreement with the recommended values, while the uranium values are in each case high. This is thought to be due to the potassium content of the sample. It was calculated that with the recommended 1.88% K of NBS 1633a with the sample mass used (7.822g) would produce the equivalent uranium concentration of 1.5 ± 0.1ppm. When corrected for this interference, one of the two uranium analyses falls within the recommended limits. The reason the other result is some 10% high is unclear, but it may be due to temporal background variations. Both the uranium and thorium results obtained for the Canadian Radioactive Reference Ore DL-1 are in excellent agreement with the recommended values, before and after removal of potassium equivalent uranium.

Comparison of the uranium results determined via the LEGS and DNC (MNR) methods (see chapter VII) show the agreement to be excellent. This agreement is also shown graphically in figure 7.5. From this figure it can also be seen that in many instances, at uranium levels below 40ppm, the results obtained by gamma-spectrometry are slightly greater than those values obtained from the DNC method. This is largely due to the potassium interference to the uranium window. To assess the accuracy and precision of the low energy gamma-spectrometry with potassium being quantified in addition to uranium and thorium, NBS 1633a was analysed, the results of which are given in table 5.2. Although the uranium results are in each case within the limits of the recommended value, they are consistently high by a factor 1.053 ± 3.41% (N=4), scatter = 2.33%. Using the inverse of this value as a correction factor and applying it to the uranium analyses, a 'corrected' weighted mean of 10.20 ± 0.39ppm U (N=4), scatter = 2.34% results. Thus the correction factor 0.95 ± 3.41% has been applied to the uranium results determined via the 3 window NaI method.

Similarly, from the same four analyses the thorium results were found to be consistently in error by a factor of 1.08 ± 1.83%. The inverse value, 0.93 ± 1.83 (N=4) scatter = 2.83% was used to 'correct' the results. It is difficult to assess the accuracy of the thorium results as the 'real' thorium contents of the Exshaw Shale samples are uncertain.

Analysis of the potassium results of NBS 1633a show the values obtained in this work to be greater than the recommended value by a factor 1.063. Using these results the correction factor 0.941 ± 4.10% (N=4), scatter = 9.77% was

Table 5.2 Low energy gamma-spectrometry for the analysis of uranium, thorium and potassium in NBS Flyash 1633a

	a.	b.	c.	d.	
U	10.6 ± 0.8	10.8 ± 0.7	11.1 ± 0.7	10.4 ± 0.7	ppm.
Th	27.7 ± 1.0	27.1 ± 0.9	25.7 ± 0.8	26.2 ± 1.0	ppm.
K_2O	2.68 ± 0.19	2.19 ± 0.17	2.53 ± 0.18	2.12 ± 0.18	%

	Recommended values.	Corrected results.	
U	10.2 ± 0.1	10.2 ± 0.4	ppm.
Th	24.7 ± 0.3	24.7 ± 0.5	ppm.
K_2O	2.26 ± 0.07	2.25 ± 0.14	%

calculated and applied to the NaI values. Once applied the agreement between the results of the NaI and XRF methods are generally within the calculated limits (see table 7.1).

In summary therefore, both gamma-spectrometry methods provide a relatively cheap (as neither a nuclear reactor, semiconductor detector nor sophisticated data reduction system is necessary) and rapid means of uranium and thorium analysis. The LEGS method is both accurate and precise for both elements at normal Th/U ratios, and may be used for rapid screening of samples and more precise analyses. The three window gamma-spectrometry method offers the advantage of being able to analyze simultaneously for all three of the major heat producing elements at little or no extra expense. The precision or uncertainty in such measurements is largely controlled by the counting time and relative concentrations of uranium, thorium and potassium of each sample. Two sources of random or unsystematic error may manifest themselves when analyzing for uranium by either method. Firstly, a disequilibrium break in the ^{238}U decay chain at, or above ^{226}Ra, will give spurious results. This would become apparent if the sample was re-analyzed by INAA or DNC where uranium is measured directly. Secondly, if the samples to be analyzed have a high average atomic number (e.g. mineralized or panned heavy concentrate samples) attenuation and/or self-absorption of the low energy radiation of window 1 (^{234}Th, ^{214}Pb plus Bi conversion X-rays) will occur. Self-absorption would be readily apparent from the high count rates observed and the higher energy, more conventional gamma-spectrometry method may be used. Sample density, and hence mass, (as vials are packed to the same height as closely as possible) may be used to identify those samples in which matrix absorption may be a problem and those samples analyzed by an alternative method.

6. X-Ray Fluorescence

6.1 Introduction

All X-ray fluorescence (XRF) analyses were carried out commercially at the University of Nottingham, England using a fully automated Philips PW 1400 wavelength dispersive spectrometer and rhodium tube. A full description of the methodology and corrections employed may be found in Leake et al. (1969) and Harvey and Atkin (1982).

For accurate major oxide determinations sample aliquots of 1-2g were fused to make glass beads. The trace element concentrations (and in some instances the Si and K contents) of the samples were determined via pressed pellets. Approximately 7g of < 200 um of homogenized material was required to produce a disc of 'infinite' thickness, needed for the short Rh wavelengths.

6.2 Analyses

Five samples (of various U content) were analyzed for the major oxides to :-

1. classify the sedimentary pelites
2. see if there was any obvious correlation between U, and Th, and any of the major oxides.
3. compare the results with those of INAA.

The same five samples, plus another 35 were analyzed for the trace elements Cu, Pb, Zn, Th and U (and in addition, the 35 samples were also analyzed for SiO_2 and K_2O). The U, Th and

K contents were determined for direct comparison with the other techniques employed, while Cu, Pb and Zn were determined because they are difficult to analyze for via INAA at trace levels.

The reported approximate 2 sigma detection limits for the XRF analysis, based on a variety of rock types for a number of trace elements is given in table 6.1 (written communication B. Atkin). It can be seen that the detection limits for U and Th by XRF are not as low as those of DNC, INAA or FTA. However, Galson _et al_. (1982) have been able to lower the 2 sigma detection limits to 0.2 ppm U, 1.0 ppm Th and 0.001 % K with better precision than previously obtained, but still using a single pressed pellet. These results are obtained using analytical counting times of 4800s, 480s and 72s for U, Th and K respectively. Increasing the counting times by a factor N would lower these detection limits by the square-root of N.

Table 6.1 Detection limits for X-Ray fluorescense

Element	Lower limit of detection
Ag*	1.0 ppm.
As	1.1 ppm.
Ba	8.3 ppm.
Bi	1.0 ppm.
Ce	7.0 ppm.
Co	2.5 ppm.
Cr	2.8 ppm.
Cu	0.8 ppm.
Mo	0.9 ppm.
Nb	1.2 ppm.
Ni	1.7 ppm.
Pb	1.5 ppm.
Rb	0.7 ppm.
S	8.0 ppm.
Sb*	1.4 ppm.
Sn*	2.0 ppm.
Sr	0.9 ppm.
Th	0.6 ppm.
U	1.4 ppm.
V	1.9 ppm.
W	1.6 ppm.
Zn	3.0 ppm.
Zr	3.1 ppm.

(* - Cr X-ray tube; all other elements Rh X-ray excitation)

(written communication B. Atkin, 1982)

7. Evaluation of the various methods for uranium analysis

Which of the various methods for uranium analysis employed in this study is the 'best'? Such a question does not have a straightforward answer as the term 'best' is ambiguous. Does it mean the most precise, most sensitive, cheapest, quickest or simplest method, to name a few possible interpretations? Clearly, the 'best' method depends upon the requirements of the analysis and the availability of the various techniques.

For example, in the case of a geochemical exploration programme for uranium, where there are many thousands of samples to be analyzed solely for uranium, then the easily automated delayed neutron counting method should be employed on account of its speed, sensitivity, lack of interferences and low cost. However, as is apparent from the earlier discussion on the technique, access to a nuclear reactor is essential. If only very small samples (≤20 mg) are available for analysis[*] and/or the uranium content of the sample is expected to be very low (say <500 ppb) for example in ultramafic or tholeiitic rocks, then the extremely sensitive fission track method should be used (Fisher, 1970,1975). Once again however, a reactor is necessary to bombard the samples.

For samples where more than U and possibly Th are to be determined, DNC and FTA will not be able to satisfy all the requirements. For example, when determining the concentrations of the major heat-producing elements U, Th and K in rocks, K would have to analyzed by an alternative method. For these three elements, the increased speed with which they may now be determined using a sodium-iodide detector and the lower energy part of the spectrum, makes γ-spectrometry an attractive alternative to the expensive (approximately $60 CDN/sample 1982 prices) XRF method of Galson _et_ _al_. (1982). The former method suffers from the disadvantage that disequlibrium in the uranium chain may lead to spurious results, while XRF has the advantage that many others elements may be determined from the same pressed pellet with some extra analysis time. If uranium is determined by DNC or INAA in conjunction with natural γ-spectrometry, this may give useful information regarding the state of disequilibrium in the ^{238}U decay chain and hence the levels of the intermediate daughter products may be calculated. With 'conventional' XRF however the accuracy and precision of uranium and thorium analyses are poor (see figures 7.1 and 7.6).

---

[*] for example lunar or meteoritic material

INAA, as has been shown, is a multielemental technique and extremely sensitive for a large number of elements. Once again access to a reactor and gamma-ray spectrometry system is necessary. For optimum Th sensitivity, decay periods of two weeks or so are required making the method more expensive than say DNC. Because such small samples are generally used for INAA care must be exercised in sample preparation to avoid sample inhomogeneity.

When comparing various analytical techniques for determining U, Th and K in granitic rocks Stuckless *et al.* (1977) concluded that γ-spectrometry was adequate for the concentrations normally present in such rock types, but as disequlibrium in the ^{238}U decay chain was occasionally a problem, they suggest that the method be combined with DNC for uranium analysis. Hart *et al.* (1980) found when comparing INAA, XRF and mass spectrometry isotope dilution (MSID) for U and Th analysis that at concentrations above 10 ppm U and Th, INAA and XRF are alternatives to the expensive and time comsumming MSID technique. As a wide variety of geological samples will have lower concentrations than 10 ppm U they state that INAA is to be preferred over the less precise XRF.

The uranium results of the various techniques employed in this work are listed in table 7.1 and are shown graphically in figures 7.1 to 7.5. Of the methods utilized XRF and FTA are the least precise[19]. The agreement between the INAA short- and long-irradiations, and the gamma-spectrometry and DNC results is most satisfactory. Figures 7.6 and 7.7 show the comparison of thorium analysis by low energy gamma-spectrometry and XRF with INAA determination of thorium.

The choice of which method to use for uranium analysis therefore depends ultimately upon the user requirements and it is hoped therefore that this part of the thesis on

---

[19] in the case of FTA the imprecision is largely due to hetrogeneities in the comparator standards.

Table 7.1 Results of various methods of uranium analysis applied to Exshaw shale samples

Sample ID.	DNC.	4 min INAA.	2 hr INAA.	NaI(2)*	NaI(3)*	FTA.	XRF.
1 Ex.	27.0 ± 0.3	29.6 ± 0.2	25.2 ± 0.4	26.8 ± 1.0	25.4 ± 1.1	28.0 ± 2.9	31
2 Ex.	4.53 ± 0.13	5.0 ± 0.2	5.11 ± 1.27	6.8 ± 0.4	3.89 ± 0.37	5.0 ± 0.6	3
3 Ex.	38.2 ± 0.4	42.0 ± 0.2	38.2 ± 0.4	36.1 ± 1.2	37.3 ± 1.6	n.a.	49
4 Ex.	24.0 ± 0.3	24.7 ± 0.2	25.1 ± 0.4	23.4 ± 0.9	23.9 ± 1.0	23.8 ± 2.5	28
5 Ex.	55.3 ± 0.5	60.6 ± 0.3	54.0 ± 0.6	52.2 ± 1.8	48.3 ± 2.2	n.a.	54
6 Ex.	30.6 ± 0.4	31.4 ± 0.2	31.9 ± 0.5	31.2 ± 1.2	30.6 ± 1.3	n.a.	n.a.
7 Ex.	15.8 ± 0.3	17.3 ± 0.2	15.6 ± 0.9	15.7 ± 0.6	14.3 ± 0.6	15.8 ± 1.7	17
8 Ex.	18.1 ± 0.3	19.1 ± 0.2	18.8 ± 0.6	17.7 ± 0.8	17.7 ± 0.9	17.8 ± 1.9	18
9 Ex.	6.19 ± 0.15	6.9 ± 0.2	5.48 ± 0.32	7.5 ± 0.4	3.76 ± 0.29	6.9 ± 0.8	11
10 Ex.	12.9 ± 0.3	12.9 ± 0.1	12.8 ± 0.3	13.2 ± 0.6	12.4 ± 0.6	n.a.	13
11 Ex.	11.9 ± 0.2	10.8 ± 0.1	11.1 ± 0.4	12.7 ± 0.6	12.6 ± 0.7	n.a.	12
12 Ex.	4.31 ± 0.13	2.8 ± 0.1	4.03 ± 0.45	5.4 ± 0.4	5.23 ± 0.30	4.4 ± 0.6	n.a.
13 Ex.	15.6 ± 0.3	14.8 ± 0.1	14.4 ± 0.3	16.7 ± 1.0	n.a.	n.a.	17
14 Ex.	31.7 ± 0.4	28.1 ± 0.2	32.8 ± 0.5	33.1 ± 1.2	32.1 ± 1.4	30.5 ± 3.1	n.a.
15 Ex.	10.5 ± 0.3	8.7 ± 0.1	8.23 ± 0.21	11.8 ± 0.6	10.1 ± 0.5	10.5 ± 1.1	n.a.
16 Ex.	13.3 ± 0.2	11.3 ± 0.2	12.2 ± 0.5	14.3 ± 0.6	13.5 ± 0.7	n.a.	15
17 Ex.	9.69 ± 0.21	7.4 ± 0.1	7.49 ± 0.28	10.4 ± 0.5	8.31 ± 0.47	9.9 ± 1.1	10
18 Ex.	15.3 ± 0.2	13.9 ± 0.2	14.2 ± 0.5	15.1 ± 0.6	14.7 ± 0.8	n.a.	n.a.
19 Ex.	16.3 ± 0.3	18.9 ± 0.2	17.4 ± 0.6	18.5 ± 0.8	16.0 ± 0.8	n.a.	n.a.
20 Ex.	3.40 ± 0.11	2.5 ± 0.1	3.20 ± 0.29	3.9 ± 0.3	2.86 ± 0.26	3.5 ± 0.5	1
21 Ex.	5.72 ± 0.15	5.7 ± 0.1	4.41 ± 0.36	8.9 ± 0.4	5.30 ± 0.45	6.1 ± 0.7	n.a.
22 Ex.	20.6 ± 0.3	23.3 ± 0.2	22.0 ± 1.2	20.5 ± 0.8	20.0 ± 0.9	n.a.	n.a.
23 Ex.	4.75 ± 0.13	4.6 ± 0.1	4.92 ± 0.53	6.0 ± 0.4	n.a.	n.a.	6
24 Ex.	41.0 ± 0.4	39.6 ± 0.2	40.6 ± 0.5	41.9 ± 1.5	41.1 ± 1.7	40.0 ± 4.0	n.a.
25 Ex.	4.53 ± 0.13	3.4 ± 0.1	3.54 ± 0.25	5.4 ± 0.3	4.24 ± 0.24	4.5 ± 0.6	6
26 Ex.	91.4 ± 0.7	95.4 ± 0.2	91.1 ± 0.6	90.3 ± 3.2	89.9 ± 3.7	84.4 ± 8.3	11
27 Ex.	34.3 ± 0.4	30.4 ± 0.2	29.4 ± 0.6	34.8 ± 1.3	33.6 ± 1.5	n.a.	n.a.
28 Ex.	14.8 ± 0.2	14.1 ± 0.1	13.3 ± 0.5	16.5 ± 0.7	14.7 ± 0.7	n.a.	n.a.
29 Ex.	5.72 ± 0.15	6.1 ± 0.2	4.61 ± 0.44	7.7 ± 0.4	4.62 ± 0.39	6.1 ± 0.7	4
30 Ex.	24.5 ± 0.3	20.4 ± 0.1	24.2 ± 0.5	23.1 ± 0.9	23.1 ± 1.0	n.a.	25
31 Ex.	25.0 ± 0.3	21.1 ± 0.2	25.2 ± 0.5	26.5 ± 1.0	25.3 ± 1.1	n.a.	n.a.
32 Ex.	21.5 ± 0.3	17.5 ± 0.2	22.5 ± 0.5	23.1 ± 1.1	n.a.	20.7 ± 2.2	24
33 Ex.	5.54 ± 0.14	5.8 ± 0.2	4.93 ± 0.14	6.7 ± 0.3	5.83 ± 0.31	5.8 ± 0.7	n.a.
34 Ex.	92.2 ± 0.8	99.3 ± 0.2	87.7 ± 0.6	94.6 ± 3.2	92.4 ± 3.9	n.a.	100
35 Ex.	9.32 ± 0.20	8.2 ± 0.2	10.5 ± 0.7	10.6 ± 0.5	9.39 ± 0.49	9.5 ± 1.0	9
36 Ex.	15.2 ± 0.2	17.1 ± 0.2	12.4 ± 0.4	17.0 ± 0.8	16.3 ± 0.8	n.a.	16
37 Ex.	17.4 ± 0.3	17.3 ± 0.2	18.1 ± 0.5	17.2 ± 0.8	15.9 ± 0.8	n.a.	19
38 Ex.	21.8 ± 0.3	18.4 ± 0.2	21.2 ± 1.4	n.a.	21.0 ± 1.2	n.a.	n.a.
39 Ex.	5.55 ± 0.15	4.3 ± 0.1	5.13 ± 0.44	6.7 ± 0.4	5.06 ± 0.40	n.a.	4
40 Ex.	12.2 ± 0.2	13.8 ± 0.2	12.7 ± 0.4	13.8 ± 0.6	12.2 ± 0.6	n.a.	n.a.
41 Ex.	37.8 ± 0.4	40.2 ± 0.3	38.5 ± 0.6	34.3 ± 1.2	35.2 ± 1.5	n.a.	n.a.
42 Ex.	9.82 ± 0.19	8.1 ± 0.1	9.70 ± 0.23	9.9 ± 0.4	8.54 ± 0.38	9.8 ± 1.1	10

(2)* gamma-spectrometry with no potassium correction

(3)* gamma-spectrometry with potassium measurement and correction

n.a. not analyzed

instrumental analytical methods of uranium, thorium and potassium analysis will be of use to the prospective analyst.

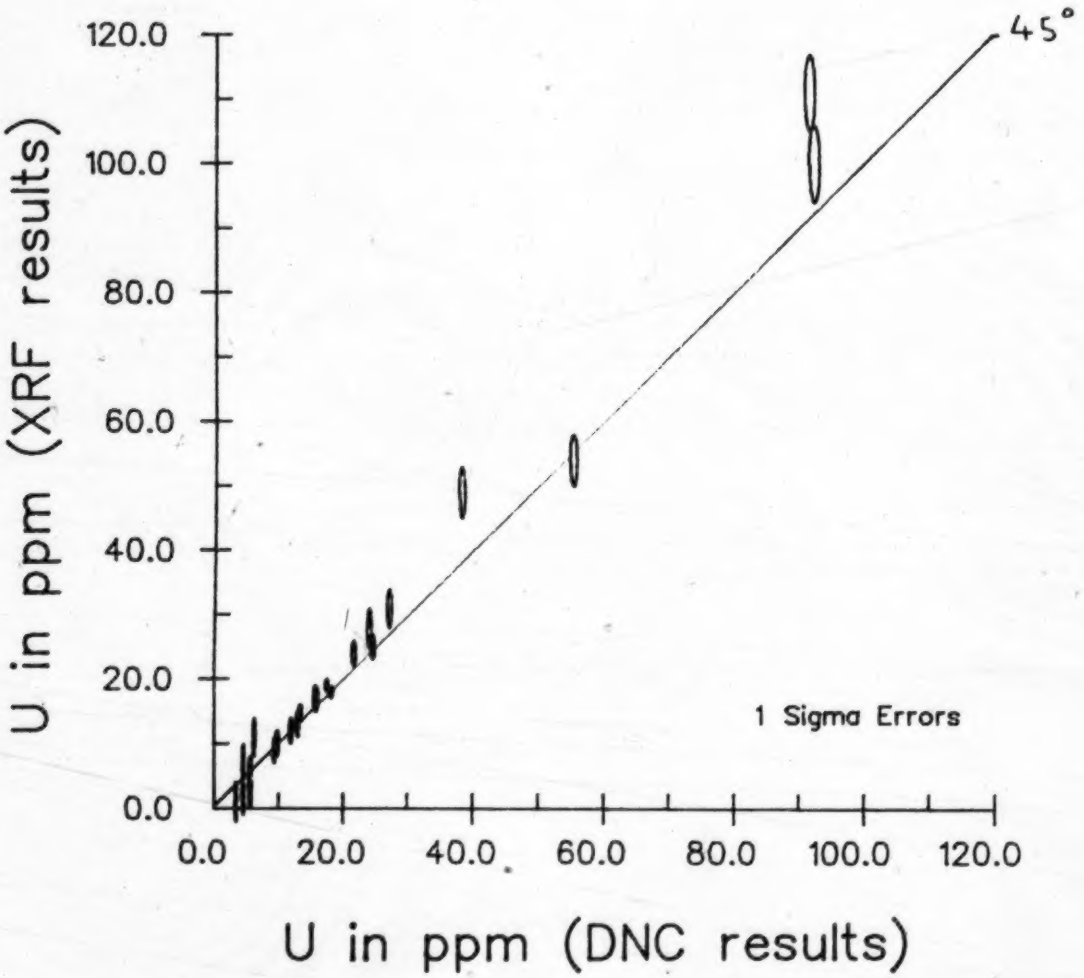

Figure 7.1 Linear plot of uranium content obtained by DNC versus XRF

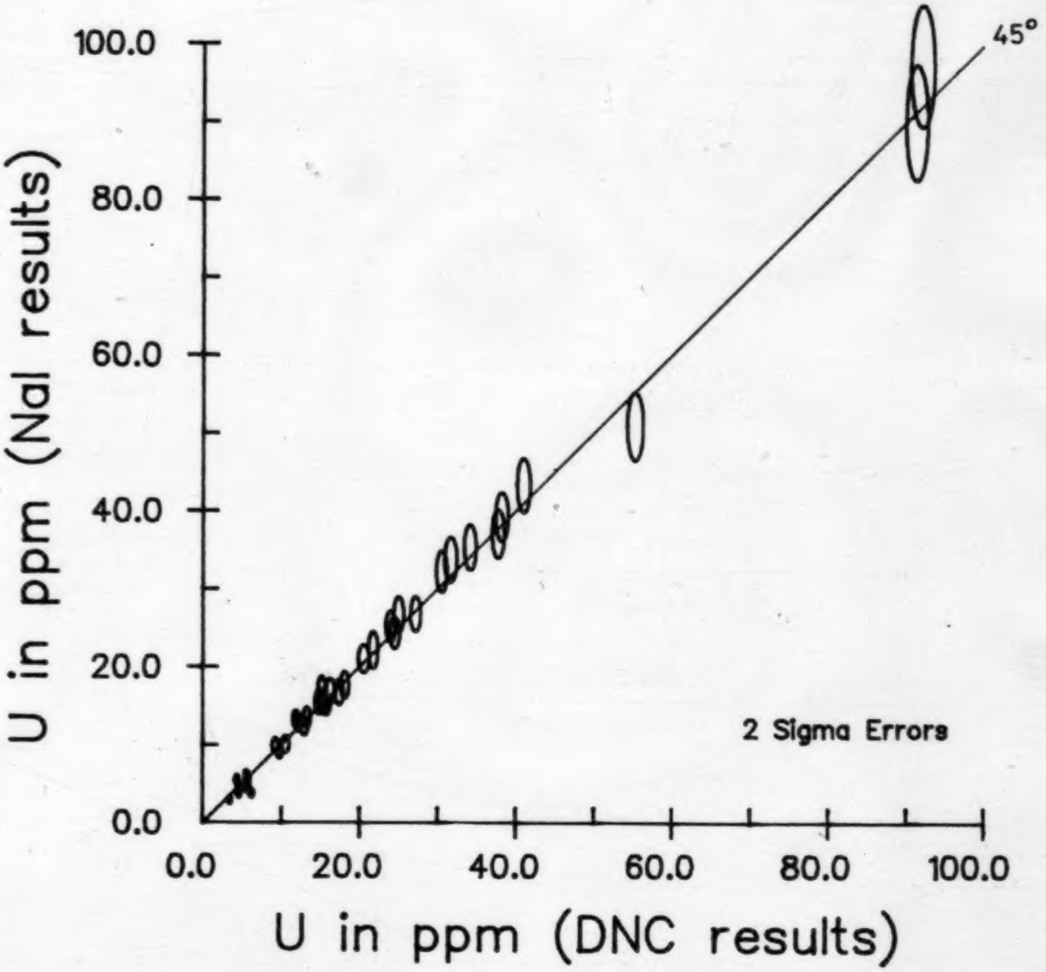

Figure 7.2 Linear plot of uranium content obtained by DNC versus low energy gamma-spectrometry NaI analysis

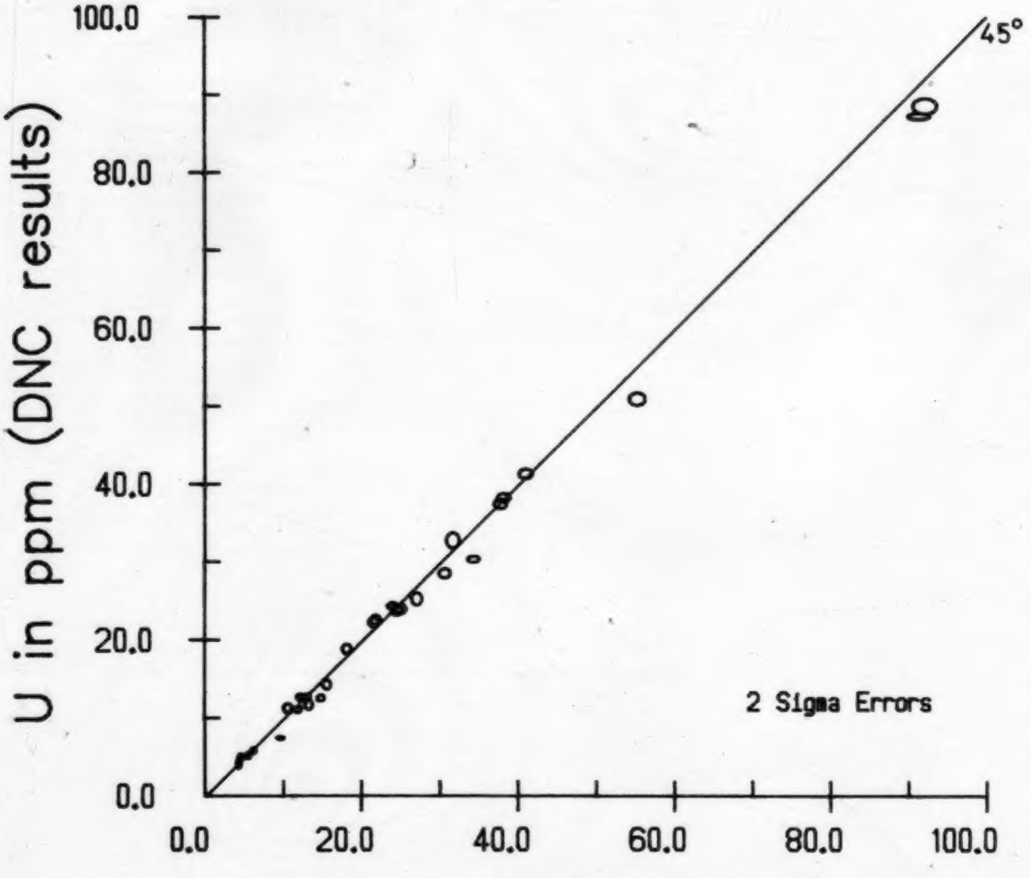

Figure 7.3 Linear plot of uranium content obtained by DNC versus INAA 2 hour irradiation

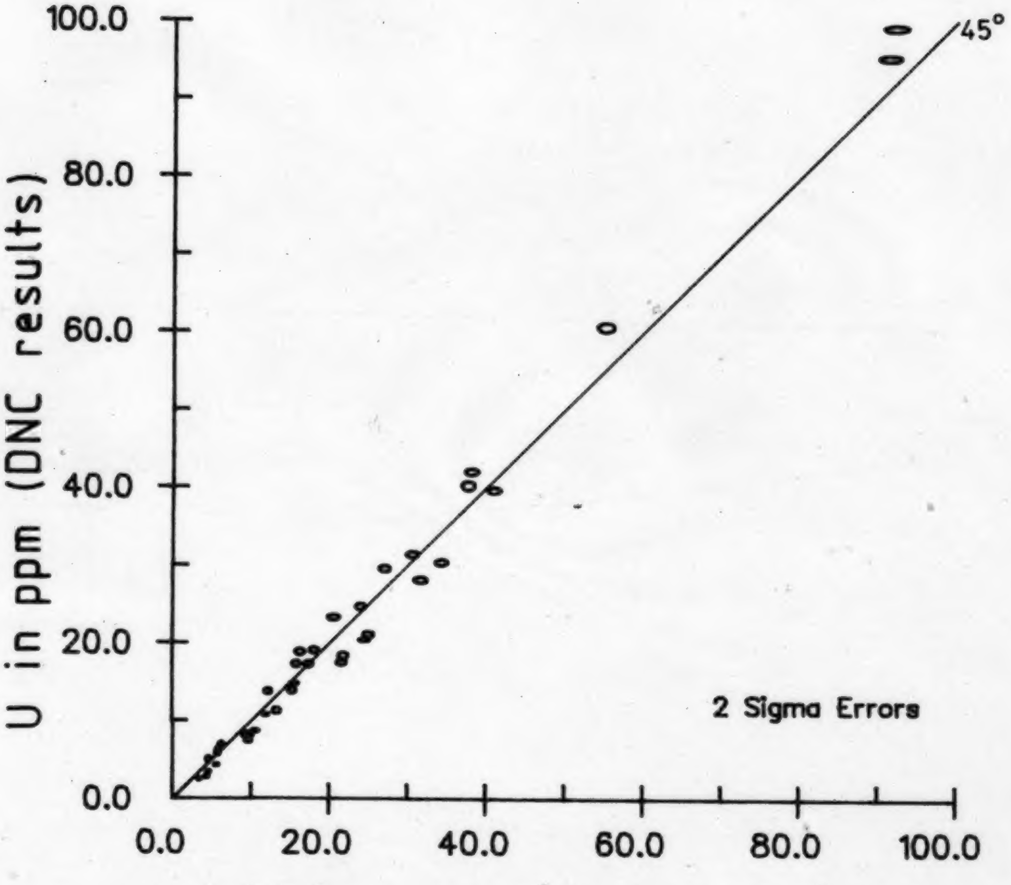

Figure 7.4 Linear plot of uranium content obtained by DNC versus INAA 4 minute irradiation

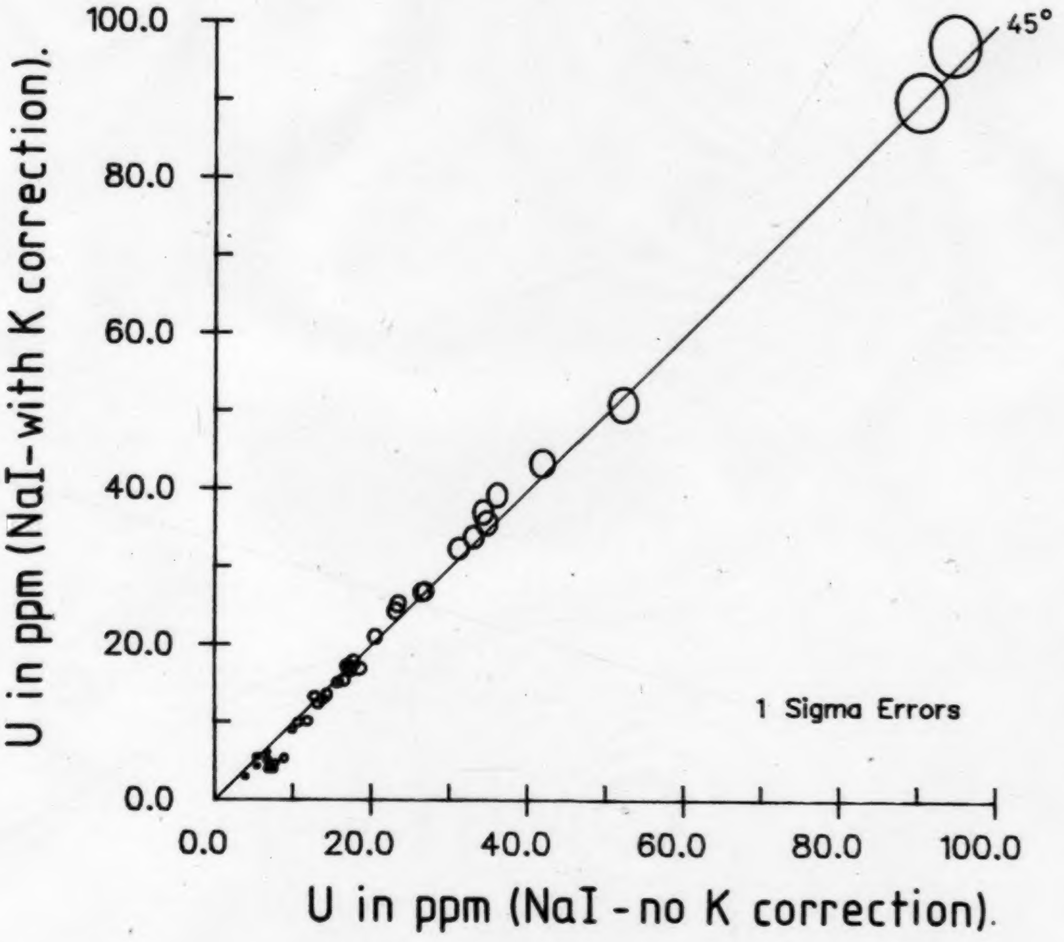

Figure 7.5 Linear plot of uranium content obtained by low energy gamma-spectrometry with and without correction for potassium

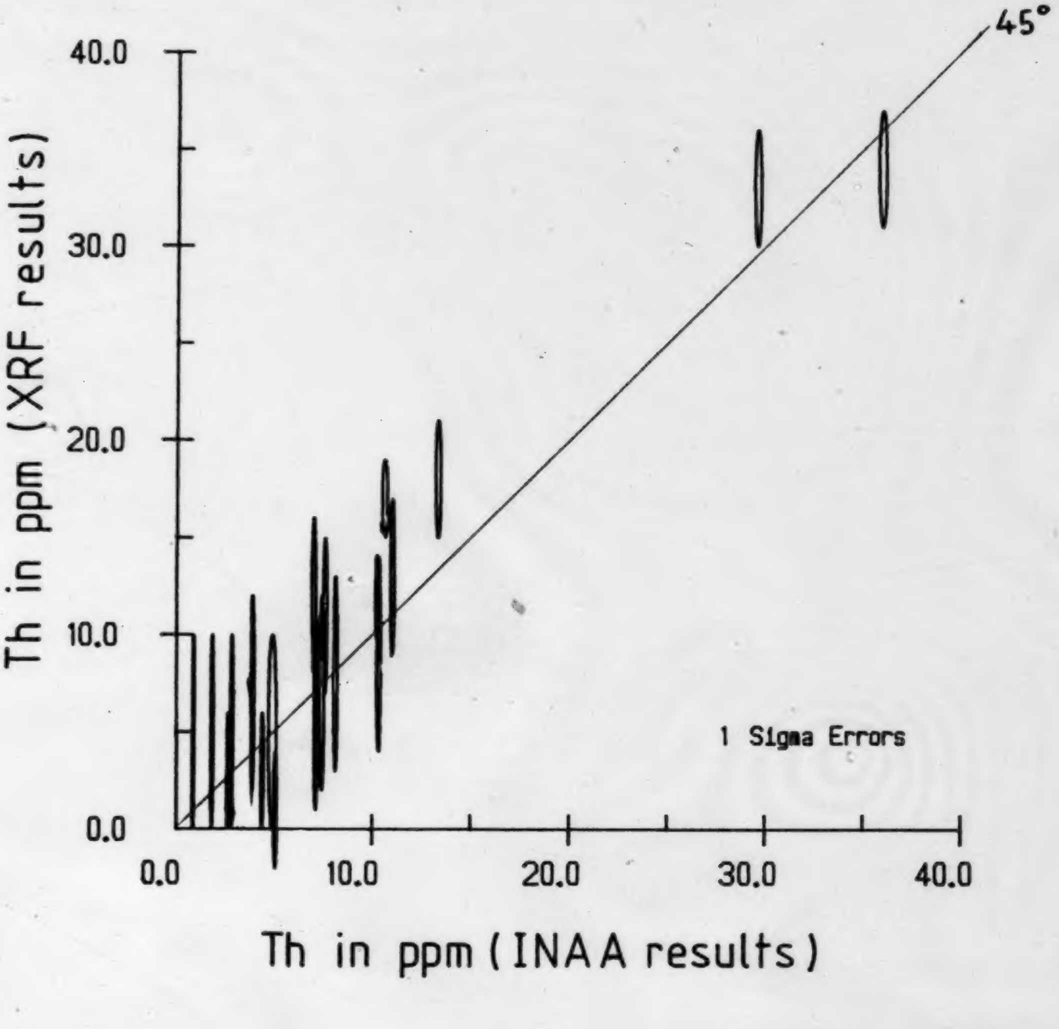

Figure 7.6 Linear plot of thorium content obtained by 2 hour INAA versus XRF

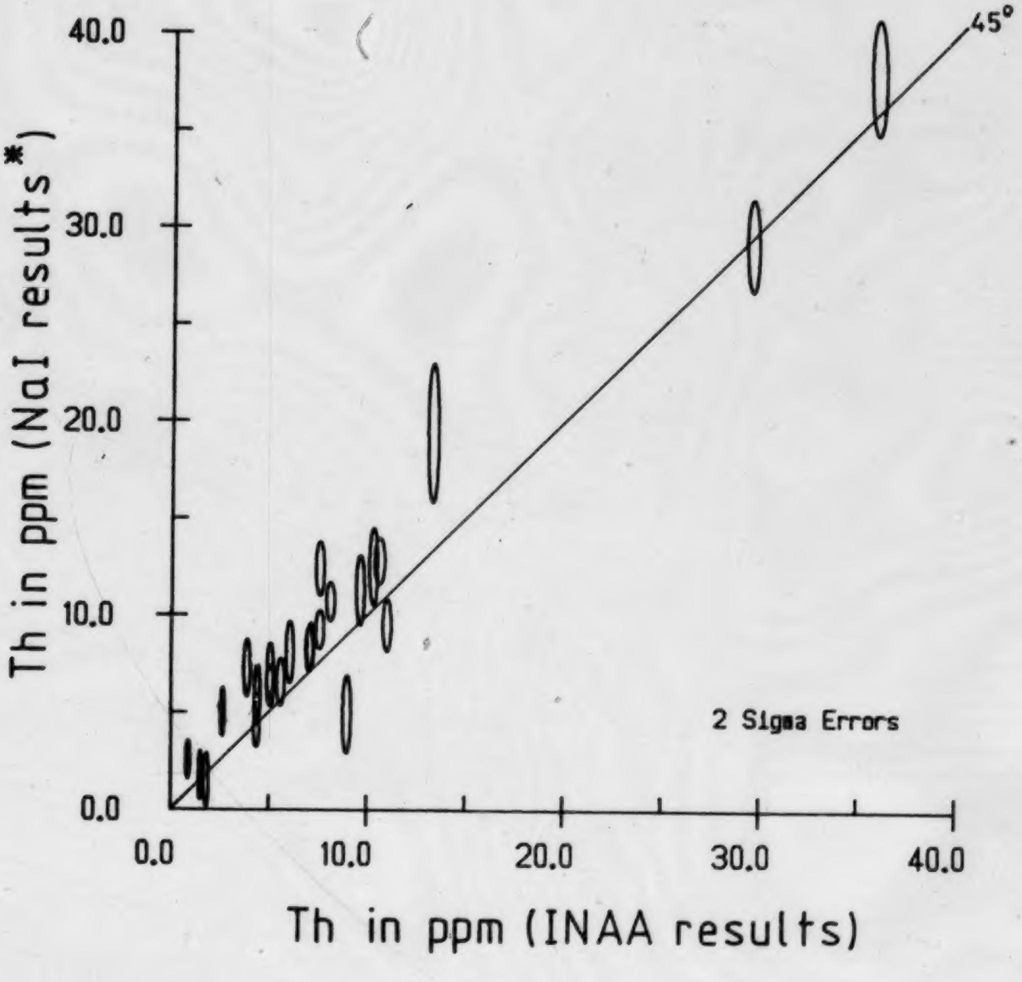

Figure 7.7 Linear plot of thorium content obtained by low energy gamma-spectrometry NaI, corrected for potassium versus XRF

PART II

Geochemistry of the Exshaw Shale.

8. The Exshaw Shale

The Exshaw Formation, although originally thought to have been Devonian in age (Warren, 1937), was dated by Folinsbee and Baadsgaard (1958) at 267 ± 13 My., making it Mississippian (Lower Carboniferous) in age.

The Formation is marine in nature and consists essentially of two units in Alberta - an upper silty limestone and a lower black shale (Havard, ibid) overlying the Wabamum Formation on the plains and the Palliser Formation in the Rocky Mountains and Foothills. On a regional scale, the Exshaw Formation is an extension of a continent wide Devonian - Mississippian black shale sequence and as early as 1948 was correlated with the uraniferous Chattanooga Shale of the Mississippi Valley and Mid-Continent regions of the United States (Fox, 1948).

Ettensohn and Barron (1981) proposed a depositional model to explain the extent and conditions responsible for this continent wide black shale sequence. They suggest that the Acadian Mountains, produced by continent-continent collision, formed a north-south trending barrier across the equator on the east side of the Old Red Sandstone Continent. This mountain range acted as a barrier to moisture-laden trade winds, producing rain shadow conditions west of the mountains were two epicontinental seas, separated intermittently by the Trans-Continental Arch, were located. As a result of being in this rainshadow area, the reduced clastic influx and restricted circulation within the basin, led to the deposition of black, euxinic, organic-rich muds.

8.1 Mineralogy

In hand specimen the shales are fine-grained, fissile and vary in colour from black to dark grey, depending upon their organic and carbonate content. Examination of a number of back-packed, randomly orientated bulk samples was carried out by X-ray diffraction (XRD) analysis to determine sample mineralogy and to see if there was any obvious mineralogical control on the U, Th and K contents of the samples. To this end a Philips wide-angle goniometer-diffractometer and strip chart recorder were used. Samples were selected from their U, Th and K contents and run over a 2θ range of 2-60° at constant instrument settings. This allows the direct comparison of peak intensities between samples so that relative concentrations of the different mineral phases may be obtained. Cu Kα radiation was used for all the 2-60° runs. However, due to a variable 'spike' at the lower 2θ angles in these runs, the majority of the samples were re-run over 2-20° 2θ on a second Philips system using Co Kα radiation.

The 'd'-spacing for each major reflection was calculated and from them the minerals identified. Reflections due to quartz, calcite and dolomite dominated the traces, although those of orthoclase and muscovite were also present in some samples. Although not easily identified (as no clay seperate was taken for analysis) illite was found to be the dominant clay mineral group present in the samples studied. This is in agreement with Havard ibid who carried out more extensive XRD analyses on Exshaw Shale samples from southern Alberta, and various other workers who found illite to be the dominant clay group present in Palaeozoic black shales (e.g. Bloxam, 1964; Leventhal and Hosterman 1982).

No obvious mineralogical control was seen for U and Th. However, as might be expected, K enrichment seems to be related to the orthoclase and illite or muscovite content of the shales.

The relative amounts of dolomite/calcite versus illite may possibly be used as a broad guide for differentiating the Exshaw Formation into its two divisions: the upper silty limestone or dolomite and the lower black shale unit.

8.2 Geochemistry

Ahrens (1954) noted that in most instances the major, minor and trace elements of samples taken from the same population displayed a log-normal distribution. Histograms of the results of this work were found to either follow a log-normal distribution or to closely approach it within the limits of the number of samples analyzed. This is important as many parametric statistical tests commonly employed (e.g. correlation coefficients, cluster analysis etc.) assume a normal distribution. Consequently, before any statistical analysis of the data could be attempted using these tests, log transformation of the data had to be completed. This, and subsquent statistical analysis of the data on the Exshaw Shale, was carried out using the Michigan Interactive Data Analysis System - MIDAS (Fox and Guire, 1976) run on the University of Alberta Amdahl 470/6 computer.

In an attempt to determine and aid in explaining the relationships between the various elements analyzed Pearson product-moment correlation coefficients were determined for all pairs of variables. This coefficient is a measure of the strength of the **linear** relationship between any two variables in queston, that is, how well the variation in one element can be explained by that of another.

The samples were first arbitarily divided into 'black' and 'calcareous' shales based on their CaO content. Those samples with more than 5.0% CaO being classified as 'calcareous'. This was carried out so that any subtle correlations would not 'cancel' each other.

The median values for each element determined in the course of this study are listed in table 8.1 together with 'average' shale values from Turekian and Wedepohl (1960) and metal-rich black shales taken from Vine and Tourlelot (1970).

8.2.1 Major elements

Silicon.

The median silica content for all the Exshaw samples is 48.5% SiO_2 while the calcareous and black shales give 36.9%

Table 8.1 Comparison of average shale values with those of the Exshaw Shale determined in this study

Element	Average Exshaw Shale	Black Shale	Calcareous Shale	Average* Shale	Average † black shale
SiO_2	48.5	58.6	39.6	58.1	——
Al_2O_3	7.20	9.65	5.45	15.1	13.2
Fe_2O_3	3.88	4.46	3.43	6.75	2.86
MgO	1.21	0.84	1.71	2.49	1.16
CaO	4.92	1.69	13.0	3.09	2.10
Na_2O	0.30	0.34	0.25	1.29	0.94
K_2O	2.67	3.32	2.16	3.20	2.41
TiO_2	0.36	0.42	0.31	0.77	0.33
As	21.0	27.8	16.3	13	——
Ba	325	355	299	580	300
Cl	470	565	394	180	——
Co	20.6	24.1	17.9	19	10
Cr	55.3	66.0	47.0	90	100
Cs	4.08	5.33	3.16	5	——
Cu	72	82	62	45	70
Ga	12.3	17.2	9.11	19	20
Hf	2.3	2.9	1.9	2.8	——
Mo	27.6	21.6	35.0	2.6	10
Ni	107	123	92	68	50
Pb	26	30	22	20	20
Rb	78	101	61	140	——
Sb	3.56	4.36	2.93	1.5	——
Sc	9.11	10.9	7.74	13	10
Sr	222	157	303	300	200
Ta	0.65	0.76	0.55	0.8	——
Th	9.2	10.7	8.2	12	——
U	15.6	15.9	15.2	3.7	——
V	227	267	191	130	150
Zn	102	108	95	95	30

* Average shale values from Mason (1966) after Turekian and Wedepohl (1961).

† Average black shale values form Vine and Tourlelot (1970).

(Major elements in weight percent, trace elements in parts per million, ppm.)

and 58.6% respectively. The black shales show a strong negative correlation with Al(r=-0.86) and Ti (r=-0.86) which is contrary to Havard's findings. He notes however, that much of the silica present was biogenetically precipitated as sponge spicules. Therefore, it would be surprising to find that Si would covary with Al and Ti except by chance, when much of the silica present has a completely different origin to that of the clay. The silica content of the calcareous shales shows a strong negative correlation with Ca (r=-0.82) which as expected shows that conditions conducive to limestone formation are very different to those suitable for black shale formation.

Iron.

All the samples gave a median Fe_2O_3 content of 3.88%, while the black shales give 4.46%. The Exshaw black shale value is greater than the average black shale concentration listed by Vine and Tourlelot (1970). Except for a moderate correlation with As (r=0.75) for all the samples (0.76 for the black shales) iron was not found to covary significantly with any other element. Iron pyrites, macroscopically present in many of the samples (particularly the black shales), obviously accounts for much of the iron present. Arsenic, which is concentrated at more than twice the average shale value in the black shales, is presumably incorporated largely within the pyrite structure. The median Fe values obtained are greater than those reported by Havard. This may in part be explained by the fact that a number of his samples were from surface exposures and consequently it may have been difficult to obtain fresh, unweathered samples.

Aluminium.

Good agreement is found between the median Al_2O_3 values of this work and that determined by Havard. For all the samples Al shows strong positive correlations with Rb (r=0.90, 0.98 for the black shales alone), Ga (r=0.86), Ti (r=0.82), Sc (r=0.81), K (r=0.79), Cr (r=0.78), Th (r=0.77) and Ta (r=0.76) (see figures 8.1 and 8.2) and to a lesser extent with Hf, As, Ce, Cs and V. The majority of these are hydrolysate elements (see figure 8.3) and are either structurally combined within the clay minerals and/or are adsorbed by them. The correlations with the soluble cations Rb, K and Cs, suggests that much of the Al also occurs within potassium feldspars, both detrital and authigenic in origin. The poor correlation between Al and the REE suggests, together with other information given later, that the REE's are associated with the clay minerals and that the low REE content of feldspars serves to 'dilute' the correlation with the clays. The negative correlation between Al and Ca (r=-0.63) in the calcareous shales supports the silica-calcium carbonate conclusion that limestone and black shale formation are incompatable.

Calcium and Magnesium.

The median values of CaO and MgO differ markedly from the black to calcareous shales, namely 1.69% to 13.04% CaO, and 0.84% to 1.71% MgO, respectively. As shown from some of the

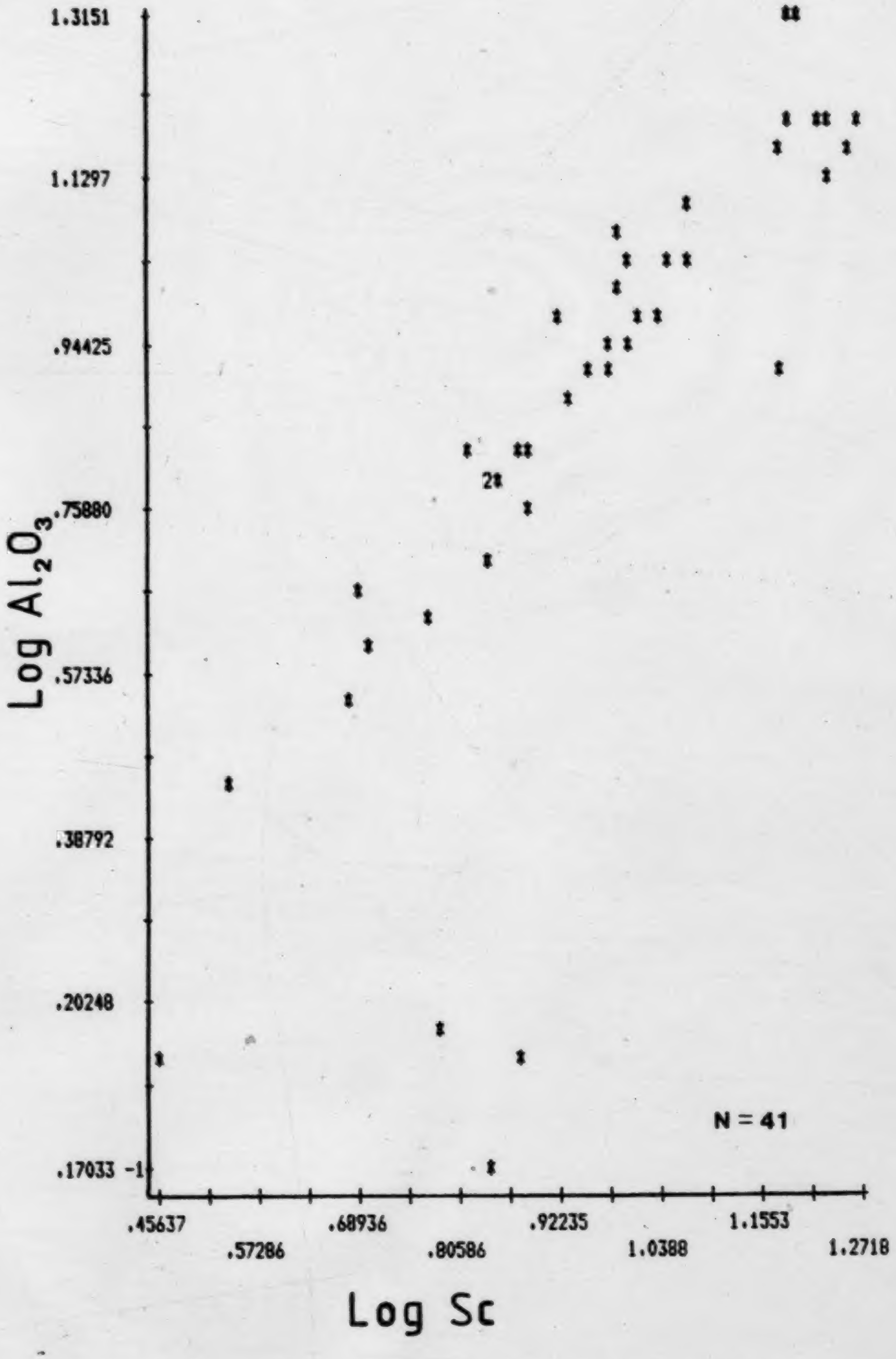

Figure 8.1 Log-log plot of Al_2O_3 versus Sc for the Exshaw Shale

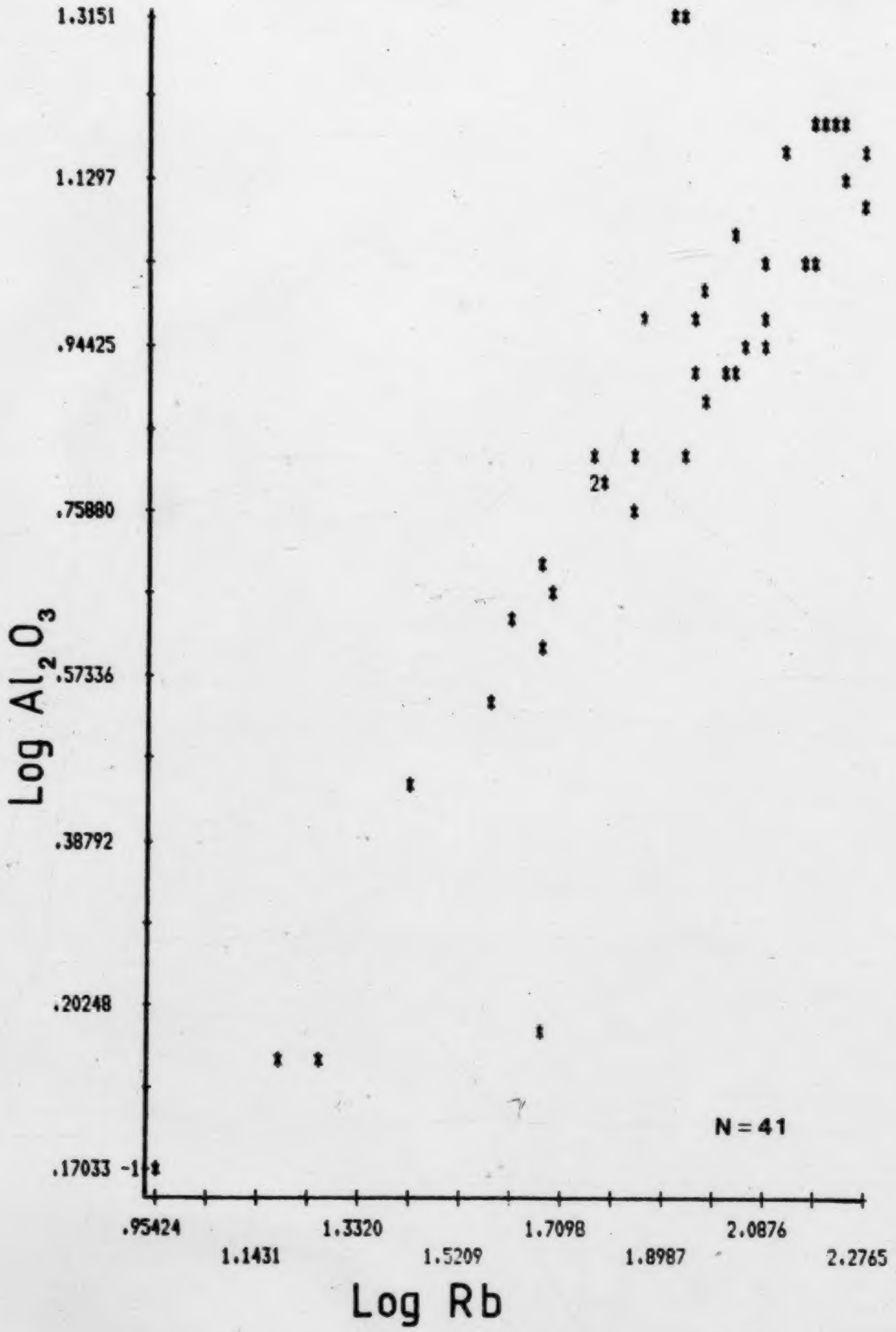

Figure 8.2 Log-log plot of Al_2O_3 versus Rb for the Exshaw Shale

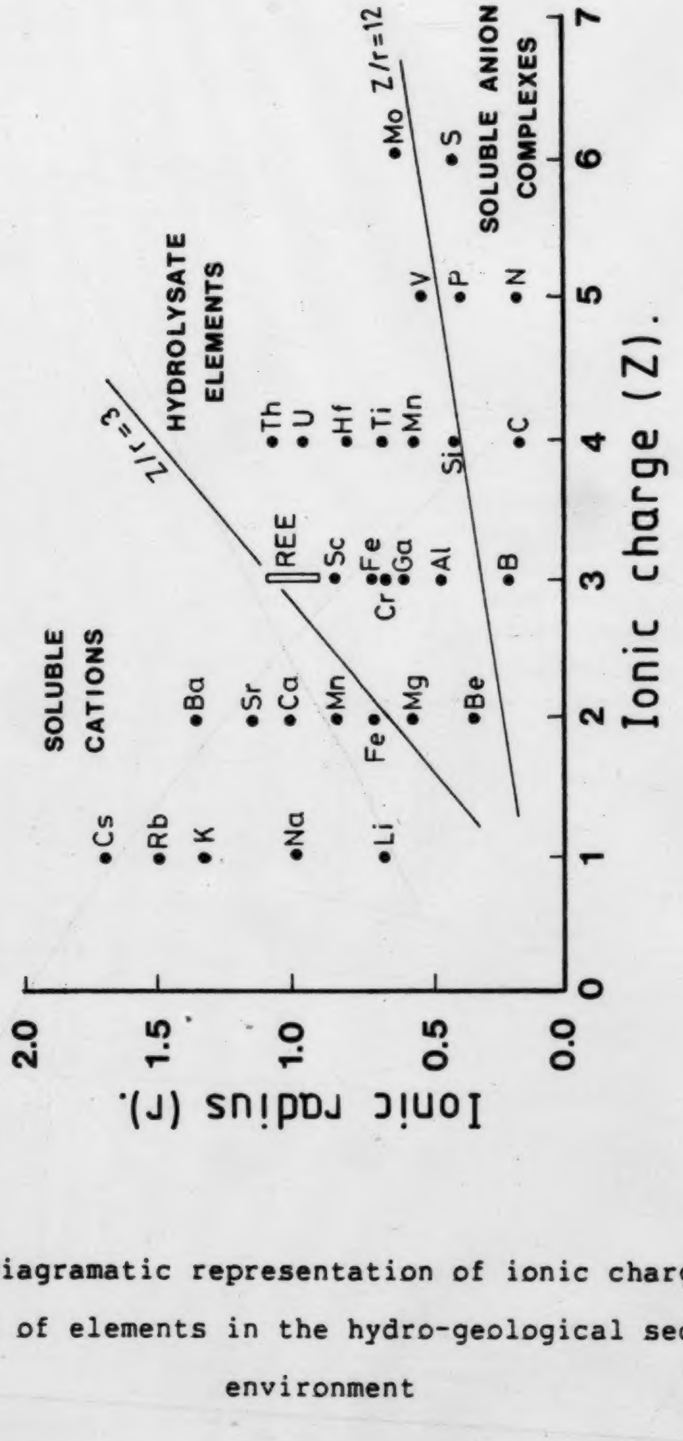

Figure 8.3 Diagramatic representation of ionic charge versus ionic radius of elements in the hydro-geological sedimentary environment

XRD analyses a number of samples contain calcite or dolomite and clearly these are the major sites for the two elements. There is practically a random relationship between Ca and Mg in the calcareous shales in agreement with the general observation that calcite and dolomite do not often occur together.

Potassium.

The median K_2O content varies from 3.32% for the black shales, which is close to the 3.24% of the 'average' shale and in good agreement with Havard's 3.29% for all his samples, to 2.16% K_2O for the calcareous shales. The strongest correlation observed is with Rb ($r=0.79$ for all samples, see figure 8.4) which is not unexpected on account of their similar ionic radii and identical charge. From the correlations with many of the other hydrolysates and soluble cations potassium, like aluminium, is thought to be located in both the clay minerals (dominantly illite) and in detrital and authigenic potassium feldspars.

Sodium.

Of particular note is the very low concentration of Na_2O (0.32% for all samples) compared to the average shale value of 1.30%. Slightly more than four times lower than the average shale this emphasises the dominance of illite as the major clay group present (as opposed to the more sodic smectites), and potassic detrital and authigenic feldspars. The little sodium that is present probably does occur with the clay minerals.

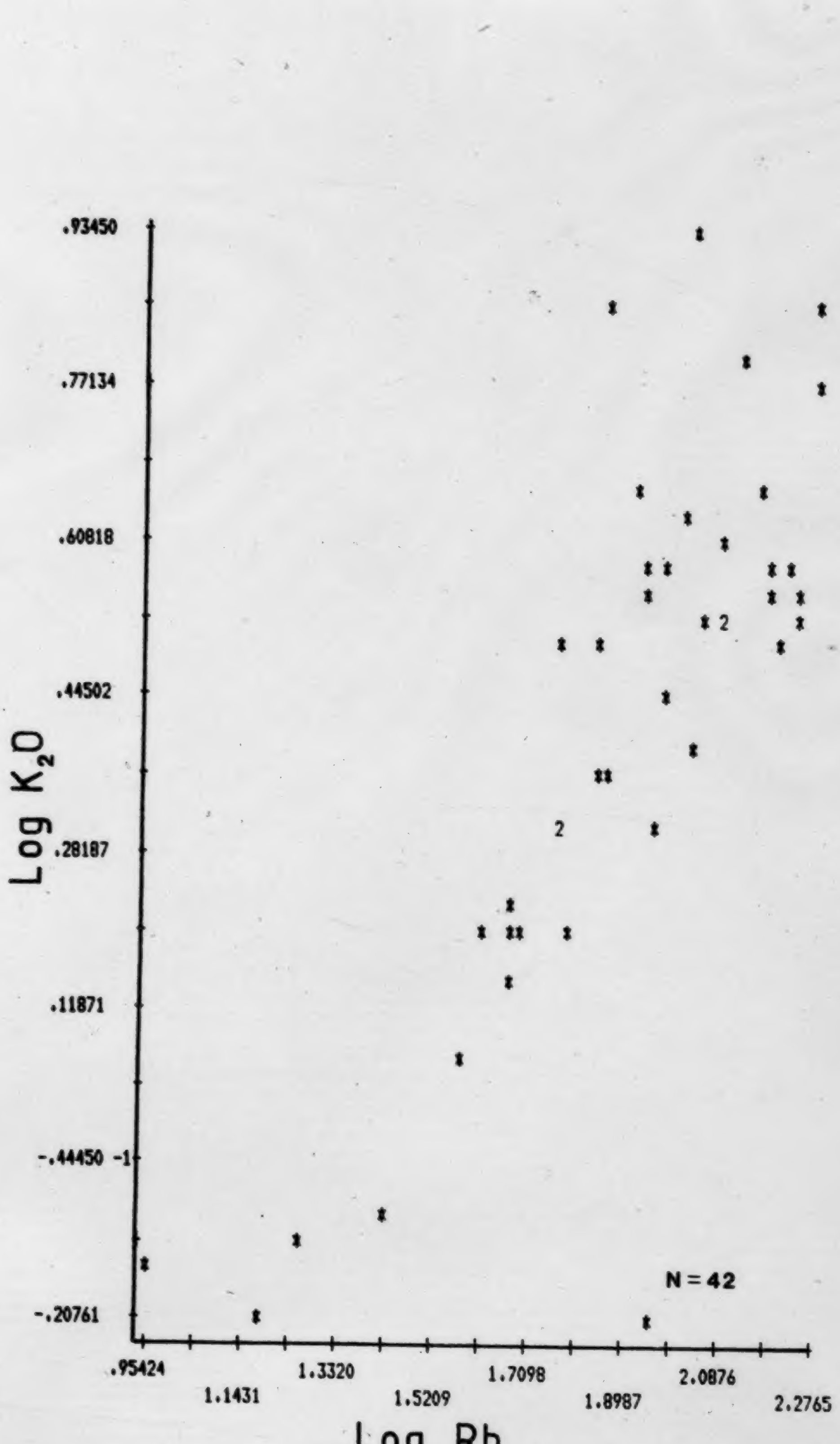

Figure 8.4 Log-log plot of K_2O versus Rb for Exshaw Shale

Titanium.

The median TiO_2 value for all the samples is 0.36%. Although in excellent agreement with Havard's average value of 0.35%, it is much lower than the average shale value of 0.76%. The strong correlation with Al and K, two of the major clay forming elements, together with the hydrolysate elements Sc, Cr, Ga, Th, Ta and Hf show titanium to be largely associated with the clay fraction and not, as is often the case, only with detrital resistates such as ilmenite and sphene. Hirst (1962) noted from studying the geochemistry of modern sediments in the Gulf of Paria that the Al_2O_3/TiO_2 ratio of the sediments was fairly constant and that it was unlikely that much Ti was precipitated out of solution. He suggested that it was more likely that the Ti was associated with the clay fraction during weathering and transportation. As the Exshaw shale sedimentation rate is thought to be have been very low, and there is a lack of coarse clastic material present, the low Ti content may therefore be a consequence of the paucity of detrital material.

8.2.2 Rare Earth Element Geochemistry

As noted earlier, in the process of analyzing samples for uranium, thorium and potassium by INAA a number of other elements may be determined simultaneously. Depending upon the rock type and matrix, seven to nine of the fourteen rare earth elements (REE) may routinely be quantified by the procedure described. Due to their similar ionic radii and preferred trivalent oxidation state the REE generally behave coherently[20], and consequently they have been the basis of many geochemical studies. Traditionally, they have been utilized in hardrock research, though over the past two decades their application to sedimentary problems has been on the increase.

Overview of REE in sedimentary rocks

From the early work of Haskin and Gehl(1962), Haskin and Frey(1966), Haskin *et al*. (1966), and Ronov *et al*. (1967,1974) a number of features became apparent regarding the REE contents and patterns of sedimentary rocks. Of particular note was the similarity of REE patterns (when normalized to chondrite REE values) between shales of various ages and locations (albeit that the relative abundances differed). This helped compound the idea that during shale formation exposed upper crustal material was both representively sampled and mixed in an efficient manner.

In addition it was found that the total REE contents in clays > sands > carbonates, and that the REE are generally adsorbed by clay minerals and transferred almost quantitatively into clastic sediments. Relative to chondrites, sediments are enriched in all the REE, with an increasing enrichment of the light REE (La-Sm).

Due to the similar REE patterns of sedimentary rocks Haskin and Frey (1966) published the results of the analysis of a composite of forty shale samples, called the North American Shale Composite (NASC) with which most sediments and sedimentary rocks have been compared (see for example Haskin et al. (1966), and Dypvik and Brunfelt (1976,1979)).

---

[20] Eu and Ce are exceptions, Eu^{3+} may be reduced to the $^{2+}$ state and Ce^{3+} oxidized to the $^{4+}$ state.

As REE contents and patterns of clastic sediments were thought to reflect the parent material of the sediment, Ronov et al. (1967) suggested that there may be a major change in the patterns and absolute abundance of the REE at the Archaean-Protoerozic boundary, when major additions of felsic material to a predominantly mafic continental crust were thought to have occurred. Their few analyses seemed to support this idea. Work by Nance and Taylor (1976), and McLennan et al. (1980) showed conclusively that such a pattern change does infact occur. Analysis of essentially unaltered Archaean (world-wide distribution) and post-Archaean sedimentary rocks (from Australia) showed the former to have no negative Eu anomaly when chondrite normalized compared to the post-Archaean Australian sedimentary rock (PAAS) and the NASC. In addition analysis of the various shales of different ages that made up the PAAS showed there to be an increase in the absolute abundance of the REE with time (figure 8.5).

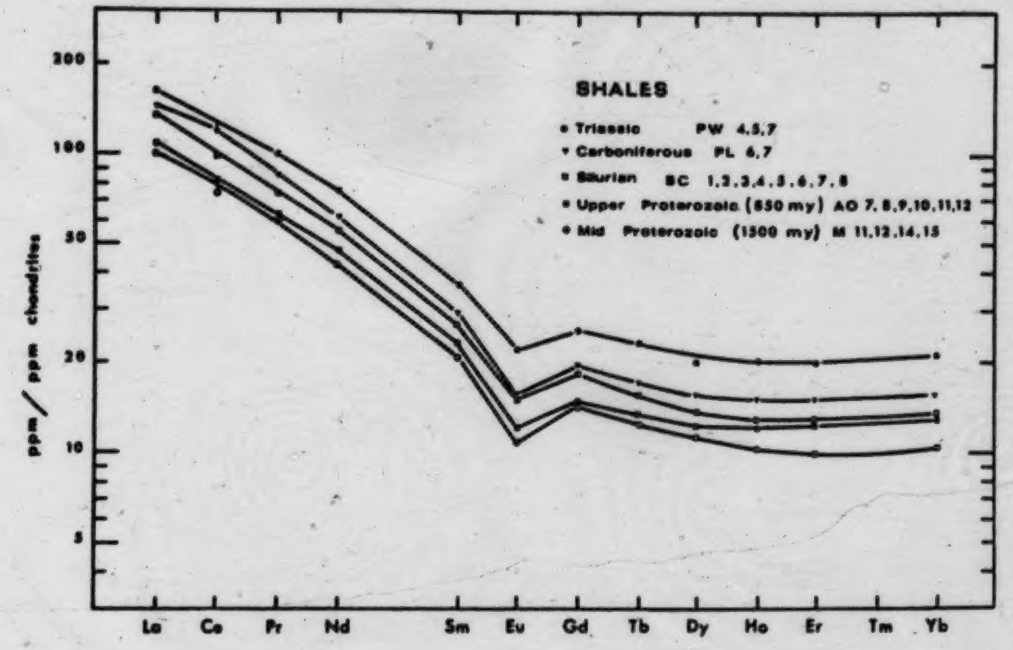

Figure 8.5 REE normalized patterns for Australian shales of various ages

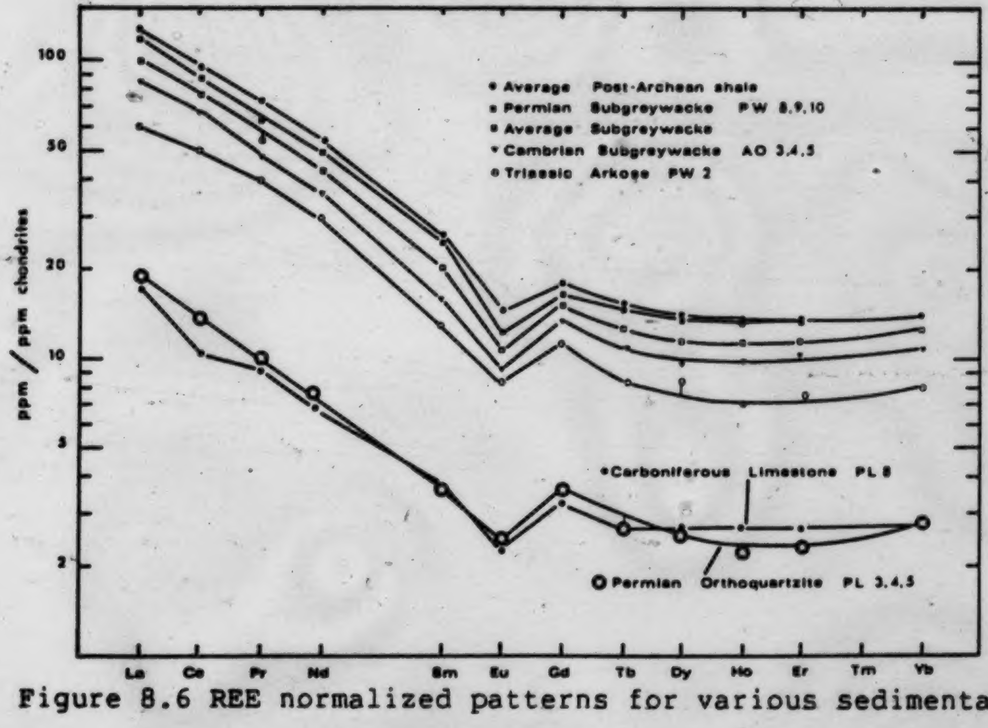

Figure 8.6 REE normalized patterns for various sedimentary rocks

Results of this work

The results for each Exshaw Shale sample analyzed are given in Appendix 1. The median and extreme values, normalized to chondritic values (Nakamura,1974) are plotted in figure 8.7, together with the North American Shale Composite, Post Archaean Australian Shale and the Alun Shale of Norway (Dypvik and Brunfelt, 1976). The Alun Shale is lower Palaeozoic in age, slightly uraniferous (Bjørlykke,1974), is thought to have been deposited in a shallow epicontinental sea, and the samples analyzed:

> "represent typical black shales high in organic carbon and sulphides, deposited under extremely slow sedimentation rates, about 1mm/1000 years." Dypvik and Brunfelt (1976) p.372.

Clearly then the conditions under which both the Alun and Exshaw Shales formed were very similar, and this may allow analogies to be drawn between them. In addition to the conditions under which they formed, their REE patterns are quite similar even to the extent that they both have negative Ce anomalies (see figure 8.7).

To compare the mean Exshaw results with other shales the median values have been normalized to the PAAS and the results plotted in figure 8.8. From this diagram, it can be seen that the total REE of the Exshaw Shales are less than those of both the PAAS and NASC. This is in part due to the older age of the Exshaw Frm. compared to many of the samples making up the PAAS (see figure 8.5) but more importantly it is thought to be due to dilution of the shales by carbonates

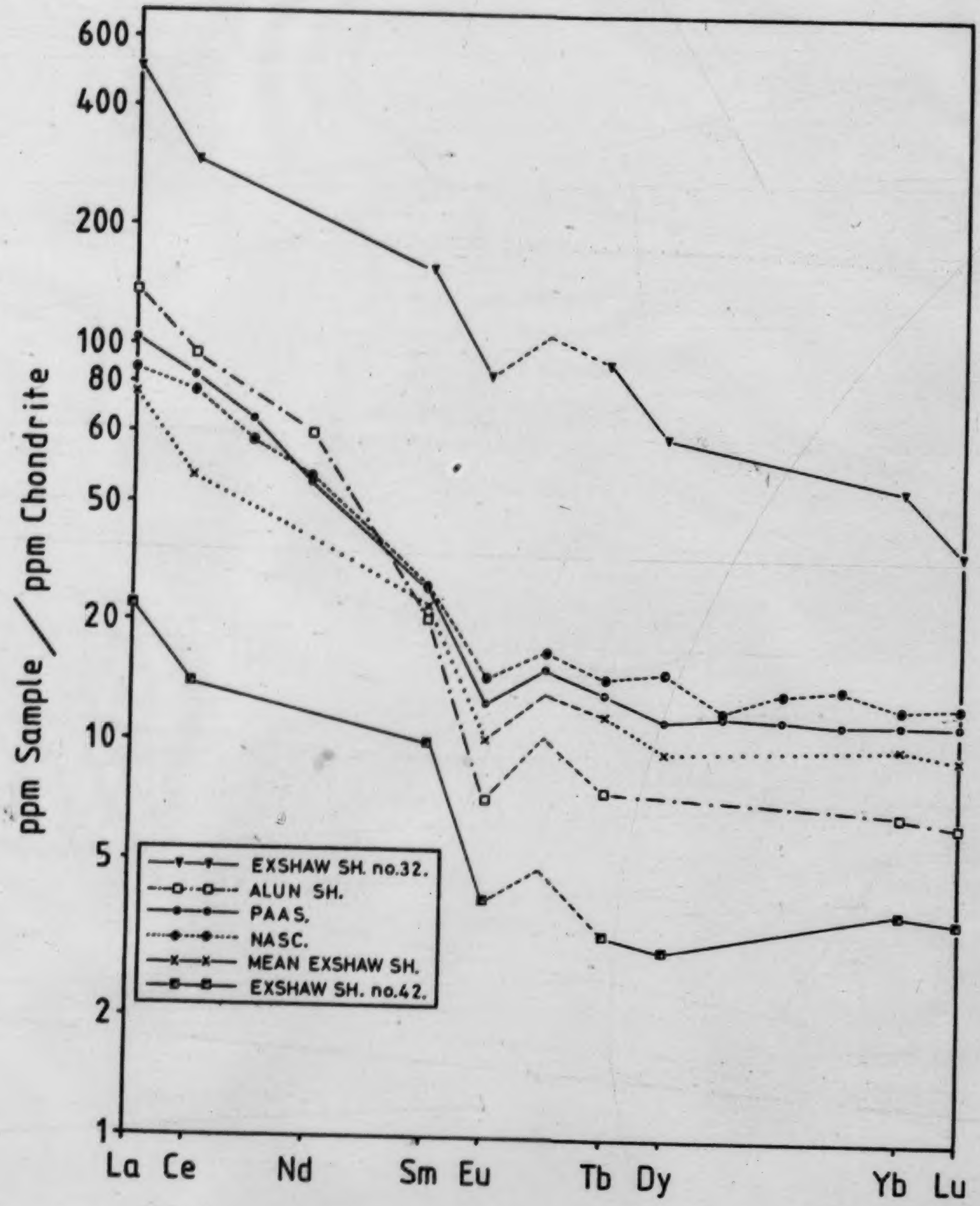

Figure 8.7 REE normalized patterns of the Exshaw Shale and comparatory shales

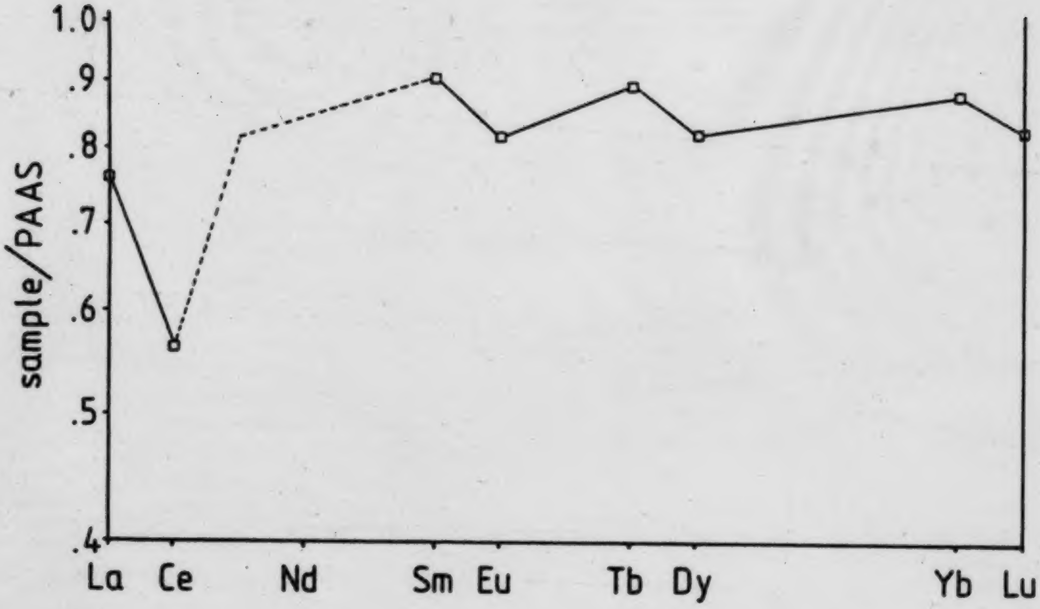

Figure 8.8 REE pattern of the mean Exshaw Shale normalized to the post-Archaean Australian shale

(see figure 8.6) and possibly by biogenetic silica (see later) both of which are known to be depleted in the REE relative to clays (Nance and Taylor (1976) and Piper (1974)). A similar effect was observed in some of the samples from the Oslo epicontinental sequence, where it was suggested that depletion in the total REE contents of two samples, 56 and 57 was:

> "probably the result of dilution by relatively large amounts of calcite in 56 and quartz in 57." p.373 Dypvik and Brunfelt (1976).

The smaller Exshaw Eu anomaly suggests that there is less feldspar in the Exshaw than in the PAAS, as feldspar concentrates Eu during magmatic processes. From the PAAS normalized plot Sm and the heavy REE (HREE) Dy, Tb, Yb and Lu are quite smooth (although depleted relative to the PAAS by 10 - 20%) while the light REE (LREE) La and Ce are significantly depleted relative to the PAAS. Of particular note is the negative Ce anomaly.

What is the cause of this negative anomaly in the Exshaw Shale? Ronov *et al.*(1967) noted that Ce^{3+} may be oxidized to the Ce^{4+} in zones of weathering and sedimentation, and that in this oxidized state its behaviour is more similar to the HREE than the LREE. In addition, of all the REE only Ce may be oxidized in seawater to the

> "highly insoluble quadrivalent state" (Piper 1974, p.286)

Piper (1974) found that Ce was significantly depleted in seawater as well as in foraminifera (after Spirn, 1965) and diatoms, these organisms inheriting their REE patterns from seawater. Nance and Taylor (1976) analyzed and plotted the REE pattern of a Carboniferous limestone which displayed a negative Ce anomaly and Ce/La ratio of 1.68 (cf. NASC and PAAS ratios of 2.28 and 2.10 respectively). They did not however find a Ce anomaly in the PAAS and explained it as follows:

> "The absence of cerium anomalies observed in this study indicates that equilibrium during deposition with seawater, which has a pronounced negative cerium anomally, does not take place" (Nance and Taylor,1976, p.1543)[21]

A number of factors appear therefore to have contributed to the negative Ce anomaly of the Exshaw Shale. Dilution of the black shale component by the calcareous shales appears in part to have been responsible, as is shown by the chondrite normalized plots of the two shale components in figure 8.7. The extremely slow sedimentation rate of the Exshaw Shale would also have offered greater opportunity for equilibrium to have been approached, if not gained between sediment and seawater, than would more rapid deposition. This idea is supported by the extreme similarity of the REE contents of the Exshaw black shales and the sedimentary rocks from the Oslo region of Norway (Dypvik and Brunfelt, 1976). Finally, as mentioned earlier, much of the silica present in the Exshaw Shale is of a biogenetic origin (Havard, 1967). Presumably the silica of sponge spicules precipated from seawater would also have a negative Ce anomaly similar to that found for diatoms (also siliceous) and foraminifera.[22]

---

[21] 'anomally' spelt as reported in publication.

[22] The author knows of no REE analyses of sponge spicules to

Towards the end of this study the publication by Tlig and Steinberg (1982) regarding recent sediments of the Indian Ocean added weight to this idea. One of their findings was:

> "The negative Ce anomaly of the coarsest fraction is associated with the biogenic components (foraminifera, diatoms) which inheret their REE distribution from seawater." (Tlig and Steinberg (1982) p.331)

However, it is not possible to explain the observed anomaly soley by dilution of an 'average' shale, say the NASC or PAAS, by sponge spicules. It is therefore concluded that the anomaly is the combined result of dilution by carbonates and the contribution of biogenetic fractions.

REE and other element correlations

As one would expect, all the REE are strongly correlated with each other. For example the correlation between La and Ce is 0.96, between Dy and Sm 0.98 and between Tb and Sm 0.93 (see figures 8.9, 8.10, 8.11). Most of the remaining strong REE correlations are with hydrosylate elements, in particular Hf, Ta, Ga and Th which agrees with the hypothesis that the REE are largely associated with the clay minerals. The correlation between Th and the REE (in particular La) is of particular interest and is the subject of a publication by McLennan and Taylor (1980). They note that the La/Th ratio of mafic igneous rocks is greater than that of felsic igneous rocks. Statistically they were able to show that the La/Th ratio

---

[22](cont'd)support this idea.

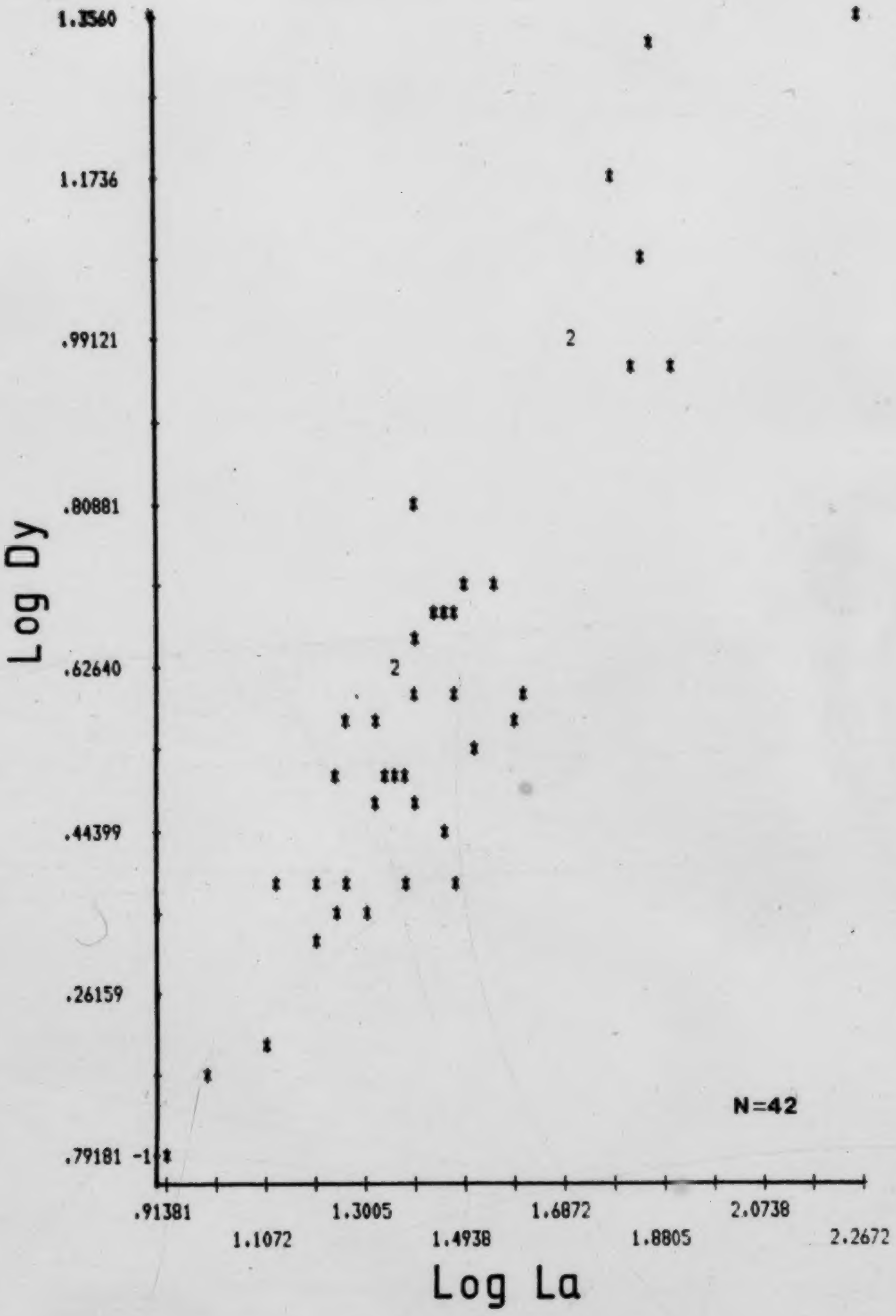

Figure 8.9 Log-log plot of La versus Dy for Exshaw Shale

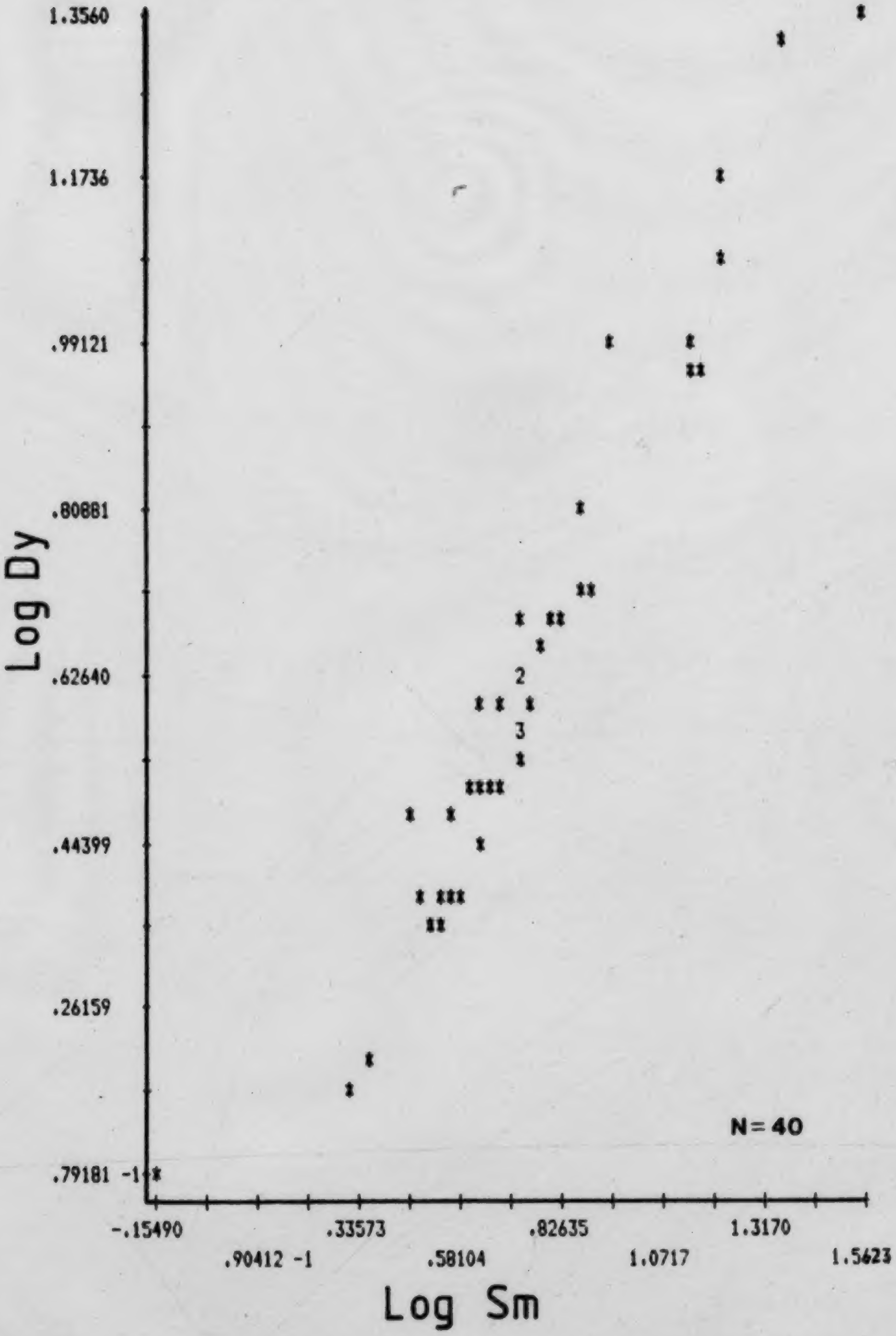

Figure 8.10 Log-log plot of Dy versus Sm for Exshaw Shale

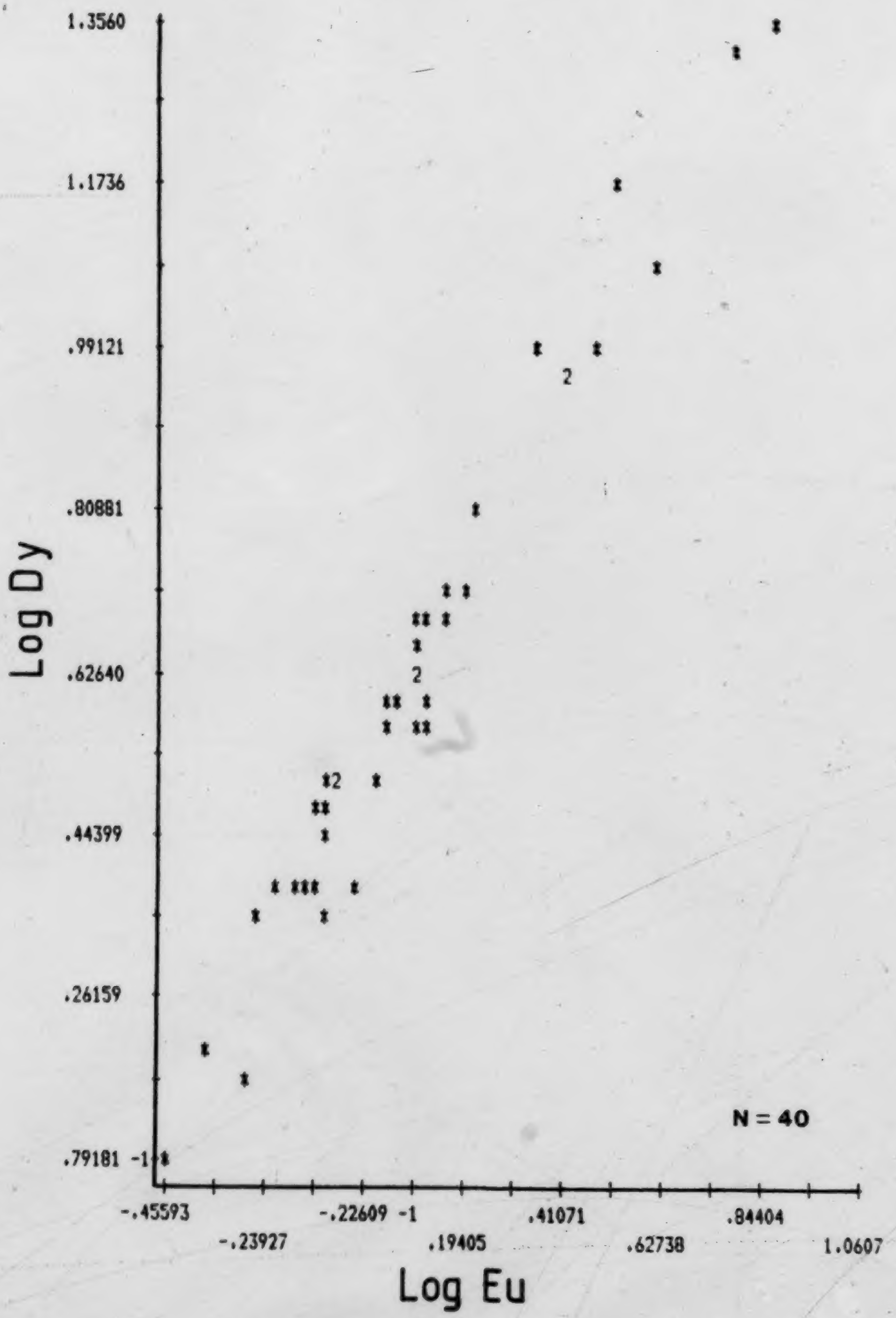

Figure 8.11 Log-log plot of Dy versus Eu for Exshaw Shale

for the Australian Archaean Shale (AAS) is greater than that of the PAAS and suggest that this is additional evidence for a more mafic upper crust in Archaean times than at present. Some 75% of the PAAS analyses lie between the La/Th ratio of 2 and 4. Results of this work show greater variability, which possibly suggests that during Palaeozoic times the exposed Canadian Shield was quite variable in composition.

Of interest are the average La, Th, U, Rb and K_2O values for the Archaean and post-Archaean crust calculated by McLennan and Taylor (1980). These values, together with the median values for all the Exshaw Shale samples and the black shale samples are listed in table 8.2. Except for the anomalous uranium values, the agreement between the black Exshaw Shale samples and both the PAAS and the average values for the Canadian Shield (Shaw et al. 1967, 1976) are excellent. This agreement suggests that black shales may be used to estimate the average composition of the source area. On a regional scale they may possibly therefore, be used to evaluate the average composition of the continental crust. As suggested by McLennan and Taylor (1980, 1980b) it would then be possible to demonstrate whether the composition of the continental crust has been changing with time. Once again dilution of the shales by the carbonate component may account for the lower median Exshaw Shale values.

Table 8.2 Comparison of some elemental concentrations in the post-Archaean upper continental crust with the Exshaw Shale

	a.	b.	c.	d.	e.
La (ppm)	30	30	32	27.9	29.7
Th (ppm)	11.1	10.5	10.3	9.2	10.7
U (ppm)	2.9	2.5	2.45	15.6	15.9
Rb (ppm)	115	110	100	78	101
K_2O (%)	3.5	3.30	3.11	2.67	3.32

(after McLennan and Taylor,1980)

a. The post-Archean upper continental crust (McLennan et al.,1980)
b. The post-Archean upper continental crust (Taylor and McLennan, 1980)
c. The average exposed Canadian Shield (Shaw et al., 1967, 1976)
d. The median of all Exshaw Shale samples analyzed (this study)
e. The median of all black Exshaw Shale samples analyzed (this study)

8.2.3 Uranium and Thorium geochemisty

Uranium

Maximum and minimum U values for the Exshaw Shale samples range from 92.2 ppm to 3.4 ppm, with a median value of 15.6 ± 2.2 ppm. This value is in agreement with the 13 ± 8 ppm mean and standard deviation reported by Campbell (1980) for the Exshaw Shale from a frequency vs. log uranium plot. The 15.6 ppm is a factor of four greater than the 'average' shale value of 3.7 ± 0.5 ppm (Adams and Weaver, 1958) and a factor of five greater than the average post-Archaean shale at 3.1 ± 0.2 ppm (McLennan and Taylor, 1980b). The level is however less than the Chattanooga Shale median uranium value of 20 ppm (Landis, 1962). In a given core large variations in the uranium concentrations were found, for example, one core showed a minimum and maximum concentration of 12.9 and 91.4 ppm U. Variations, similar in magnitude to this have been observed in Devonian black shale cores by Leventhal (1978).

The median values for the black and calcareous shales at 15.9 and 15.2 ppm U respectively show that there appears to have been no obvious mineralogical control in either group which controlled the enrichment.

A number of workers (Bloxam, 1964, Mo *et al*. 1973, Kelepertsis, 1981, Leventhal, 1978 and Leventhal and Hosterman, 1982) found there to be a strong correletion between uranium and the organic carbon content of black and calcareous shales. This suggests that uranium was precipitated out of solution by the reduction of the soluble U^{6+} ion to the insoluble U^{4+} ion which was then either adsorbed by, or complexed with, the organic material present. The tabulated U, Th, K_2O and organic C correlation coefficients for the Exshaw Shale samples are given in table 8.3. Uranium is most strongly correlated with organic carbon, particularly in the black shales. This suggests that uranium was supplied in solution (as it has only weak correlations with most of the remaining thirty or so elements determined) from a low lying source area and precipitated out of solution in a reducing environment under conditions suitable for the preservation of organic matter, and was able to attain the concentrations found due to the very low sedimentation rate.

The only other element which uranium is found to correlate significantly with is nickel (0.70). This finding is in partial agreement with the sympathetic variation of U with Ni and Zn observed in the Exshaw Shale by Campbell (1980).

Thorium

In the Exshaw samples analyzed thorium concentrations ranged from 1.8 to 43.8 ppm, with a median value of 9.2 ± 1.9 ppm (N=42, ±1 sigma). This is slightly lower than the average shale value of 12 ± 1 ppm Th reported by Adams and Weaver (1958), or the 12.3 ppm Th average concentration reported by Bloxam (1964) for Carboniferous black shales from South Wales and is less than the post-Archaean sedimentary rock

Table 8.3 Correlation coefficients for U, Th, K_2O and organic C for the Exshaw Shale

	U	Th	K_2O	C org.
U	——			
Th	0.16	——		
K_2O	0.18	0.62	——	
C org.	0.73	-0.28	-0.14	——

All Samples.

	U	Th	K_2O	C org.
U	——			
Th	0.23	——		
K_2O	0.34	0.72	——	
C org.	0.76	-0.26	-0.11	——

Black Shales.

	U	Th	K_2O	C org.
U	——			
Th	0.08	——		
K_2O	-0.00	0.43	——	
C org.	0.70	-0.31	-0.05	——

Calcareous Shales.

average value of 14.6 ± 1.2 ppm (2 sigma) (McLennan and Taylor, 1980b). The median black Exshaw Shale concentration of 10.7 ± 2.1 (N=19) is however in better agreement with the average shale values. The respective calcareous and black shale median thorium values of 8.2 ± 1.3 ppm (N=23) and 10.7 ± 2.1 ppm (N=19) show there to be little or no significant difference between the Exshaw calcareous and black shale thorium concentrations. Kelepertsis (1981) found the average Th content of intercalated Carboniferous calcareous and black shales in Anglesey, North Wales to be 16 ± 2 ppm (N=5) and 11.5 ± 1.3 ppm (N=4)respectively.[23] However, due to the few samples analyzed little significance may be attached to his findings.

From the earlier disscussions regarding LREE-Th relationships and the correlation coefficients between Th and K_2O shown in table 8.3, it is apparent that much, if not all, of the Th in the Exshaw Shale samples is associated (adsorbed) with the clay minerals. The strong correlations with Al (0.79), Hf (0.90) and Ga (0.82) supports this hypothesis. Bloxam (1964) found that Th and K exhibited some degree of covariance and suggested, as did Pliler and Adams (1962) and Kelepertsis (1981) that Th was most likely associated with the clay fraction (usually illite) of the shales they studied.

---

[23] Kelepertsis (1981) actually reports 19 and 12 ppm Th respectively for the calcareous and black shales but failed to log-transform his data before analysis.

As Th is extremely insoluble in near neutral waters (Kelepertsis, 1981) the slightly lower than average Th content of the Exshaw samples agrees with the hypothesis that during deposition of the sediments, detrital influx was low as the Th was most likely incorporated in detrital clays.

8.2.4 Geochemistry of remaining elements

Alkali metals and Alkaline Earths.

Particularly in the black shales, cesium is found to correlate with Rb and K while Rb is strongly correlated with Al (0.92), Ga (0.90) Ba, K, Sc and Cr. Barium is also found to correlate strongly with these elements. This suggests that Cs, Rb and Ba are largely associated with the clay minerals. Strontium however, is clearly associated with the calcareous shales. This association was also noted by Havard *ibid* and more generally in shales by Vine and Tourlelot (1970).

The Base Metals - Cu, Ni, Pb, Zn and Co

The transitional metals and Pb are all enriched in the Exshaw black shales compared to the average shale values of Turekian and Wedepohl(1961). With the exception of Pb, no significant correlations are observed between these metals and any other element. When enriched these metals are often found to be strongly correlated with organic carbon, with which they often form organo-metallic complexes (Leventhal and Hosterman 1982). Lead is correlated with the LREE, Th and many of the other hydrosylate elements suggesting that it is associated with the clays. The correlation with Th (0.64) agrees with the findings of Weiss and Amstutz (1966), who noted that Pb^{2+} could interchange with Th^{4+} in clays. Their experimental studies showed that between 2 - 6 weight percent Pb may be contained within the illite structure.

9. Conclusions

9.1 Methodology

Of the various methods of uranium analysis used the delayed neutron counting method is to be favoured if only uranium is to be quantified and sufficient sample is available. Where only small quantities of sample are available, fission track analysis or INAA are sensitive alternatives to DNC.

When DNC is used in conjunction with the gamma-ray spectrometry of naturally occurring radioisotopes cases of 5% disequlibrium or greater can be identified. Where, in addition to uranium, multielement information is required, INAA is to be prefered. Conventional XRF analysis for the quantification of U and Th although reasonably accurate lacks precision at typical rock concentrations.

From the analyses of the great variety of rock types analyzed (standards and samples) INAA has shown to be an accurate, and in most instances precise, method for use in the earth sciences.

9.2 Geochemistry

The anomalous radioactivity of the Exshaw Shale is largely due to uranium enrichment (up to 92 ppm), though potassium levels are in certain instances high (maximum of almost 8% K_2O by weight). The median thorium value for all the Exshaw Shale samples is less than the 'average' shale value.

Uranium appears to have been transported in solution, and upon reduction to the insoluble tetravalent state, was either adsorbed or complexed with the organic matter present. In most instances the concentrations of elements from the Exshaw Shale agree well with the values from Turekian and Wedepohl (1961).

Exshaw Shale rare earth element patterns show a negative Ce anomaly in many of the samples analyzed; the anomaly being the result of dilution of the black shale component by calcareous matter and by biogenetic silica.

Agreement between the median elemental concentrations of the black Exshaw Shales and the average values of the Canadian shield (Shaw *et al*., 1967, 1976) suggests that during black shale formation variations in the source area geochemistry are throughly mixed. Consequently, median values, determined from many shale samples, or from a composite shale sample, may be used to estimate the average composition of the exposed source area, and if over a large enough area, the average composition of the exposed continental crust.

References

Abbey, S. 1980. Studies in 'standard samples' for use in the general analysis of silicate rocks and minerals. Part 6:1979 edition of usable values. *Geolological Survey of Canada,* Paper 80-14.

Adams, J.A.S. and Weaver, C.E. 1958. Thorium-to-uranium ratios as indicators of sedimentary processes: example of concept of geochemical facies. *Bull. American Ass. Petrol. Geol.,* V.42, No.2, p.387-430.

Amiel, S. 1962. Analytical applications of delayed neutron emission in fissionable elements. *Anal. Chem.,* V.34, No.13, p.1683-1692.

Amiel, S. ed., 1981. *Nondestructive Activation Analysis - with nuclear reactors and radioactive neutron sources.* (Studies in Analytical Chemistry;3) Elsevier Scientific Publishing Company, The Netherlands. pp.369.

Apps, M.J. 1978. Development of INAA facilities. *University of Alberta SLOWPOKE Facility Annual Report,*. p.11.

Apps, M.J. and Apps, K.S. 1981. NAARUN: a simple to use neutron activation analysis computer program. *University of Alberta SLOWPOKE Facility Annual Report,* R4-5.

Atherton, M.P. and Brotherton, M.S. 1979. Thorium and uranium in some pelitic rocks from the Dalradian, Scotland. *Chem. Geol.,* V.27, p.329-342.

Baedecker, P.A., Rowe, J.J. and Steinnes, E. 1977. Application of epithermal neutron activation in multielement analysis of silicate rocks employing both coaxial Ge(Li) and low energy photon detector systems. *J. Radioanal. Chem.,* V.40, p.115-146.

Bell, R.T. 1978. Uranium in black shales- a review *in* Short course in uranium deposits: Their mineralogy and origin. Kimberley, M.M., ed., Mineral Ass. of Canada, short course handbook, V.3, p.307-329.

Boyce,R.E. and Bode, G.W. 1972. Carbon and carbonate analyses, Leg 9. in Initial Reports on the Deep Sea Drilling Project. Vol. IX, p797.

Bergerioux, C., Kennedy, G., Zikovsky, L. 1979. Use of the semi-absolute method in neutron activation analysis. J. Radioanal. Chem., V.50, No.1-2, p.229-234.

Bloxam, T.W. 1964. Uranium, thorium, potassium and carbon in some black shales from the South Wales coalfield. Geochim. Cosmochim. Acta., V.28, p.1177-1185.

Boulanger, A., Evans, D.J.R. and Raby, B.F. 1975. Uraniun analysis by neutron activation delayed neutron counting. Atomic Energy of Canada Ltd. Commercial Products Report. pp.15

Bouzigues, H., Boyer, R.J.M., Teulires, P. 1975. Proc. Symp. Oklo Phenomenon, and French Atomic Energy Commission, Libreville. 23-27 June, 1975. pp237.

Brenner, I.B. and Hamel, A. 1976. Titanium and trace element elememt data in USGS standard rocks SCo-1 and SGR-1 in Flanagan, F.J(ed.), Description and analyses of eight new USGS rock standards. U.S. Geol. Survey Prof. Paper 840, p.49-58.

Brunfelt, A.O. and Steinnes, E. 1978. Neutron activation analysis for trace element determination in geostandards. Geostandards Newsletter, V.2, No.1, p.3-7.

Bunker, C.M. and Bush, C.A. 1966. Uranium, thorium, and radium analyses by gamma-ray spectrometry (0.184-0.352 million electron volts)., Geological Survey Research: U.S. Geol. Survey Prof. Paper 550-B, p.B176-B181.

Campbell, F.A. 1980. The uranium content of the Exshaw Formation and Belloy Group in Alberta. Current Research, Part B, Geol. Sur. Can., Paper 80-1B, p.145-148.

Chattopadhyay, A and Katz, S.A. 1978. Determination of 22 elements in geological samples by instrumental neutron activation analysis. J. Radioanal. Chem., V.46, p.321-332.

Culbert, R.R. and Leighton, D.G. 1981. Low energy gamma spectrometry in the geochemical exploration for uranium. J. Geochem. Expl., V.14, p.49-68.

Cullers, R.L, Chaudhuri, S., Arnold, B., Lee, M. and Wolf, C.W. Jr. 1975. Rare earth distributions in clay minerals and in the clay-sized fraction of the Lower Permian Havensville and Eskridge shales of Kansas and Oklahoma., Geochim. Cosmochim. Acta. V.39, p.1691-1703.

Currie, L.A., 1968. Limits for qualitative detection and quantitative determination- application to radiochemistry. Anal. Chem., V.40, p.586-593.

DeSoete, D., Gijbels, R. and Hoste, J. 1972. Neutron Activtion Analysis. Elving, P.J. and Kolthoff, eds., John Wiley and Sons, London. pp. 836

Duke, M.J.M. and Apps, M.J. 1980. Mapping the spatial distribution of uranium in geological materials by fission track analysis. University of Alberta SLOWPOKE Facility Annual Report., R28.

Dypvik, H. and Brunfelt, A.O. 1976. Rare earth elements in lower Palozoic epicontinental and eugeosysoclinal sediments from the Oslo and Trondheim region. Sedimentology, V.23, p.363-378.

Dypvik, H. and Brunfelt, A.O. 1979. Distribution of rare earth elements in some North Atlantic Kimmeridgean black shales. Nature., V.278, p.339-341.

Ehmann, W.D., Bruckner, J. and McKown, D.M. 1980. Epithermal neutron activation anaysis using a boron carbide irradiation filter. J. Radioanal. Chem., V.57, No.2, p.491-502.

Ettensohn, F.R. and Barron, L.S. 1981. Depositional model for the Devonian-Mississippian black-shale sequence of North america: a tectono-climatic approach. Prepared for U.S. Dept. of Energy. Contract No. DE-AC21-76ET12040.

Fabbi, B.P. and Espos, L.F. 1976. X-ray fluorescence analyses of 21 selected major, minor and trace elements in eight new USGS rock standards. in Flanagan, F.J.(ed.), Description and analysis of eight new USGS rock standards. U.S. Geol. Survey Prof. Paper 840, p.89-94.

Fisher, D.E., 1970. Homogenized fission track dertermination of uranium in whole rock geological samples. Analyst. Chem., V.42, p.414-416.

Flanagan, F.J. 1976.(ed.) Description and analyses of eight new USGS rock standards. US Geol. Surv. Prof. Pap., 840. pp.189.

Fisher, D.E. 1975. Geoanalytic applications of particle tracks. Earth Sci. Review., V.11, p.291-335.

Fleischer, R.L., and Price, P.D. 1964. Uranium contents of ancient man-made glass.Science V.144, p.841-842.

Fleischer, R.L., Price, P.B. and Walker, R.H. 1975. Nuclear tracks in solids: principles and applications. Berkeley, University of California Press.

Folinsbee, R.E. and Baadsgaard, H. 1958. An absolute age for the Exshaw Shale. Alta. Soc. Petrol. Geol., 8th Annual Field Conference Guide Book. p.69-73.

Fox, D.J and Guire, K.E. 1976. Documentation for MIDAS. Statistical research laboratory, University of Michigan.

Fox, F.G. 1948. The stratigraphy of the Devonian and Mississippian rocks in the Foothills of Southern Alberta. Unpublished Ph.D. Thesis, University of Oklahoma.

Galson, D.A., Atkin, B.P, and Harvey, P.K. 1983. The determination of low concentrations of U, Th and K by XRF. Chem. Geol., V.38, p.225-237.

Gladney, E.S., Owens, J.W. and Starner, J.W., 1978. Simultaneous determination of uranium and thorium in ores by instrumental epithermal neutron activation analysis. Analytica Chemica Acta., V.14, p.157-166.

Gordon, G.E., Randle, K., Goles, G.G., Corliss, J.B., Beeson, M.H. and Oxley, S.S. 1968. Instrumental activation analysis of standard rocks with high resolution gamma-ray detectors. Geochim. Cosmochim. Acta., V.32, p.369-396.

Gryntakis, E.M. and Kim, J.I. 1976. A compilation of resonance integrals PART I, Z = 1-52 (Hydrogen-Tellurium). J. Radioanal. Chem., V.29, p.175-224.

Gryntakis, E.M. and Kim, J.I. 1978. A compilation of resonance integrals PART II, Z = 53-100 (Iodine-Fermium). J. Radioanal. Chem., V.42, p.118.

Hancock, R.G.V. 1982. On the determination of silicon in pottery. J. Radioanal. Chem., V.69, p.313-328.

Hamilton, E.I. 1966. Distribution of uranium in some natural minerals. Science, V.151., p.570-572.

Hart, R.J., Reid, D.L., Stuckless, J.S. and Welke, H.J. 1980. Comparison of three techniques for the determination of uranium and thorium in rocks. Chem. Geol., V.29, p.345-350

Haskin,L.A. and Gehl, M.A. 1962. The rare-earth distribution in sediments. J. Geophys. Res., V.67, p.2537-2541.

Haskin, L.A. and Frey, F.A. 1966a. Dispersed and not-so-rare earths. Science,. V.152, No. 3720, p.299-314.

Haskin, L.A. and Frey, F.A. 1966b. Meteoritic, solar and terrestrial rare-earth distributions. in Physics and Chemistry of the Earth. ed. L.H. Ahrens. V.7, p.167-321.

Havard, K.R. 1967. Mineralogy and geochemistry: Exshaw Frm., southern Alberta. unpublished M.Sc. thesis, Dept. of Geology and Geophysics, University of Calgary.

Hirst, D.M. 1962a. The geochemistry of modern sediments from the Gulf of Paria - I. The relationship between the mineralogy and the distribution of major elements. Geochim. Cosomchim. Acta., V.26, p.309-334.

Hirst, D.M. 1962b. The geochemistry of modern sediments from the Gulf of Paria - II, The location and distribution of trace elements. Geochim. Cosmochim. Acta., V.26, p.1147-1187.

Hoede, D. and Das, H.A. 1981. Accuracy and precision of instrumental neutron activation analysis based on gamma-spectrometry with a planar intrinsic Ge detector. J. Radioanal. Chem., V.62, p.171-186.

Holmberg, P. and Reippo, R. 1973. Monte Carlo calculations of efficiency volume for well-type NaI detectors with self absorption in the source. Int. J. of Appl. Radn. and Isotopes., V.24, p.99-105.

James, G.W. 1977. Low-level determinations of uranuium and thorium in geological samples by X-ray spectrometry. Anal. Chem., V.49, p.967-969.

Katcoff, S. 1960. Fission-product yields from neutron induced fission. Nature, V. 18, No.11, p.201

Katz, A. and Grossman, L. 1976. Intercalibration of 17 standard silicates for 14 elements by instrumental neutron activation analysis. in Flanagan, F.J.(ed.) Description and analyses of eight new USGS rock standards U.S. Geol. Survey Prof. Paper 840, p.49-58.

Kay, R.E., Stevens-Guille, P.D., Hilborn, J.W. and Jervis, R.E. 1973. SLOWPOKE: A new low-cost laboratory reactor. Inter. J. Appl. Radiation and Isotopes, V.24, p.509-518.

Keepin, G.R., Wimett, T.F. and Ziegler, R.K. 1957. J. Nuc. Energy., V.6, p.1-21.

Kelepertsis, A. E. 1981. The geochemistry of uranium and thorium in some lower Carboniferous sedimentary rocks (Great Britain). Chem. Geol., V.34, p.275-288.

Kennedy, G. and Fowler, A. 1983. Interference from uranium in neutron activation analysis of rare-earths in silicate rocks. J. Radioanal. Chem., V.78, No.1, p.165-169.

Kleeman, J.D. and Lovering, J.F. 1967. Uranium distribution in rocks by fission track registration in Lexan plastic. Science, V.156, p.512-513.

Knoll, G.F. 1979. Radiation Detection and Measurement. John Wiley and Sons, New York. pp.816.

Kruger, P. 1971. Principles of Activation Analysis. John Wiley and Sons, Inc., New York. pp.522

Kubota, M. 1977. Interference by neutron induced second order nuclear reaction in activation analysis of REE. J. Radioanal. Chem., V.36, p.565-576.

Kuleff, I. and Kasladinow, K. 1981. Epithermal neutron activation analysis of uranium by neptumium-239 using high resolution gamma-spectrometry. J. Radioanal. Chem., V.63, No.2, p.397-404.

Kunzendorf, H. and Løvborg, L. 1981. Elemental interferences in the analysis of uranium by delayed-neutron counting. J. Geochem. Expl., V.15. p.583-595.

Landis, E.R. 1962. Uranium and other trace elements in Devonian and Mississippian black shales in the central and mid-continent area. U.S. Geol. Survey Bull. 1107-E, p.289-336.

Leake, B.E., Hendry, G.L., Kemp, A., Plant, A.G., Harvey, P.K., Wilson, J.R., Coats, J.S., Aucott, J.W., Lunel, T. and Howarth, R.J. 1969. The chemical analysis of rock powders by automatic X-ray fluorescence. *Chem. Geol.,* V.5, p.7-86.

Lederer, C.M. and Shirley, V. 1978 eds., *Table of Isotopes.* seventh edition. John Wiley and Sons, New York.

Leventhal, J.S. 1978. Trace element, carbon and sulfur in Devonian black-shale cores from Perry County, Kentucky; Jackson and Lincoln Counties, West Virginia; and Cattaraugus County, New York. *U.S. Geol. Survey, Open-File Rep*. 78-504, pp44.

Leventhal, J.S. and Hosterman, J.W. 1982. Chemical and mineralogical analysis of Devonian black-shale samples from Martin County, Kentucky; Caroll and Washington Counties, Ohio; Wise County, Virginia; and Overton County, Tennessee, U.S.A. *Chem. Geol.*, V.37, p.239-264.

Levinson, A.A. and Coetzee, G.L. 1978. Implications of disequilibrium in exploration for uranium ores in the surficial environment using radiometric techniques- a review. *Minerals Sci. Engng.,* V.10, No.1, p.19-27.

Mason, B. 1966.*Principles of Geochemistry.* 3rd. edition. John Wiley and Sons, Inc., Japan. pp.329.

McLennan, S.M. and Taylor, S.R. 1980. Geochemical standards for sedimentary rocks: trace element data for USGS standards SCo-1, MAG-1 and SGR-1. *Chem. Geol.,* V.29, p.333-343.

McLennan, S. M. and Taylor, S.R. 1980b. Th and U in sedimentary rocks: crustal evolution and sedimentary recycling *Nature*, V.285, p.621-624.

McLennan, S.M., Nance, W.B. and Taylor, S.R. 1980. Rare earth element- thorium correlations in sedimentary rocks, and the composition of the continental crust. *Geochim. Cosmchim. Acta.,* V.44, p.1833-1839.

Millard, H.T., Jr. 1976. Determinations of uranium and thorium in USGS standard rocks by the delayed neutron technique. in Flanagan, F.J.(ed.) Description and analyses of eight new USGS rock standards: U.S. Geol. Survey Prof. Paper 840, p.61-65.

Millard, H.T., Jr. and Keaten, B.A. 1982. Precision of uranium and thorium determinations by delayed neutron counting. J. Radioanal. Chem., V.72, No.1-2, p.489-500.

Mo, T., Suttle, A.D. and Sackett, W.M. 1973. Uranium concentrations in marine sediments. Geochim. Cosmochim. Acta., V.37, p.35-51.

Muecke, G.K. (ed.) 1980. Short course in Neutron Activation Analysis in the Geosciences. Mineral Ass. of Canada Short Course Handbook., V.5, pp.279.

Nakamura, N. 1974. Determination of REE, Ba, Fe, Na and K in carbonaceous and ordinary chondrites. Geochim. Cosmochim. Acta., V.38, p.757-775.

Nance, W. B. and Taylor, S.R. 1976. Rare earth element patterns and crustal evolution I. Australian past-Archean sedimentary rocks. Geochim. Cosmochim. Acta., V.40, p.1539-1551.

Nishimura, S. 1970. The determination of uranium content of standard rocks by fission track registration in muscovite. Radioisotopes., V.19, p.194-196.

Piper, D.Z. 1974. Rare earth elements in the sedimentary cycle: a summary. Chem. Geol., V.14, p.285-304.

Pliler, R. and Adams, J.A.S. 1962. The distribution of thorium, uranium and potassium in the Mancos Shale. Geochim. Cosmochim. Acta., V.26, p.1115-1135.

Potts, P.J., Thorpe, O.W. and Watson, J.S. 1981. Determination of the rare-earth element abundances in 29 international rock standards by instrumental neutron activation analysis: a critical appraisal of calibration error. *Chem. Geol.,* V.34, p.331-352.

Price, P.B. and Walker, R.M., 1963. A simple method of measuring low uranium concentrations in natural crystals. *Appl. Phys. Lett.* V.2, p.23-25.

Pulman, I.I. 1975. Distribution of uranium, thorium and potassium in the sedimentary rocks of the west Siberian platform. *Geochem. Int.,* V.12, part 3, p.97-107.

Rakovic, M. 1970. *Activation Analysis.* The Press, (Ilifte),London. pp.339.

Reynolds, S.A. and Mullins, W.T. 1963. Neutron flux perturbation in activation analysis. *Int. J. Appl. Radn. Isotopes.,* V.14, p.421-426.

Ritchie, J.C. and McHenry, J.R. 1973. Determination of fallout ^{137}Cs and naturally occurring gamma-ray emitters in sediments. *Int. J. Appl. Radn. Isotopes.,* V.24, p.575-578.

Ronov, A.B., Balashov, Yu.A. and Migdisov, A.A. 1967 Geochemistry of the rare earths in the sedimentary cycle. *Geochem. Int.,* V.4, p.1-17.

Ronov, A.B, Balashov, Yu.A., Girin, Yu.A., Brotishko, R.Kh. and Kazakoo, G.A. 1974. Regularities of rare-earth element distribution in the sedimentary shell and in the crust of the earth. *Sedimentology,* V.21, p.171-193.

Rosenberg, R.J. 1981. A simple method for the determination of uranium and thorium by delayed neutron counting. *J. Radioanal. Chem.,* V.62, No.1/2, p.145-149.

Rosholt. Jr., J.N. 1959. Natural radioactive disequilibrium of the uranium series. *U.S. Geol. Survey Bull.,* No. 1084-A, p.1-30.

Ryan, D.E., Stuart, D.C. and Chattopadhyay, A. 1978. Rapid multielement neutron activation analysis with a SLOWPOKE reactor. Anal. Chim. Acta., V.100, p.87-93.

Ryan, D.E., Brooks, R.R. and Zhang, H.F. 1981. The analytical chemistry of thorium. Rev. Anal. Chem., p.281-318.

Schock, H.H. 1977. Comparison of a coaxial Ge(Li) and a planar Ge detector in instrumental activation analysis of geologic materials. J. Radioanal. Chem., V.36, p.557-564.

Shaw, D.M., Dostal, J. and Keays, R.R. 1967. Additional estimates of continental surface Precambrian shield compostion in Canada. Geochim. Cosmochim. Acta., V.40, p.73-83.

Shaw, D.M., Reilly, G.A., Muysson, J.R., Pattenden, G.E. and Campbell, F.E. 1976. The chemical compostion of the Canadian Precambrian shield. Can. J. Earth Sci.,V.4, p.829-854.

Steinnes, E. 1971. Epithermal neutron activation analysis of geological material. in Activation Analysis in Geochemistry and Cosmochemistry. A.O. Brunfelt and E. Steinnes (eds.) Universitetsforlaget, Oslo, p.113-128.

Stuart, D.C. and Ryan, D.E. 1981. Epithermal neutron activation analysis with a SLOWPOKE reactor. Can. J. Chem., V.59, p.1470-1475.

Stuckless, J.S., Millard, H.T., Bunker, C.M., Nkomo, I.T., Roshalt, J.N., Bush, C.A., Huffman, C. and Keil, R.I. 1977. A comparison of some analytical techniques for determining uranium, thorium and potassium in granitic rocks. Jour. Research US. Geol. Survey., V.5, No.1, p.83-91.

Takeuchi, T., Uehara, S. and Hayashi, T. 1980. Comparisons of several dead time correction methods in the case of a mixture of short- and long-lived nuclides. J. Radioanal. Chem., V.56, p.25-35.

Thomas, J.A., Mountjoy, W. and Huffman, C.Jr. 1976. Copper, lithium, manganese, strontium, zinc, sodium, potassium and magnesium contents of eight new USGS standard rock samples. in Flanagan, F.J.(ed.) Description and analyses of eight new USGS rock standards. U.S. Geol. Survey Prof. Paper 840, p.119-122.

Tlig, S. and Sleinberg, M. 1982. Distribution of Rare-earth elements (REE) in size fractions of recent sediments of the Indian Ocean. Chem. Geol., V.37, p.317-333.

Vine, J.D. and Tourlelot, E.B. 1970. Geochemistry of black shale deposits - a summary report. Econ Geol., V.65, p.253-272.

Vukotić, P. 1981. Routine multielement instrumental neutron activation anlysis of silicate rocks using short-lived radionuclides. J. Radioanal. Chem., V.63, No.2, p.353-365.

Warren, P.S. 1937. Age of the Exshaw shale in the Canadian Rockies. Am. Jour. Sci., V.33, p.454-457.

Weiss, A. and Amstutz, G.C. 1966. Ion-exchange reactions on clay minerals and cation selective membrane properties as possible mechanisms of economic metal concentration. Mineralium Deposita, V.1, p.60-66.

Wyttenbach, A. 1971. Coincidence losses in activation analysis. J. Radioanal. Chem., V.8, p.335-343.

Zikovsky, L. and Galinier, J.L. 1981. Calculation of primary nuclear interferences occurring in neutron activation analysis with a SLOWPOKE reactor. J. Radionanal. Chem., V.67, p.193-202.

Appendix 1 : Chemical Analyses.

The instrumental neutron activation analysis and X-ray fluorsence results for the forty-two Exshaw Shale samples are reported in this appendix. Silica, Cu, Ni, Pb and Zn were analyzed by XRF, organic carbon with a LECO high frequency induction furnace in a manner similar to that outlined by Boyce and Bode (1972), and the remaining elements via INAA.

The INAA results are reported with ± one standard deviation uncertainty and total Fe is reported as Fe_2O_3.

NA - element not analyzed for

ND - element not detected during analysis.

Sample No.	1 Ex.	2 Ex.	3 Ex.
SiO_2	66.15	55.77	27.98
Al_2O_3	6.40 ± 0.09	13.6 ± 0.1	1.04 ± 0.03
Fe_2O_3	2.34 ± 0.03	7.17 ± 0.25	4.51 ± 0.18
MgO	0.57 ± 0.11	0.87 ± 0.21	2.71 ± 0.11
CaO	6.43 ± 0.18	0.71 ± 0.07	25.2 ± 0.4
Na_2O	0.150 ± 0.004	0.431 ± 0.003	0.113 ± 0.003
K_2O	3.09 ± 0.28	3.69 ± 0.23	0.69 ± 0.23
TiO_2	0.19 ± 0.04	0.62 ± 0.05	0.04 ± 0.02
C org.	5.4	1.2	3.9
As	16.6 ± 0.5	44.6 ± 0.4	6.65 ± 0.31
Ba	286 ± 28	406 ± 42	286 ± 28
Cl	273 ± 16	913 ± 35	393 ± 21
Co	19.7 ± 0.2	32.1 ± 0.3	14.8 ± 0.2
Cr	34.8 ± 1.0	102 ± 2	39.2 ± 1.1
Cs	3.78 ± 0.11	12.8 ± 0.2	0.58 ± 0.10
Cu	69	53	54
Ga	9.0 ± 0.8	22.9 ± 1.0	3.6 ± 0.9
Hf	1.0 ± 0.1	3.9 ± 0.1	2.3 ± 0.1
Mn	97.7 ± 2.3	122 ± 3	75.4 ± 2.1
Mo	59 ± 2	6 ± 2	97 ± 4
Ni	132	120	175
Pb	22	107	16
Rb	58 ± 3	174 ± 5	9 ± 2
Sb	3.31 ± 0.10	8.14 ± 0.09	0.68 ± 0.05
Sc	6.44 ± 0.15	17.2 ± 0.2	7.01 ± 0.10
Sr	1060 ± 30	106 ± 25	525 ± 26
Ta	0.46 ± 0.06	0.94 ± 0.08	0.26 ± 0.05
Th	7.47 ± 0.87	11.0 ± 0.7	5.80 ± 0.63
U	27.0 ± 0.3	4.53 ± 0.13	38.2 ± 0.4
V	233 ± 5	410 ± 7	100 ± 3
Zn	255	231	397
La	17.6 ± 0.5	41.0 ± 0.5	60.0 ± 3.6
Ce	24.3 ± 0.3	72.7 ± 0.6	63.3 ± 0.6
Sm	4.10 ± 0.28	4.83 ± 0.32	16.6 ± 0.4
Eu	0.81 ± 0.06	1.06 ± 0.07	3.28 ± 0.15
Tb	ND	ND	2.44 ± 0.07
Dy	3.20 ± 0.10	3.90 ± 0.10	15.3 ± 0.2
Yb	1.51 ± 0.15	2.73 ± 0.24	7.19 ± 0.40
Lu	0.30 ± 0.01	0.40 ± 0.03	1.21 ± 0.04

Sample No.	4 Ex.	5 Ex.	6 Ex.
SiO_2	59.48	38.76	NA
Al_2O_3	3.52 ± 0.05	9.31 ± 0.09	NA
Fe_2O_3	1.43 ± 0.13	17.8 ± 0.3	2.55 ± 0.18
MgO	0.70 ± 0.09	1.37 ± 0.17	NA
CaO	13.2 ± 0.3	9.35 ± 0.21	7.80 ± 0.21
Na_2O	0.286 ± 0.006	0.101 ± 0.003	0.197 ± 0.009
K_2O	1.16 ± 0.18	7.33 ± 0.61	2.35 ± 0.26
TiO_2	0.16 ± 0.04	0.53 ± 0.05	NA
C org.	9.1	5.7	NA
As	10.6 ± 0.3	124 ± 2	21.1 ± 0.4
Ba	252 ± 24	413 ± 37	372 ± 36
Cl	618 ± 29	234 ± 18	950 ± 37
Co	10.7 ± 0.2	21.7 ± 0.1	15.9 ± 0.2
Cr	29.1 ± 0.9	41.4 ± 1.4	62.5 ± 1.3
Cs	1.74 ± 0.10	2.59 ± 0.18	3.20 ± 0.13
Cu	216	86	NA
Ga	5.5 ± 0.3	11.8 ± 0.9	11.7 ± 1.0
Hf	1.0 ± 0.1	2.0 ± 0.1	2.0 ± 0.1
Mn	246 ± 4	320 ± 4	161 ± 3
Mo	70 ± 3	44 ± 3	96 ± 3
Ni	99	162	NA
Pb	17	53	NA
Rb	38 ± 3	72 ± 5	74 ± 3
Sb	3.04 ± 0.06	14.9 ± 0.2	4.10 ± 0.07
Sc	4.81 ± 0.10	8.42 ± 0.21	7.90 ± 0.11
Sr	143 ± 30	255 ± 33	143 ± 26
Ta	0.28 ± 0.06	0.70 ± 0.08	0.72 ± 0.07
Th	5.43 ± 0.81	8.60 ± 0.11	10.4 ± 0.2
U	24.0 ± 0.3	55.3 ± 0.5	30.6 ± 0.4
V	280 ± 6	289 ± 6	NA
Zn	7	218	NA
La	15.9 ± 0.9	18.5 ± 0.7	29.7 ± 1.7
Ce	24.5 ± 0.5	19.8 ± 0.6	48.0 ± 0.5
Sm	2.96 ± 0.32	5.45 ± 0.38	5.53 ± 0.28
Eu	0.67 ± 0.06	1.26 ± 0.09	1.29 ± 0.07
Tb	0.43 ± 0.05	ND	0.56 ± 0.06
Dy	2.50 ± 0.08	3.80 ± 0.09	4.70 ± 0.10
Yb	1.37 ± 0.15	1.44 ± 0.21	1.96 ± 0.19
Lu	0.28 ± 0.02	0.37 ± 0.02	0.31 ± 0.03

Sample No.	7 Ex.	8 Ex.	9 Ex.
SiO_2	13.73	51.15	38.73
Al_2O_3	1.39 ± 0.03	5.4 ± 0.2	8.97 ± 0.09
Fe_2O_3	0.82 ± 0.13	6.04 ± 0.24	3.47 ± 0.19
MgO	11.6 ± 0.3	1.78 ± 0.24	3.06 ± 0.18
CaO	33.3 ± 0.5	0.54 ± 0.08	21.0 ± 0.3
Na_2O	0.107 ± 0.003	0.774 ± 0.014	0.177 ± 0.003
K_2O	0.73 ± 0.11	3.27 ± 0.25	4.08 ± 0.24
TiO_2	0.06 ± 0.03	0.65 ± 0.04	0.36 ± 0.05
C org.	NA	5.7	2.9
As	8.82 ± 0.26	44.9 ± 0.6	9.78 ± 0.47
Ba	247 ± 25	891 ± 68	290 ± 34
Cl	497 ± 25	506 ± 29	337 ± 23
Co	14.0 ± 0.2	24.3 ± 0.2	18.0 ± 0.2
Cr	35.5 ± 0.9	125 ± 2	56 ± 1
Cs	1.33 ± 0.09	8.75 ± 0.14	7.04 ± 0.12
Cu	45	65	57
Ga	2.8 ± 0.7	26.3 ± 1.3	13.3 ± 0.5
Hf	0.6 ± 0.1	3.4 ± 0.2	1.9 ± 0.1
Mn	128 ± 3	111 ± 3	560 ± 6
Mo	107 ± 5	58 ± 4	6 ± 2
Ni	164	274	40
Pb	14	24	21
Rb	18 ± 2	173 ± 5	122 ± 4
Sb	1.19 ± 0.04	13.3 ± 0.1	1.21 ± 0.07
Sc	7.61 ± 0.02	18.7 ± 0.2	10.1 ± 0.2
Sr	478 ± 30	150 ± 27	616 ± 31
Ta	0.22 ± 0.05	1.01 ± 0.09	0.61 ± 0.04
Th	2.03 ± 0.63	14.5 ± 1.0	7.61 ± 0.61
U	15.8 ± 0.3	18.1 ± 0.3	6.19 ± 0.15
V	110 ± 3	1080 ± 10	95 ± 4
Zn	498	385	55
La	25.5 ± 1.8	32.2 ± 1.2	21.0 ± 0.6
Ce	32.5 ± 0.4	65.3 ± 0.6	35.8 ± 0.4
Sm	7.40 ± 0.33	5.20 ± 0.33	2.90 ± 0.38
Eu	1.62 ± 0.08	0.97 ± 0.07	0.73 ± 0.09
Tb	1.09 ± 0.05	ND	0.32 ± 0.05
Dy	6.35 ± 0.12	3.50 ± 0.09	2.91 ± 0.10
Yb	3.16 ± 0.21	2.80 ± 0.26	1.56 ± 0.18
Lu	0.41 ± 0.02	0.29 ± 0.04	0.29 ± 0.02

Sample No.	10 Ex.	11 Ex.	12 Ex.
SiO_2	45.67	79.88	NA
Al_2O_3	6.73 ± 0.10	2.85 ± 0.05	6.13 ± 0.09
Fe_2O_3	2.11 ± 0.15	1.19 ± 0.12	3.14 ± 0.16
MgO	2.40 ± 0.15	0.24 ± 0.07	3.20 ± 0.15
CaO	18.8 ± 0.4	3.65 ± 0.16	12.6 ± 0.3
Na_2O	0.160 ± 0.004	0.267 ± 0.006	0.847 ± 0.016
K_2O	3.48 ± 0.24	0.80 ± 0.10	1.59 ± 0.11
TiO_2	0.30 ± 0.04	0.11 ± 0.03	0.43 ± 0.05
C org.	4.2	5.5	1.9
As	10.9 ± 0.5	6.62 ± 0.40	16.0 ± 0.6
Ba	288 ± 33	189 ± 30	203 ± 32
Cl	187 ± 17	540 ± 25	289 ± 23
Co	22.0 ± 0.2	31.6 ± 0.2	22.0 ± 0.2
Cr	52.8 ± 1.2	20.8 ± 0.9	68.4 ± 1.2
Cs	6.95 ± 0.11	1.13 ± 0.09	2.73 ± 0.12
Cu	37	104	NA
Ga	10.4 ± 0.5	6.6 ± 0.3	11.2 ± 1.5
Hf	1.4 ± 0.1	ND	4.9 ± 0.1
Mn	157 ± 3	48.2 ± 1.7	242 ± 5
Mo	52 ± 3	8 ± 2	9 ± 2
Ni	100	69	NA
Pb	18	14	NA
Rb	86 ± 4	27 ± 3	62 ± 3
Sb	3.88 ± 0.10	1.60 ± 0.07	6.10 ± 0.12
Sc	7.7 ± 0.2	3.42 ± 0.11	7.09 ± 0.16
Sr	1090 ± 30	111 ± 18	139 ± 31
Ta	0.53 ± 0.60	0.48 ± 0.06	0.85 ± 0.07
Th	8.42 ± 0.73	1.77 ± 0.69	9.55 ± 0.59
U	12.9 ± 0.3	11.9 ± 0.2	4.31 ± 0.13
V	489 ± 8	158 ± 4	317 ± 6
Zn	237	32	NA
La	19.6 ± 0.7	9.8 ± 0.3	28.5 ± 0.3
Ce	26.2 ± 0.4	12.3 ± 0.3	49.8 ± 0.5
Sm	3.50 ± 0.30	1.96 ± 0.24	6.55 ± 0.35
Eu	0.56 ± 0.06	0.51 ± 0.05	1.21 ± 0.08
Tb	ND	ND	0.48 ± 0.05
Dy	2.17 ± 0.07	1.47 ± 0.05	4.91 ± 0.10
Yb	1.00 ± 0.21	ND	2.18 ± 0.30
Lu	0.16 ± 0.02	0.12 ± 0.02	0.34 ± 0.03

Sample No.	13 Ex.	14 Ex.	15 Ex.
SiO_2	44.75	NA	NA
Al_2O_3	10.7 ± 0.1	10.5 ± 0.1	8.41 ± 0.12
Fe_2O_3	4.91 ± 0.22	4.94 ± 0.21	3.16 ± 0.18
MgO	1.31 ± 0.18	1.16 ± 0.17	1.72 ± 0.15
CaO	8.26 ± 0.23	1.25 ± 0.08	16.4 ± 0.3
Na_2O	0.667 ± 0.012	0.212 ± 0.004	0.153 ± 0.003
K_2O	3.42 ± 0.17	4.49 ± 0.38	4.33 ± 0.28
TiO_2	0.76 ± 0.05	0.31 ± 0.05	0.54 ± 0.05
C org.	NA	8.3	NA
As	39.7 ± 0.6	31.9 ± 0.4	12.4 ± 0.3
Ba	525 ± 42	290 ± 28	297 ± 33
Cl	1400 ± 50	218 ± 16	184 ± 18
Co	18.4 ± 0.2	26.2 ± 0.2	16.0 ± 0.1
Cr	99.7 ± 1.7	78.1 ± 1.6	49.6 ± 1.2
Cs	5.06 ± 0.17	8.55 ± 0.17	6.56 ± 0.14
Cu	58	NA	NA
Ga	31.1 ± 1.4	20.6 ± 1.0	12.0 ± 0.3
Hf	14.9 ± 0.1	2.3 ± 0.1	1.6 ± 0.1
Mn	75.7 ± 1.5	92.1 ± 2.2	352 ± 5
Mo	17 ± 2	83 ± 2	30 ± 1
Ni	71	NA	NA
Pb	71	NA	NA
Rb	123 ± 4	144 ± 5	101 ± 3
Sb	2.01 ± 0.08	9.63 ± 0.09	1.82 ± 0.05
Sc	11.8 ± 0.2	10.2 ± 0.1	9.60 ± 0.11
Sr	448 ± 30	853 ± 29	314 ± 36
Ta	1.60 ± 0.10	0.67 ± 0.07	0.60 ± 0.06
Th	43.8 ± 1.7	10.0 ± 1.0	8.27 ± 0.71
U	15.6 ± 0.3	31.7 ± 0.4	10.5 ± 0.3
V	95 ± 5	360 ± 7	105 ± 5
Zn	14	NA	NA
La	185 ± 2	27.5 ± 0.3	18.3 ± 0.3
Ce	279 ± 2	55.6 ± 0.5	33.1 ± 0.6
Sm	36.5 ± 0.5	6.64 ± 0.32	3.52 ± 0.30
Eu	7.42 ± 0.20	1.43 ± 0.07	0.62 ± 0.07
Tb	5.25 ± 0.10	0.56 ± 0.07	0.18 ± 0.06
Dy	22.7 ± 0.3	4.75 ± 0.09	2.48 ± 0.08
Yb	11.1 ± 0.6	1.75 ± 0.18	1.38 ± 0.16
Lu	1.17 ± 0.03	0.37 ± 0.04	0.22 ± 0.02

Sample No.	16 Ex.	17 Ex.	18 Ex.
SiO_2	57.38	72.81	NA
Al_2O_3	9.06 ± 0.09	9.32 ± 0.09	15.7 ± 0.2
Fe_2O_3	2.88 ± 0.18	3.78 ± 0.19	5.82 ± 0.23
MgO	1.88 ± 0.16	0.92 ± 0.16	1.11 ± 0.24
CaO	5.34 ± 0.18	1.30 ± 0.10	0.52 ± 0.85
Na_2O	0.565 ± 0.011	0.460 ± 0.009	0.701 ± 0.013
K_2O	3.31 ± 0.24	2.00 ± 0.08	3.93 ± 0.28
TiO_2	0.47 ± 0.05	0.46 ± 0.05	0.62 ± 0.06
C org.	4.2	2.4	4.2
As	15.7 ± 0.6	26.9 ± 0.4	45.2 ± 0.5
Ba	365 ± 36	563 ± 51	714 ± 49
Cl	346 ± 22	608 ± 30	665 ± 30
Co	18.6 ± 0.2	21.4 ± 0.2	26.0 ± 0.2
Cr	83.8 ± 1.3	74.6 ± 1.4	112 ± 2
Cs	5.20 ± 0.18	4.40 ± 0.15	8.70 ± 0.15
Cu	59	61	NA
Ga	15.8 ± 1.0	13.5 ± 0.5	25.0 ± 1.2
Hf	3.8 ± 0.1	4.5 ± 0.1	4.1 ± 0.1
Mn	145 ± 3	101 ± 3	94.9 ± 2.9
Mo	42 ± 2	8 ± 1	51 ± 3
Ni	99	103	NA
Pb	20	19	NA
Rb	114 ± 4	92 ± 4	169 ± 4
Sb	4.84 ± 0.12	4.85 ± 0.07	10.6 ± 0.1
Sc	9.56 ± 0.21	10.5 ± 0.1	17.4 ± 0.2
Sr	84 ± 25	104 ± 22	129 ± 26
Ta	1.04 ± 0.08	0.84 ± 0.07	0.90 ± 0.08
Th	12.4 ± 0.6	10.7 ± 0.50	14.1 ± 0.1
U	13.3 ± 0.2	9.69 ± 0.21	15.3 ± 0.2
V	401 ± 7	475 ± 8	927 ± 7
Zn	110	188	NA
La	22.5 ± 0.4	25.2 ± 1.1	39.7 ± 1.9
Ce	43.1 ± 0.6	51.8 ± 0.5	69.6 ± 0.6
Sm	4.42 ± 0.30	4.30 ± 0.28	5.40 ± 0.30
Eu	0.76 ± 0.07	1.11 ± 0.07	1.13 ± 0.07
Tb	ND	0.23 ± 0.06	ND
Dy	3.34 ± 0.08	3.86 ± 0.09	3.66 ± 0.08
Yb	1.98 ± 0.31	2.51 ± 0.21	2.40 ± 0.24
Lu	0.35 ± 0.03	0.43 ± 0.03	0.41 ± 0.02

Sample No.	19 Ex.	20 Ex.	21 Ex.
SiO_2	NA	59.05	NA
Al_2O_3	14.2 ± 0.1	8.32 ± 0.12	14.6 ± 0.2
Fe_2O_3	4.18 ± 0.23	2.64 ± 0.17	3.76 ± 0.20
MgO	2.75 ± 0.23	2.09 ± 0.16	2.79 ± 0.24
CaO	4.08 ± 0.16	6.84 ± 0.21	3.95 ± 0.16
Na_2O	0.301 ± 0.006	0.522 ± 0.006	0.252 ± 0.005
K_2O	5.83 ± 0.39	2.40 ± 0.15	6.45 ± 0.39
TiO_2	0.57 ± 0.06	0.41 ± 0.04	0.58 ± 0.06
C org.	NA	2.3	1.3
As	12.9 ± 0.6	6.60 ± 0.51	6.60 ± 0.35
Ba	413 ± 39	838 ± 48	329 ± 40
Cl	1370 ± 50	272 ± 20	418 ± 21
Co	23.7 ± 0.2	15.0 ± 0.1	22.4 ± 0.2
Cr	87 ± 2	78.5 ± 1.3	70.2 ± 1.5
Cs	10.0 ± 0.2	5.21 ± 0.11	8.12 ± 0.13
Cu	NA	64	NA
Ga	26.2 ± 1.0	11.7 ± 1.2	19.7 ± 0.6
Hf	3.3 ± 0.1	3.2 ± 0.1	3.1 ± 0.1
Mn	367 ± 5	107 ± 3	432 ± 4
Mo	32 ± 2	ND	ND
Ni	NA	51	NA
Pb	NA	21	NA
Rb	189 ± 5	106 ± 4	136 ± 4
Sb	3.51 ± 0.09	ND	0.80 ± 0.05
Sc	18.1 ± 0.4	15.1 ± 0.3	14.9 ± 0.1
Sr	138 ± 36	165 ± 24	361 ± 40
Ta	0.85 ± 0.06	0.87 ± 0.07	0.84 ± 0.07
Th	13.1 ± 0.1	9.76 ± 0.7	12.5 ± 0.7
U	16.3 ± 0.3	3.40 ± 0.11	5.72 ± 0.15
V	210 ± 6	185 ± 5	122 ± 5
Zn	NA	139	NA
La	31.6 ± 0.5	25.5 ± 0.3	25.3 ± 1.4
Ce	58.1 ± 0.5	44.2 ± 0.5	49.8 ± 0.5
Sm	7.30 ± 0.40	3.74 ± 0.28	5.91 ± 0.35
Eu	1.42 ± 0.09	0.77 ± 0.06	1.23 ± 0.09
Tb	ND	0.31 ± 0.06	ND
Dy	5.21 ± 0.12	3.04 ± 0.08	4.38 ± 0.10
Yb	3.14 ± 0.27	2.34 ± 0.29	2.45 ± 0.21
Lu	0.37 ± 0.03	0.30 ± 0.02	0.28 ± 0.03

Sample No.	22 Ex.	23 Ex.	24 Ex.
SiO_2	NA	65.07	NA
Al_2O_3	6.06 ± 0.09	7.87 ± 0.08	5.87 ± 0.08
Fe_2O_3	1.90 ± 0.14	12.3 ± 0.3	2.60 ± 0.17
MgO	0.78 ± 0.12	0.38 ± 0.13	0.75 ± 0.11
CaO	9.39 ± 0.24	1.05 ± 0.08	1.38 ± 0.08
Na_2O	0.392 ± 0.009	0.181 ± 0.003	0.117 ± 0.003
K_2O	2.07 ± 0.20	3.84 ± 0.19	3.11 ± 0.29
TiO_2	0.24 ± 0.04	0.32 ± 0.04	0.22 ± 0.04
C org.	NA	1.8	14.5
As	12.1 ± 0.7	24.4 ± 0.4	21.3 ± 0.4
Ba	232 ± 25	215 ± 32	527 ± 43
Cl	994 ± 38	386 ± 19	524 ± 23
Co	13.1 ± 0.1	16.8 ± 0.2	36.6 ± 0.3
Cr	49.6 ± 1.0	56.0 ± 1.3	49.7 ± 1.3
Cs	2.41 ± 0.11	5.72 ± 0.19	3.79 ± 0.13
Cu	NA	123	NA
Ga	7.3 ± 0.1	11.6 ± 0.4	16.6 ± 0.9
Hf	1.7 ± 0.1	1.6 ± 0.1	1.5 ± 0.1
Mn	121 ± 3	145 ± 3	47.0 ± 1.6
Mo	60 ± 2	51 ± 2	2 ± 1
Ni	NA	68	NA
Pb	NA	22	NA
Rb	58 ± 3	95 ± 4	70 ± 4
Sb	2.36 ± 0.07	1.69 ± 0.05	5.31 ± 0.07
Sc	6.95 ± 0.10	8.55 ± 0.10	7.62 ± 0.11
Sr	160 ± 24	32 ± 22	231 ± 22
Ta	0.53 ± 0.05	0.55 ± 0.70	0.64 ± 0.07
Th	6.85 ± 0.90	7.37 ± 0.60	3.11 ± 1.03
U	20.8 ± 0.3	4.75 ± 0.13	41.0 ± 0.4
V	285 ± 6	81 ± 4	586 ± 9
Zn	NA	260	NA
La	22.7 ± 0.6	13.6 ± 1.0	25.5 ± 1.4
Ce	32.2 ± 0.4	27.2 ± 0.4	31.3 ± 0.4
Sm	5.30 ± 0.30	3.59 ± 0.28	3.88 ± 0.27
Eu	1.21 ± 0.07	0.73 ± 0.06	0.71 ± 0.05
Tb	0.28 ± 0.05	ND	ND
Dy	4.12 ± 0.09	2.48 ± 0.08	2.40 ± 0.07
Yb	1.66 ± 0.17	1.09 ± 0.16	1.29 ± 0.17
Lu	0.30 ± 0.02	0.19 ± 0.02	0.14 ± 0.02

Sample No.	25 Ex.	26 Ex.	27 Ex.
SiO_2	80.60	53.05	NA
Al_2O_3	1.50 ± 0.02	11.7 ± 0.1	6.49 ± 0.09
Fe_2O_3	2.30 ± 0.15	8.76 ± 0.25	4.51 ± 0.19
MgO	0.14 ± 0.08	0.72 ± 0.19	2.42 ± 0.15
CaO	0.46 ± 0.06	2.42 ± 0.12	6.43 ± 0.21
Na_2O	0.152 ± 0.003	0.197 ± 0.004	0.517 ± 0.010
K_2O	1.63 ± 0.11	8.60 ± 0.83	2.30 ± 0.28
TiO_2	0.06 ± 0.01	0.76 ± 0.05	0.24 ± 0.04
C org.	5.9	5.0	11.7
As	14.7 ± 0.3	77.6 ± 0.6	43.8 ± 0.6
Ba	150 ± 23	1050 ± 60	377 ± 35
Cl	421 ± 20	221 ± 17	950 ± 38
Co	20.5 ± 0.2	38.9 ± 0.6	22.6 ± 0.2
Cr	37.9 ± 0.9	34.1 ± 1.5	50.4 ± 1.2
Cs	2.44 ± 0.11	4.47 ± 0.19	3.13 ± 0.14
Cu	124	131	NA
Ga	7.6 ± 0.7	13.0 ± 1.0	10.5 ± 1.4
Hf	1.6 ± 0.1	2.4 ± 0.1	1.6 ± 0.1
Mn	51.0 ± 1.0	257 ± 3	212 ± 4
Mo	7 ± 1	90 ± 2	39 ± 1
Ni	63	325	NA
Pb	31	41	NA
Rb	48 ± 3	106 ± 5	71 ± 3
Sb	0.90 ± 0.04	10.9 ± 0.2	10.3 ± 0.2
Sc	6.14 ± 0.09	9.82 ± 0.13	7.58 ± 0.11
Sr	192 ± 19	1780 ± 40	118 ± 28
Ta	0.55 ± 0.05	0.63 ± 0.90	0.59 ± 0.06
Th	4.90 ± 0.59	22.5 ± 2.1	6.57 ± 0.77
U	4.53 ± 0.13	91.4 ± 0.7	34.3 ± 0.4
V	18 ± 1	280 ± 6	252 ± 6
Zn	11	293	NA
La	29.5 ± 1.5	73.7 ± 4.6	36.2 ± 1.7
Ce	33.1 ± 0.4	100 ± 1	57.8 ± 0.5
Sm	3.37 ± 0.23	23.6 ± 0.5	7.94 ± 0.36
Eu	0.91 ± 0.06	5.93 ± 0.15	1.58 ± 0.10
Tb	0.19 ± 0.06	3.91 ± 0.10	1.10 ± 0.06
Dy	2.43 ± 0.06	21.6 ± 0.3	5.24 ± 0.11
Yb	1.48 ± 0.17	4.69 ± 0.32	2.24 ± 0.22
Lu	0.20 ± 0.02	0.54 ± 0.17	0.38 ± 0.15

Sample No.	28 Ex.	29 Ex.	30 Ex.
SiO_2	NA	54.72	67.92
Al_2O_3	10.8 ± 0.2	15.1 ± 0.2	4.49 ± 0.07
Fe_2O_3	4.64 ± 0.64	4.34 ± 0.22	3.23 ± 0.16
MgO	1.24 ± 0.18	1.33 ± 0.23	0.74 ± 0.10
CaO	9.33 ± 0.10	1.26 ± 0.12	2.06 ± 0.11
Na_2O	0.209 ± 0.004	0.754 ± 0.013	0.375 ± 0.007
K_2O	4.48 ± 0.30	3.79 ± 0.18	1.54 ± 0.18
TiO_2	0.44 ± 0.03	0.63 ± 0.06	0.19 ± 0.02
C org.	3.5	2.3	7.4
As	17.6 ± 0.4	29.1 ± 0.5	19.8 ± 0.6
Ba	358 ± 120	464 ± 44	108 ± 12
Cl	325 ± 20	2040 ± 70	955 ± 37
Co	27.2 ± 0.5	21.3 ± 0.2	22.4 ± 0.3
Cr	61.6 ± 4.4	96.4 ± 1.5	34.4 ± 1.0
Cs	7.97 ± 0.59	8.67 ± 0.19	2.53 ± 0.12
Cu	NA	47	131
Ga	19.0 ± 0.9	23.3 ± 1.9	9.9 ± 0.9
Hf	2.9 ± 0.4	2.4 ± 0.1	1.0 ± 0.1
Mn	268 ± 5	157 ± 3	63.8 ± 2.0
Mo	26 ± 2	16 ± 2	110 ± 2
Ni	NA	106	82
Pb	NA	25	21
Rb	150 ± 13	151 ± 4	50 ± 3
Sb	2.54 ± 0.06	5.64 ± 0.08	5.65 ± 0.11
Sc	11.3 ± 0.1	16.8 ± 0.2	4.92 ± 0.16
Sr	535 ± 57	85 ± 29	56 ± 20
Ta	ND	0.81 ± 0.08	0.31 ± 0.04
Th	10.2 ± 0.9	12.3 ± 0.6	5.05 ± 0.93
U	14.8 ± 0.2	5.72 ± 0.15	24.5 ± 0.3
V	185 ± 5	499 ± 9	138 ± 4
Zn	NA	143	15
La	23.8 ± 1.4	29.7 ± 1.3	12.9 ± 0.5
Ce	41.1 ± 1.5	55.5 ± 0.5	23.4 ± 0.4
Sm	2.06 ± 0.14	5.58 ± 0.35	2.33 ± 0.25
Eu	0.48 ± 0.04	1.29 ± 0.08	0.42 ± 0.05
Tb	ND	0.20 ± 0.05	ND
Dy	1.53 ± 0.04	4.05 ± 0.10	1.66 ± 0.06
Yb	1.54 ± 0.17	2.37 ± 0.22	ND
Lu	0.65 ± 0.02	0.37 ± 0.03	0.33 ± 0.02

Sample No.	31 Ex.	32 Ex.	33 Ex.
SiO_2	NA	37.82	NA
Al_2O_3	4.30 ± 0.14	20.4 ± 0.2	4.05 ± 0.07
Fe_2O_3	6.76 ± 0.19	6.49 ± 0.24	1.59 ± 0.13
MgO	1.03 ± 0.11	0.36 ± 0.28	1.86 ± 0.11
CaO	12.7 ± 0.3	3.04 ± 0.13	27.9 ± 0.5
Na_2O	0.423 ± 0.008	0.344 ± 0.006	0.115 ± 0.003
K_2O	1.56 ± 0.21	3.77 ± 0.19	1.68 ± 0.12
TiO_2	0.25 ± 0.04	1.06 ± 0.06	0.19 ± 0.04
C org.	NA	NA	4.4
As	29.8 ± 0.4	87.1 ± 0.7	8.03 ± 0.25
Ba	348 ± 37	221 ± 22	653 ± 47
Cl	628 ± 30	469 ± 22	180 ± 4
Co	11.8 ± 0.1	16.7 ± 0.2	28.2 ± 0.2
Cr	36.0 ± 1.2	82.0 ± 1.6	33.6 ± 1.0
Cs	1.92 ± 0.13	5.43 ± 0.18	5.32 ± 0.11
Cu	NA	49	NA
Ga	3.5 ± 1.5	28.1 ± 1.1	3.7 ± 0.5
Hf	2.3 ± 0.1	8.7 ± 0.2	0.9 ± 0.1
Mn	277 ± 4	81.4 ± 2.2	248 ± 4
Mo	50 ± 2	23 ± 1	8 ± 1
Ni	NA	51	NA
Pb	NA	81	NA
Rb	42 ± 4	88 ± 4	48 ± 3
Sb	3.47 ± 0.07	2.52 ± 0.07	2.38 ± 0.05
Sc	5.85 ± 0.10	16.1 ± 0.2	5.08 ± 0.09
Sr	276 ± 33	48 ± 24	526 ± 40
Ta	0.47 ± 0.06	2.41 ± 0.10	0.36 ± 0.06
Th	11.0 ± 1.1	33.7 ± 1.4	4.10 ± 0.44
U	25.0 ± 0.3	21.5 ± 0.3	5.54 ± 0.14
V	219 ± 5	104 ± 5	207 ± 5
Zn	NA	17	NA
La	50.2 ± 0.4	80.6 ± 3.2	16.1 ± 0.8
Ce	73.8 ± 0.6	154 ± 1	22.3 ± 0.5
Sm	8.88 ± 0.36	14.7 ± 0.3	4.57 ± 0.30
Eu	2.24 ± 0.09	2.53 ± 0.80	0.54 ± 0.06
Tb	1.65 ± 0.07	2.31 ± 0.08	ND
Dy	7.15 ± 0.13	8.88 ± 0.15	2.15 ± 0.07
Yb	2.33 ± 0.21	4.25 ± 0.31	1.24 ± 0.13
Lu	0.38 ± 0.03	0.43 ± 0.03	0.13 ± 0.02

Sample No.	34 Ex.	35 Ex.	36 Ex.
SiO_2	48.44	39.02	57.74
Al_2O_3	12.4 ± 0.1	8.26 ± 0.12	9.87 ± 0.15
Fe_2O_3	10.5 ± 0.2	2.81 ± 0.18	2.38 ± 0.17
MgO	1.21 ± 0.19	1.80 ± 0.16	ND
CaO	1.33 ± 0.11	17.1 ± 0.4	5.59 ± 0.18
Na_2O	0.166 ± 0.004	0.166 ± 0.004	0.556 ± 0.010
K_2O	7.02 ± 0.77	2.63 ± 0.18	2.75 ± 0.22
TiO_2	0.63 ± 0.05	0.39 ± 0.05	0.52 ± 0.06
C org.	12.8	3.6	4.1
As	74.1 ± 0.6	9.22 ± 0.28	18.7 ± 0.4
Ba	419 ± 27	209 ± 33	283 ± 33
Cl	354 ± 18	238 ± 23	400 ± 23
Co	38.0 ± 0.3	17.7 ± 0.2	21.5 ± 0.2
Cr	77.8 ± 1.3	46.9 ± 1.3	72.0 ± 1.3
Cs	7.09 ± 0.18	5.23 ± 0.16	4.71 ± 0.15
Cu	143	43	69
Ga	46.1 ± 1.4	12.6 ± 0.4	12.6 ± 1.4
Hf	3.3 ± 0.1	1.4 ± 0.1	3.5 ± 0.1
Mn	103 ± 2	428 ± 6	175 ± 3
Mo	167 ± 9	18 ± 1	45 ± 2
Ni	391	69	105
Pb	49	19	22
Rb	186 ± 6	91 ± 4	95 ± 4
Sb	9.69 ± 0.10	1.14 ± 0.04	5.75 ± 0.08
Sc	12.0 ± 0.2	9.18 ± 0.11	9.94 ± 0.12
Sr	476 ± 30	533 ± 41	93 ± 25
Ta	0.88 ± 0.09	0.78 ± 0.06	0.87 ± 0.07
Th	16.0 ± 2.1	7.86 ± 0.72	13.1 ± 0.9
U	92.2 ± 0.8	9.32 ± 0.20	15.2 ± 0.2
V	523 ± 9	95 ± 5	450 ± 10
Zn	216	46	208
La	55.1 ± 0.3	17.4 ± 0.6	21.3 ± 0.5
Ce	83.9 ± 0.8	34.1 ± 0.6	36.8 ± 0.4
Sm	13.8 ± 0.5	3.21 ± 0.36	5.40 ± 0.30
Eu	2.93 ± 0.09	0.78 ± 0.07	1.07 ± 0.07
Tb	1.70 ± 0.08	ND	ND
Dy	9.80 ± 0.14	2.20 ± 0.09	3.60 ± 0.08
Yb	3.49 ± 0.27	1.76 ± 0.17	1.93 ± 0.19
Lu	ND	0.19 ± 0.02	0.27 ± 0.02

Sample No.	37 Ex.	38 Ex.	39 Ex.
SiO_2	52.90	NA	59.42
Al_2O_3	15.1 ± 0.2	20.7 ± 0.2	13.0 ± 0.1
Fe_2O_3	5.42 ± 0.22	7.17 ± 0.24	5.90 ± 0.23
MgO	1.51 ± 0.23	0.75 ± 0.29	0.76 ± 0.20
CaO	0.62 ± 0.09	3.27 ± 0.13	0.48 ± 0.09
Na_2O	0.731 ± 0.013	0.322 ± 0.007	0.389 ± 0.008
K_2O	3.16 ± 0.24	4.47 ± 0.36	4.18 ± 0.25
TiO_2	0.56 ± 0.06	1.07 ± 0.06	0.67 ± 0.06
C org.	5.7	NA	1.3
As	40.1 ± 0.5	86.7 ± 0.8	35.4 ± 0.7
Ba	799 ± 58	185 ± 32	361 ± 45
Cl	760 ± 33	473 ± 22	477 ± 23
Co	33.2 ± 0.3	16.7 ± 0.2	32.7 ± 0.2
Cr	111 ± 2	77.5 ± 1.5	102 ± 2
Cs	8.56 ± 0.19	5.19 ± 0.18	12.1 ± 0.2
Cu	58	NA	53
Ga	26.4 ± 1.4	27.1 ± 1.0	23.9 ± 1.0
Hf	3.6 ± 0.1	9.5 ± 0.2	4.2 ± 0.1
Mn	96.6 ± 2.6	75.4 ± 2.1	122 ± 3
Mo	65 ± 2	2 ± 1	11 ± 1
Ni	254	NA	107
Pb	27	NA	77
Rb	162 ± 5	81 ± 4	178 ± 5
Sb	10.4 ± 0.2	2.67 ± 0.07	6.97 ± 0.13
Sc	15.4 ± 0.2	15.4 ± 0.2	17.7 ± 0.2
Sr	183 ± 26	107 ± 23	112 ± 24
Ta	0.82 ± 0.09	2.24 ± 0.09	1.05 ± 0.13
Th	13.4 ± 1.0	32.3 ± 1.4	14.8 ± 0.7
U	17.4 ± 0.3	21.8 ± 0.3	5.55 ± 0.15
V	963 ± 13	109 ± 5	429 ± 7
Zn	388	NA	269
La	28.8 ± 0.7	65.2 ± 3.6	34.9 ± 0.3
Ce	53.5 ± 0.9	129 ± 1	63.6 ± 0.6
Sm	4.23 ± 0.30	14.3 ± 0.4	4.38 ± 0.29
Eu	0.78 ± 0.70	2.53 ± 0.09	0.98 ± 0.70
Tb	ND	2.03 ± 0.08	ND
Dy	2.85 ± 0.08	9.05 ± 0.14	3.45 ± 0.08
Yb	1.98 ± 0.21	3.49 ± 0.28	2.51 ± 0.25
Lu	0.32 ± 0.03	0.44 ± 0.03	0.41 ± 0.03

Sample No.	40 Ex.	41 Ex.	42 Ex.
SiO_2	NA	NA	24.24
Al_2O_3	9.20 ± 0.09	4.95 ± 0.08	1.38 ± 0.04
Fe_2O_3	3.82 ± 0.19	14.3 ± 0.3	5.82 ± 0.18
MgO	2.04 ± 0.17	0.60 ± 0.11	ND
CaO	18.3 ± 0.3	14.8 ± 0.3	29.3 ± 0.5
Na_2O	0.170 ± 0.004	0.342 ± 0.006	0.121 ± 0.003
K_2O	3.39 ± 0.24	1.42 ± 0.26	0.14 ± 0.06
TiO_2	0.29 ± 0.03	0.29 ± 0.04	ND
C org.	3.5	8.8	8.0
As	16.5 ± 0.3	74.3 ± 0.6	7.66 ± 0.25
Ba	333 ± 37	336 ± 40	61 ± 14
Cl	271 ± 21	612 ± 28	284 ± 22
Co	15.5 ± 0.1	14.4 ± 0.1	34.1 ± 0.3
Cr	54.4 ± 1.4	36.6 ± 1.3	15.0 ± 0.9
Cs	7.50 ± 0.12	1.58 ± 0.15	0.86 ± 0.10
Cu	NA	NA	52
Ga	14.9 ± 0.8	10.9 ± 1.0	4.5 ± 0.3
Hf	1.9 ± 0.1	2.6 ± 0.1	0.3 ± 0.1
Mn	410 ± 6	222 ± 3	562 ± 6
Mo	60 ± 2	40 ± 2	23 ± 1
Ni	NA	NA	65
Pb	NA	NA	11
Rb	125 ± 4	47 ± 9	15 ± 3
Sb	2.23 ± 0.05	9.10 ± 0.10	2.22 ± 0.05
Sc	11.0 ± 0.1	6.90 ± 0.12	2.86 ± 0.07
Sr	387 ± 39	291 ± 31	179 ± 36
Ta	0.49 ± 0.10	0.33 ± 0.07	ND
Th	9.39 ± 0.92	14.4 ± 0.8	2.95 ± 0.54
U	12.2 ± 0.2	37.8 ± 0.4	9.82 ± 0.20
V	ND	ND	170 ± 4
Zn	NA	NA	59
La	22.1 ± 0.8	70.1 ± 0.5	8.2 ± 0.2
Ce	39.7 ± 0.4	92 ± 1	13.3 ± 0.3
Sm	4.30 ± 0.35	16.7 ± 0.5	2.43 ± 0.25
Eu	0.83 ± 0.08	4.07 ± 0.14	0.35 ± 0.07
Tb	0.25 ± 0.06	2.31 ± 0.08	ND
Dy	3.10 ± 0.07	12.2 ± 0.2	1.17 ± 0.08
Yb	1.86 ± 0.18	3.99 ± 0.30	1.23 ± 0.14
Lu	0.27 ± 0.02	0.45 ± 0.03	0.14 ± 0.02

Appendix 2 : Sample Locations.

Sample ID.	Well location.
1 Ex, 10 Ex and 26 Ex	14 - 29 - 48 - 6W5
2 Ex	6 - 4 - 84 - 7W6
3 Ex and 7 Ex	14 - 28 - 52 -11W5
4 Ex, 11 Ex and 44 Ex	12 - 11 - 78 -22W5
5 Ex, 24 Ex and 34 Ex	9 - 6 - 52 -11W5
6 Ex and 27 Ex	1 - 12 - 79 -22W5
8 Ex and 17 Ex	15 - 16 -110 - 6W6
9 Ex, 23 Ex and 35 Ex	4 - 36 - 51 - 1W5
12 Ex, 16 Ex, 20 Ex and 36 Ex	4 - 23 - 72 -10W6
13 Ex, 25 Ex, 32 Ex and 38 Ex	10 - 28 - 83 - 7W6
14 Ex and 33 Ex	15 - 10 - 58 - 5W5
15 Ex and 40 Ex	15 - 10 - 50 - 2W5
18 Ex and 37 Ex	10 - 36 -110 - 7W6
19 Ex	8 - 18 - 44 -25W4
21 Ex	1 - 20 - 46 -26W4
22 Ex, 29 Ex, 30 Ex and 42 Ex	13 - 18 - 80 -23W5
28 Ex	4 - 36 - 51 - 1W6
31 Ex	1- 12 - 79 -23W5
39 Ex	16 - 18 -107 - 6W6